

**Domain Decomposition Methods for Reissner-Mindlin
Plates discretized with the Falk-Tu Elements
TR2011-937**

by

Jong Ho Lee

A dissertation submitted in partial fulfillment

of the requirements for the degree of

Doctor of Philosophy

Department of Mathematics

New York University

January 2011

Professor Olof B. Widlund

© Jong Ho Lee
All rights reserved, 2011

Acknowledgements

I thank my advisor Professor Olof Widlund. Without his help, I could not do this dissertation. Thanks so much for his effort and advice, and I am fortunate to work with him. He encouraged me to do research and gave me a lot of help to write dissertation.

I also thank my colleague Duksoon Oh for discussion and help. I got much help from him for research and computing.

Thanks also to all members in Courant.

Abstract

The Reissner-Mindlin plate theory models a thin plate with thickness t . The condition number of finite element approximations of this model deteriorates badly as the thickness t of the plate converges to 0. In this thesis, we develop an overlapping domain decomposition method for the Reissner-Mindlin plate model discretized by Falk-Tu elements with a convergence rate which does not deteriorate when t converges to 0. We use modern overlapping methods which use the Schur complements to define coarse basis functions and show that the condition number of this overlapping method is bounded by $C(1 + \frac{H}{\delta})^3(1 + \log\frac{H}{h})^2$. Here H is the maximum diameter of the subdomains, δ the size of overlap between subdomains, and h the element size. Numerical examples are provided to confirm the theory. We also modify the overlapping method to develop a BDDC method for the Reissner-Mindlin model. We establish numerically an extension lemma to obtain a constant bound and an edge lemma to obtain a $C(1 + \log\frac{H}{h})^2$ bound. Given such bounds, the condition number of this BDDC method is shown to be bounded by $C(1 + \log\frac{H}{h})^2$.

Contents

Acknowledgements	iii
Abstract	iv
List of Figures	vii
List of Tables	ix
1 Introduction	1
1.1 An Overview	1
1.2 Functional Analysis Tools	2
1.3 The Conjugate Gradient Method	5
1.4 Mixed Finite Element Methods	7
2 Domain Decomposition Methods and an Abstract Theory	9
2.1 Introduction	9
2.2 Abstract Theory of Schwarz Methods	10
2.3 Problem Setting	11
2.4 Notation	12
2.5 Schur Complement Systems and Discrete Harmonic Extensions	14
2.6 Overlapping Schwarz Methods	15
2.7 BDDC Methods	17
3 The Reissner-Mindlin Plate Theory	20
3.1 Introduction	20
3.2 Linear Elasticity	21
3.3 Finite Elements for Reissner-Mindlin Plate	26
4 Overlapping Methods Using the Falk-Tu Elements for the Reissner-Mindlin Plate	32
4.1 Introduction	32
4.2 Definition of the Operator \mathcal{C} and Bilinear Forms	32
4.3 Discrete Harmonic Extension	34
4.4 The Coarse Problem	37
4.5 Local Problems	52

4.6	The Additive and Multiplicative Operators	56
4.7	The Case of $t=\infty$	57
4.8	Changes of Thickness t or the Lamé constants	59
4.9	Higher Order Falk-Tu Elements	59
4.10	Numerical Experiments	59
5	BDDC methods for the Reissner-Mindlin Plate	71
5.1	Introduction	71
5.2	Notation	71
5.3	BDDC Methods for MITC elements	72
5.4	BDDC Methods for Falk-Tu elements	75
	Bibliography	82

List of Figures

3.1	the MITC7 element.	27
3.2	the MITC9 element.	29
3.3	the Falk-Tu element with $k=2$	30
4.1	One subdomain and its vertices and edges.	37
4.2	3d plots of the θ vertex basis function $\theta_{1,v}^0$	38
4.3	Values of $w_{v_1}^0$ on the interface.	44
4.4	3d plots of the w vertex basis function w_v^0	45
4.5	Values of $\theta_{e_3}^0$ on the interface.	47
4.6	3d plots of the θ edge basis function θ_e^0	48
4.7	3d plots of the w edge basis function w_e^0	53
4.8	The condition number as a function of the number of subdomains without the w quadratic coarse basis functions.	61
4.9	The condition number as a function of the number of subdomains with the w quadratic coarse basis functions.	61
4.10	The condition number as a function of $\frac{H}{h}$ without the w quadratic coarse basis functions.	64
4.11	The condition number as a function of $\frac{H}{h}$ with the w quadratic coarse basis functions.	64
4.12	The condition number as a function of $\frac{H}{\delta}$ without the w quadratic coarse basis functions.	66
4.13	The condition number as a function of $\frac{H}{\delta}$ with the w quadratic coarse basis functions.	66
4.14	The condition number as a function of the number of subdomains with the w quadratic coarse basis functions.	68
4.15	The condition number as a function of $\frac{H}{h}$ with the w quadratic coarse basis functions.	69
4.16	The condition number as a function of $\frac{H}{\delta}$ with the w quadratic coarse basis functions.	70
5.1	Maximum eigenvalue as a function of $\frac{H}{h}$ for the extension lemma. . .	76
5.2	$\sqrt{\text{maximum eigenvalue}}$ as a function of $\frac{H}{h}$ for the edge lemma. . . .	78

5.3	Maximum eigenvalue of the preconditioned system as a function of the number of subdomains	80
5.4	$\sqrt{\text{maximum eigenvalue}}$ of the preconditioned system as a function of H/h	81
5.5	Iteration count of the preconditioned system as a function of H/h .	81

List of Tables

4.1	Results for $L = 1$, $\frac{H}{h} = 4$, $\frac{H}{\delta} = 4$, and decreasing $h = \frac{1}{n}$, and with an increasing number of subdomains $= \frac{n}{4} \times \frac{n}{4}$ without the w quadratic coarse basis functions.	60
4.2	Results for $L = 1$, $\frac{H}{h} = 4$, $\frac{H}{\delta} = 4$, and decreasing $h = \frac{1}{n}$, and with an increasing number of subdomains $= \frac{n}{4} \times \frac{n}{4}$ with the w quadratic coarse basis functions.	60
4.3	Results for $L = 1$, $\frac{H}{h} = 4$, $\frac{H}{\delta} = 4$, and decreasing $h = \frac{1}{n}$, and with an increasing number of subdomains $= \frac{n}{12} \times \frac{n}{12}$	62
4.4	Results for $L = 1$, $h = \frac{1}{n}$, $\frac{H}{\delta} = 4$, the number of subdomains 3×3 , and increasing $\frac{H}{h} = \frac{n}{3}$ without the w quadratic coarse basis functions.	63
4.5	Results for $L = 1$, $h = \frac{1}{n}$, $\frac{H}{\delta} = 4$, the number of subdomains 3×3 , and increasing $\frac{H}{h} = \frac{n}{3}$ with the w quadratic coarse basis functions.	63
4.6	Results for $h = \frac{1}{72}$, $\frac{H}{h} = 12$, and decreasing $\frac{H}{\delta} = 12, 6, 4, 3, 2.4, 2$ without the w quadratic coarse basis functions.	65
4.7	Results for $h = \frac{1}{72}$, $\frac{H}{h} = 12$, and decreasing $\frac{H}{\delta} = 12, 6, 4, 3, 2.4, 2$ with the w quadratic coarse basis functions.	65
4.8	Results for $L = 1$, $\frac{H}{h} = 4$, $\frac{H}{\delta} = 4$, decreasing $h = \frac{1}{n}$, and increasing the number of subdomains $= \frac{n}{4} \times \frac{n}{4}$ with the w quadratic coarse basis functions.	67
4.9	Results for $L = 1$, $h = \frac{1}{n}$, $\frac{H}{\delta} = 4$, the number of subdomains 3×3 , and increasing $\frac{H}{h} = \frac{n}{3}$ with the w quadratic coarse basis functions.	69
4.10	Results for $h = \frac{1}{72}$, $\frac{H}{h} = 12$, and decreasing $\frac{H}{\delta} = 12, 6, 4, 3, 2.4, 2$ with the w quadratic coarse basis functions.	70
5.1	Maximum of the generalized eigenvalues for $H = 1$, $h = \frac{1}{k}$, and increasing $\frac{H}{h} = k$ between two interior subdomains for the extension lemma.	76
5.2	Maximum of the generalized eigenvalues for $H = 1$, $h = \frac{1}{k}$, and increasing $\frac{H}{h} = k$ for the edge lemma.	77
5.3	Results for $L = 1$, $\frac{H}{h} = 4$, and with an increasing number of subdomains.	79

5.4 Results for $L = 1$, number of subdomains 4×4 , and with an increasing H/h 80

Chapter 1

Introduction

1.1 An Overview

When we solve an elliptic partial differential equation (PDE) numerically, we first need to discretize the problem using finite element, finite difference, or other methods. After discretization, we have a large sparse linear system to solve to get a numerical solution. Typically, accuracy of approximated solution from discrete methods depends on the mesh size, denoted by h . As the mesh size decreases, we can get a more exact numerical solution, but the linear system to solve becomes larger and more ill-conditioned. Therefore, we need to precondition the linear system so that the preconditioned system has a smaller condition number and converges to the solution faster when using Krylov space methods.

Domain decomposition methods give scalable and efficient preconditioners that can be used with Krylov space methods and parallel computers. In domain decomposition methods, we divide the original domain into many smaller subdomains so that we can solve a smaller linear system of each subdomain using direct solver separately. If we use only local solvers, information can be exchanged only between neighboring subdomains in each iteration. By also using a coarse solver, which has only few degrees of freedoms per subdomain, we can prevent the condition number of preconditioned system from increasing for many subdomain cases.

Domain decomposition methods can be categorized into two classes: overlapping Schwarz methods and iterative substructuring methods. In overlapping Schwarz methods, we use overlapping subdomains with an overlap δ and get better-conditioned methods with larger δ . In iterative substructuring methods, we reduce the space of unknowns to the space of interface unknowns by eliminating the unknowns in the interior of subdomains resulting in Schur complements. We will concentrate on BDDC (balancing domain decomposition methods by constraints) methods in this thesis.

We consider Reissner-Mindlin plate theory which has been developed to de-

scribe the behavior of a thin plate under exterior force. We describe the displacement of the plate by three variables: one displacement variable and two rotations, after a reduction of dimension, see subsection 3.2.1. If we use naive standard low order polynomial elements, the finite element model can suffer from locking problems. There are now many good finite elements developed on Reissner-Mindlin plate theory, which avoid this problem.

There are a number of studies which develop preconditioners for the Kirchhoff plate problem, see [13, 15, 14, 33, 39]. [33] and [39] can be extended to the Reissner-Mindlin plate problem for elements which are spectrally equivalent to Kirchhoff plate elements. For MITC element approximation of the Reissner-Mindlin plate problem, a BDDC method has also been developed, see [8].

In this dissertation, we develop overlapping Schwarz methods on Reissner-Mindlin plate theory by finding proper coarse basis functions. There is relation between the displacement variable and rotations, and we use this relation to get good coarse basis functions. We then modify overlapping Schwarz methods to a BDDC method using primal constraints of BDDC methods which are related to the coarse basis functions of the overlapping Schwarz methods. We developed methods which are independent of t for small t , quasi-optimal, and scalable.

We will first review some basic functional analysis tools, the conjugate gradient method and mixed finite element methods.

1.2 Functional Analysis Tools

1.2.1 Sobolev Spaces

We assume that Ω is a Lipschitz domain in \mathbb{R}^2 or \mathbb{R}^3 . $L^2(\Omega)$ is the space of real valued functions defined as

$$L^2(\Omega) = \left\{ u : \Omega \rightarrow \mathbb{R} \mid \int_{\Omega} u^2 d\mathbf{x} < \infty \right\}.$$

This is a Hilbert space with the inner product

$$(u, v)_{L^2(\Omega)} = \int_{\Omega} uv d\mathbf{x}$$

and an induced norm

$$\|u\|_{L^2(\Omega)}^2 = (u, u)_{L^2(\Omega)} = \int_{\Omega} u^2 d\mathbf{x}.$$

In the following when we say derivatives, they are weak derivatives as in [10, chapter 2.1]. $H^1(\Omega) \subset L^2(\Omega)$ is the space of real valued functions which have first

order weak derivatives and satisfies

$$\int_{\Omega} u^2 d\mathbf{x} < \infty \quad \text{and} \quad \int_{\Omega} \nabla u \cdot \nabla u d\mathbf{x} < \infty.$$

This is also a Hilbert space with the scaled norm

$$\|u\|_{H^1(\Omega)}^2 := \int_{\Omega} \nabla u \cdot \nabla u d\mathbf{x} + \frac{1}{H_{\Omega}^2} \int_{\Omega} u^2 d\mathbf{x}$$

where H_{Ω} is a diameter of the domain Ω ; this scaling factor is obtained by dilation from a region of unit diameter. The corresponding H^1 -seminorm is given by

$$|u|_{H^1(\Omega)}^2 = \int_{\Omega} \nabla u \cdot \nabla u d\mathbf{x}.$$

$H_0^1(\Omega)$ is the closure of $C_0^{\infty}(\Omega)$ in $H^1(\Omega)$ with respect to the H^1 -norm. In $H_0^1(\Omega)$, the H^1 -norm and H^1 -seminorm are equivalent.

Similarly, we define $H^2(\Omega)$ as the space with functions that have bounded L^2 norms and L^2 bounded first and second order derivatives.

We also define the divergence of a vector-valued function \mathbf{u} with two or three components by

$$\operatorname{div} \mathbf{u} := \nabla \cdot \mathbf{u} = \sum_{i=1}^n \frac{\partial u_i}{\partial x_i} \quad (1.1)$$

where u_i is the i -th component of \mathbf{u} . $\mathbf{H}(\operatorname{div}, \Omega) \subset L^2(\Omega)^n$ is the space with the inner product given by

$$(\mathbf{u}, \mathbf{v})_{\operatorname{div}, \Omega} = \int_{\Omega} \operatorname{div} \mathbf{u} \operatorname{div} \mathbf{v} d\mathbf{x} + \frac{1}{H_{\Omega}^2} \int_{\Omega} \mathbf{u} \cdot \mathbf{v} d\mathbf{x}.$$

We note that $H^1(\Omega)^n \subset \mathbf{H}(\operatorname{div}, \Omega)$. We define the curl of the scalar-valued function p and the rotation of the vector-valued function \mathbf{u} with two components by

$$\operatorname{curl} p := \begin{pmatrix} \frac{\partial p}{\partial x_2} \\ -\frac{\partial p}{\partial x_1} \end{pmatrix}, \quad \operatorname{rot} \mathbf{u} := \frac{\partial u_2}{\partial x_1} - \frac{\partial u_1}{\partial x_2}. \quad (1.2)$$

Similar to $\mathbf{H}(\operatorname{div}, \Omega)$, $\mathbf{H}(\operatorname{rot}, \Omega) \subset (L^2(\Omega))^2$ is the space with the inner product

$$(\mathbf{u}, \mathbf{v})_{\operatorname{rot}, \Omega} = \int_{\Omega} \operatorname{rot} \mathbf{u} \operatorname{rot} \mathbf{v} d\mathbf{x} + \frac{1}{H_{\Omega}^2} \int_{\Omega} \mathbf{u} \cdot \mathbf{v} d\mathbf{x}.$$

1.2.2 Trace and Extension Theorems

Let Ω be a Lipschitz domain in \mathbb{R}^n , $n = 2, 3$, and Γ be an open subset of $\partial\Omega$ with non-vanishing $(n - 1)$ -dimensional measure.

We define the $H^{1/2}(\Gamma)$ -seminorm by

$$|u|_{H^{1/2}(\Gamma)}^2 = \int_{\Gamma} \int_{\Gamma} \frac{|u(x) - u(y)|^2}{|x - y|^n} dx dy$$

where n is the dimension of Ω . With the $H^{1/2}(\Gamma)$ -norm defined by

$$\|u\|_{H^{1/2}(\Gamma)}^2 = |u|_{H^{1/2}(\Gamma)}^2 + \frac{1}{H_{\Gamma}} \|u\|_{L^2(\Gamma)}^2,$$

$H^{1/2}(\Gamma)$ is the space of functions which have bounded $H^{1/2}(\Gamma)$ -norms.

Lemma 1 (Trace theorem). *Let Ω be a Lipschitz domain. Then, there is a bounded linear operator $\gamma_0 : H^1(\Omega) \rightarrow H^{1/2}(\partial\Omega)$ such that $\gamma_0 u = u$ on $\partial\Omega$ if u is continuously differentiable.*

We also have the extension theorem.

Lemma 2. *Let Ω be a Lipschitz domain. Then, there exists a continuous lifting operator $\mathcal{R}_0 : H^{1/2}(\partial\Omega) \rightarrow H^1(\Omega)$ such that $\gamma_0(\mathcal{R}_0 u) = u$, $u \in H^{1/2}(\partial\Omega)$.*

1.2.3 Poincaré and Friedrichs Inequalities

In domain decomposition theory, Poincaré and Friedrichs inequalities are powerful tools for the analysis. See [41] for a proof of the following theorem.

Theorem 1. *Let $\Omega \subset \mathbb{R}^n$ be a bounded Lipschitz domain and let $f_i, i = 1, \dots, L$, be linear functionals in $H^1(\Omega)$, such that, if v is constant in Ω ,*

$$\sum_{i=1}^L |f_i(v)|^2 = 0 \quad \leftrightarrow \quad v = 0.$$

Then, there exist constants, depending only on Ω and the functionals f_i , such that, for $u \in H^1(\Omega)$,

$$\|u\|_{L^2(\Omega)}^2 \leq C_1 |u|_{H^1(\Omega)}^2 + C_2 \sum_{i=1}^L |f_i(u)|^2.$$

From Theorem 1 and simple *scaling arguments*, we have Poincaré and Friedrichs inequalities which will be used many times in our proofs, cf. [47, chapter A.4].

Lemma 3 (Poincaré and Friedrichs Inequalities). *Let $\Omega \subset \mathbb{R}^n$ be a bounded Lipschitz domain with diameter H . Then, there exists a constant C_1 , that depends only on the shape of Ω but not on its size, such that*

$$\|u - \bar{u}\|_{L^2(\Omega)}^2 \leq C_1 H_\Omega^2 |u|_{H^1(\Omega)}^2$$

for $\forall u \in H^1(\Omega)$. Here \bar{u} is the mean of u over Ω . Similarly, if $\Gamma \subset \partial\Omega$ has nonvanishing $(n-1)$ -dimensional measure and a diameter of order H_Ω , then

$$\|u\|_{L^2(\Omega)}^2 \leq C_2 H_\Omega^2 |u|_{H^1(\Omega)}^2 + C_3 H_\Omega \|u\|_{L^2(\Gamma)}^2$$

for $\forall u \in H^1(\Omega)$.

1.3 The Conjugate Gradient Method

We can solve a sparse linear system using Krylov space methods. Especially if we solve a symmetric positive definite problem

$$Au = b,$$

where A is a symmetric positive definite matrix, we can use the Conjugate Gradient method. For more detail, see [47, chapter C] and [48]. The Conjugate Gradient method is given as follows:

1. Initialize: $r^0 = b - Au^0$
2. Iterate $k = 1, 2, \dots$ until convergence

$$\beta^k = \langle r^{k-1}, r^{k-1} \rangle / \langle r^{k-2}, r^{k-2} \rangle \quad [\beta^1 = 0]$$

$$p^k = r^{k-1} + \beta^k p^{k-1} \quad [p^1 = r^0]$$

$$\alpha^k = \langle r^{k-1}, r^{k-1} \rangle / \langle p^k, Ap^k \rangle$$

$$u^k = u^{k-1} + \alpha^k p^k$$

$$r^k = r^{k-1} - \alpha^k Ap^k$$

We see that in this iterative method A is used only in a matrix-vector multiplication and we do not need to construct A explicitly.

We define the A -norm as follows:

$$\|x\|_A = \sqrt{x^T A x}.$$

Then, we have the following convergence lemma for the Conjugate Gradient method.

Lemma 4. *Let A be symmetric and positive definite. Then, the iterate u^k of the Conjugate Gradient method minimizes $\|u_* - u\|_A$ over the space*

$$u^0 + \text{span}\{A^i r^0, i = 0, 1, \dots, k-1\}$$

where u_* is the solution of $Au = b$ and $r^0 = b - Au^0$.

The Conjugate Gradient method also satisfies the error bound

$$\|u^k - u_*\|_A \leq 2 \left(\frac{\sqrt{\kappa_2(A)} - 1}{\sqrt{\kappa_2(A)} + 1} \right)^k \|u^0 - u_*\|_A$$

where $\kappa_2(A)$ is the spectral condition number of A .

As Lemma 4 suggests, the convergence rate of the Conjugate Gradient method depends greatly on the condition number of A . If we can find a good preconditioner M , a symmetric positive definite matrix with $\kappa_2(M^{-1}A) \ll \kappa_2(A)$, we can consider the modified linear system, which has a symmetric operator,

$$M^{-1/2}AM^{-1/2}v = M^{-1/2}b, \quad v = M^{1/2}u.$$

The algorithm of the preconditioned Conjugate Gradient method is given as follows:

1. Initialize: $r^0 = b - Au^0$
2. Iterate $k = 1, 2, \dots$ until convergence

Precondition: $z^{k-1} = M^{-1}r^{k-1}$

$$\beta^k = \langle z^{k-1}, r^{k-1} \rangle / \langle z^{k-2}, r^{k-2} \rangle \quad [\beta^1 = 0]$$

$$p^k = z^{k-1} + \beta^k p^{k-1} \quad [p^1 = z^0]$$

$$\alpha^k = \langle z^{k-1}, r^{k-1} \rangle / \langle p^k, Ap^k \rangle$$

$$u^k = u^{k-1} + \alpha^k p^k$$

$$r^k = r^{k-1} - \alpha^k Ap^k$$

We have the following convergence lemma.

Lemma 5. *Let A and M be symmetric and positive definite. Then, the preconditioned Conjugate Gradient method satisfies*

$$\|u^k - u_*\|_A \leq 2 \left(\frac{\sqrt{\kappa_2(M^{-1}A)} - 1}{\sqrt{\kappa_2(M^{-1}A)} + 1} \right)^k \|u^0 - u_*\|_A.$$

Therefore, we need to find M which is a good approximation to A and is computationally inexpensive when designing domain decomposition methods.

We can compute an approximation of the condition number of A when we use the Conjugate Gradient method to solve the system. For more detail, see [30] and [43]. From the coefficients of the Conjugate Gradient method, we can construct the following symmetric tridiagonal matrix,

$$J^{(k)} = \begin{pmatrix} 1/\alpha_1 & -\sqrt{\beta_1}/\alpha_1 & \cdots & \cdots \\ -\sqrt{\beta_1}/\alpha_1 & (1/\alpha_2 + \beta_1/\alpha_1) & -\sqrt{\beta_2}/\alpha_2 & \cdots \\ \cdots & \cdots & \cdots & \cdots \end{pmatrix}. \quad (1.3)$$

Then, $J^{(k)}$ is a matrix representation of the restriction of the matrix A to the space $\text{span}\{A^i r^0, i = 0, 1, \dots, k-1\}$. An approximation of the condition number of A can be obtained from the condition number of $J^{(k)}$. The eigenvalues of $J^{(k)}$ interlace those of $J^{(k+1)}$ and an improved estimate of the condition number can be obtained in each step. Extreme eigenvalues of $J^{(k)}$ typically converge quite rapidly.

1.4 Mixed Finite Element Methods

In this section, we consider abstract mixed finite element methods for saddle point problems. For more details, see [9, pp.34-41] and [10].

Let X and M be two Hilbert spaces and suppose that $a(\cdot, \cdot)$ and $b(\cdot, \cdot)$ are two continuous bilinear forms on $X \times X$ and $X \times M$ such that

$$\begin{aligned} |a(u, v)| &\leq \|a\| \|u\|_X \|v\|_X, \quad \forall u \in X, \forall v \in X, \\ |b(v, \gamma)| &\leq \|b\| \|v\|_X \|\gamma\|_M, \quad \forall v \in X, \forall \gamma \in M. \end{aligned}$$

We consider the solution of the following saddle point problem:

Given $f \in X'$ and $g \in M'$, find $(u, \gamma) \in X \times M$ such that

$$\begin{aligned} a(u, v) + b(v, \gamma) &= \langle f, v \rangle, \quad \forall v \in X, \\ b(u, \mu) &= \langle g, \mu \rangle, \quad \forall \mu \in M. \end{aligned} \quad (1.4)$$

We have the following theorem on the existence, uniqueness and stability of the saddle point problem. For a proof, see [10, chapter 3.4].

Theorem 2. *If there exists a constant $\alpha > 0$ such that*

$$a(v, v) \geq \alpha \|v\|_X^2, \quad \forall v \in V := \{v \in X \mid b(v, \mu) = 0, \forall \mu \in M\}, \quad (1.5)$$

and $\beta > 0$ such that

$$\inf_{\mu \in M} \sup_{v \in X} \frac{b(v, \mu)}{\|v\|_X \|\mu\|_M} \geq \beta, \quad (1.6)$$

then there exists a unique solution (u, γ) to (1.4) and the norms of the solution satisfy

$$\begin{aligned} \|u\|_X &\leq \alpha^{-1} \|f\|_{X'} + \beta^{-1} \left(1 + \frac{\|a\|}{\alpha}\right) \|g\|_{M'}, \\ \|\gamma\|_M &\leq \beta^{-1} \left(1 + \frac{\|a\|}{\alpha}\right) \|f\|_{X'} + \beta^{-1} \left(1 + \frac{\|a\|}{\alpha}\right) \frac{\|a\|}{\beta} \|g\|_{M'}. \end{aligned} \quad (1.7)$$

(1.6) is called the inf-sup condition and the assumption of Theorem 2 is called the *Babuška-Brezzi condition*. Next, we consider two finite element spaces $X^h \subset X$ and $M^h \subset M$. We then have the discrete saddle point problem as follows:

Find $(u^h, \gamma^h) \in X^h \times M^h$ such that

$$a(u^h, v^h) + b(v^h, \gamma^h) = \langle f, v^h \rangle, \quad \forall v^h \in X^h, \quad (1.8)$$

$$b(u^h, \mu^h) = \langle g, \mu^h \rangle \quad \forall \mu^h \in M^h. \quad (1.9)$$

For the error bound of finite element methods, we have the following theorem, cf. [10, chapter 4.3].

Theorem 3. *Suppose the hypotheses of Theorem 2 hold and suppose X_h and M_h satisfy the Babuška-Brezzi condition with $\alpha > 0$ and $\beta > 0$ which are independent of h . Then, we have*

$$\|u - u_h\|_X + \|\gamma - \gamma_h\|_M \leq C \left(\inf_{v_h \in X_h} \|u - v_h\|_X + \inf_{\mu_h \in M_h} \|\gamma - \mu_h\|_M \right). \quad (1.10)$$

In some cases, such as in Reissner-Mindlin plate theory, we need to consider saddle point problems with penalty terms. Suppose that in addition to the bilinear forms a and b , we have

$$c : M \times M \longrightarrow \mathbb{R}, \quad c(\mu, \mu) \geq 0, \quad \forall \mu \in M,$$

which is a continuous bilinear form on $M \times M$. We also will use a parameter t which is a small real number. Saddle point problem with the penalty term has the following form:

Find $(u, \gamma) \in X \times M$ such that

$$\begin{aligned} a(u, v) + b(v, \gamma) &= \langle f, v \rangle, \quad \forall v \in X, \\ b(u, \mu) - t^2 c(\gamma, \mu) &= \langle g, \mu \rangle, \quad \forall \mu \in M. \end{aligned} \quad (1.11)$$

In this problem, we need the ellipticity of a on the entire space X , rather than just on the kernel V to get the stability of the solution. If we have the ellipticity and an inf-sup condition, we then have the uniform stability and error bounds as in Theorem 2 and 3 for all $0 \leq t \leq 1$.

Chapter 2

Domain Decomposition Methods and an Abstract Theory

2.1 Introduction

Overlapping Schwarz methods have been developed to solve numerical PDE efficiently. One level additive overlapping methods were originally introduced by Matsokin and Nepomnyaschikh [40] and Nepomnyaschikh [42]. They were improved to more powerful two level overlapping methods in [25, 26, 27] and other related papers. Modern overlapping methods using Schur complements were introduced in [23] and [24]. They have been applied successfully in many fields other than for the Poisson problem. With a large overlap, we can get a small condition number for the overlapping methods.

The traditional overlapping methods are not suitable for the case where we have jumps of the coefficients. Such a problem can have a bilinear form

$$\int_{\Omega} \rho(x) \nabla u \cdot \nabla v \, dx$$

where $\rho(x)$ can vary over the domain. With proper scaling, iterative substructuring methods can handle the jumps of coefficients successfully and the condition number of operators do not depend on the change of coefficients.

Among iterative substructuring methods, the FETI-DP and BDDC (Balancing Domain Decomposition by Constraints) methods are well known. In this thesis, we mainly consider the BDDC methods. The BDDC methods were first introduced by Dohrmann in [22] as a variant of the Balancing Neumann-Neumann methods with an additional coarse level solver. It has now been applied in other fields as in [34] and three-level BDDC methods have been introduced in [49] and [50].

In this chapter, we introduce the abstract Schwarz theory. We then introduce the overlapping Schwarz methods and the BDDC methods for the Poisson problem

and give condition number bounds for them.

2.2 Abstract Theory of Schwarz Methods

We consider a finite dimensional Hilbert space W . Given a symmetric, positive definite bilinear form $a(\cdot, \cdot)$, we have a matrix representation given by A which is a symmetric, positive definite matrix; see [47, appendix B]. Similarly, we can express an element $f \in W'$ as a vector. We then have to find $u \in W$ such that

$$Au = f. \quad (2.1)$$

We consider a family of spaces $W^{(i)}, i = 0, \dots, N$ with interpolation operators

$$R^{(i)T} : W^{(i)} \rightarrow W, \quad i = 0, \dots, N,$$

and assume that W has the following decomposition

$$W = \sum_{i=0}^N R^{(i)T} W^{(i)}. \quad (2.2)$$

We next consider local symmetric, positive definite stiffness matrices

$$\tilde{A}^{(i)} : W^{(i)} \rightarrow W^{(i)}, \quad i = 0, \dots, N,$$

with corresponding local bilinear forms $a^{(i)}(\cdot, \cdot)$. If $\tilde{A}^{(i)} = R^{(i)} A R^{(i)T}$, we say that we use *exact solvers*. We then define projection-like operators

$$P_i := R^{(i)T} \tilde{A}^{(i)-1} R^{(i)} A : W \rightarrow R^{(i)T} W^{(i)} \subset W, \quad i = 0, \dots, N, \quad (2.3)$$

and if we use exact solvers, they are projections since

$$P_i^2 = R^{(i)T} \tilde{A}^{(i)-1} R^{(i)} A R^{(i)T} \tilde{A}^{(i)-1} R^{(i)} A = R^{(i)T} \tilde{A}^{(i)-1} \tilde{A}^{(i)} \tilde{A}^{(i)-1} R^{(i)} = P_i. \quad (2.4)$$

The additive Schwarz operator is defined by

$$P_{ad} = \sum_{i=0}^N P_i, \quad (2.5)$$

and the symmetric multiplicative Schwarz operator by

$$P_{mu} = I - E_{mu}, \quad (2.6)$$

where the multiplicative error propagation operator E_{mu} is defined by

$$E_{mu} = (I - P_N) \cdots (I - P_1)(I - P_0)(I - P_1) \cdots (I - P_N). \quad (2.7)$$

For bounds of the condition numbers of the Schwarz operators, we need some assumptions, cf. [47, chapter 2.3].

Assumption 1. (Stable Decomposition) A decomposition (2.2) is stable, i.e.,

$$\sum_{i=0}^N u^{(i)T} \tilde{A}^{(i)} u^{(i)} \leq C_0^2 u^T A u. \quad (2.8)$$

The minimum eigenvalue of the additive Schwarz operator P_{ad} is bounded below by C_0^{-2} , see [47, Lemma 2.5].

Assumption 2. There exist constants $0 \leq \epsilon_{ij} \leq 1, 1 \leq i, j \leq N$, such that

$$|a(R^{(i)T} u^{(i)}, R^{(j)T} u^{(j)})| \leq \epsilon_{ij} a(R^{(i)T} u^{(i)}, R^{(i)T} u^{(i)})^{1/2} a(R^{(j)T} u^{(j)}, R^{(j)T} u^{(j)})^{1/2}$$

for $u^{(i)} \in W^{(i)}$ and $u^{(j)} \in W^{(j)}$. We will denote the spectral radius of $\mathcal{E} = \{\epsilon_{ij}\}$ by $\rho(\mathcal{E})$.

For a decomposition of W , we can color the subspaces $\{W^{(i)}, i = 0, \dots, N\}$ such that if two subspaces $W^{(j)}$ and $W^{(k)}$ have the same color, then they are orthogonal, i.e.,

$$a(R^{(j)T} u^{(j)}, R^{(k)T} u^{(k)}) = 0, \quad u^{(j)} \in W^{(j)}, \quad u^{(k)} \in W^{(k)}.$$

We assume that we color the subspaces using N^c colors and can then show

$$\rho(\mathcal{E}) \leq N^c. \quad (2.9)$$

Assumption 3. There exists $\omega > 0$, such that

$$a(R^{(i)T} u^{(i)}, R^{(i)T} u^{(i)}) \leq \omega \tilde{a}^{(i)}(u^{(i)}, u^{(i)}), \quad u^{(i)} \in \text{range}(\tilde{A}^{(i)-1} R^{(i)} A), \quad 0 \leq i \leq N.$$

Basic convergence theorems on the additive and multiplicative Schwarz operators can be found in [47, chapter 2.3]

Theorem 4. Let Assumptions 1, 2, and 3 be satisfied. Then, we have the following bounds on the additive Schwarz operator and the multiplicative error propagation operator E_{mu} :

$$\begin{aligned} \kappa(P_{ad}) &\leq C_0^2 \omega (\rho(\mathcal{E}) + 1), \\ \|E_{mu}\|_a^2 &= \|I - P_{mu}\|_a^2 \leq 1 - \frac{2 - \omega}{(8\rho(\mathcal{E})^2 + 1)C_0^2} < 1, \quad \text{if } 0 < \omega < 2. \end{aligned}$$

2.3 Problem Setting

In this chapter, we mainly consider second order scalar elliptic problems on a bounded domain $\Omega \subset \mathbb{R}^n, n = 2, 3$. $\partial\Omega$ is the boundary of Ω and we impose

homogenous Dirichlet boundary conditions on $\partial\Omega$. The problem is to find $u \in H_0^1(\Omega)$ such that

$$\int_{\Omega} \rho(x) \nabla u \cdot \nabla v \, dx = \int_{\Omega} f v \, d\mathbf{x}, \quad \forall v \in H_0^1(\Omega). \quad (2.10)$$

Here we assume that there exists a constant ρ_0 such that $\rho(x) \geq \rho_0 > 0$.

Let \mathcal{T}_H be a shape-regular coarse triangulation of Ω . We decompose Ω into N nonoverlapping subdomains Ω_i , $i = 1, \dots, N$, with diameters H_i and $H = \max_i \{H_i\}$. We assume that each subdomain Ω_i is the union of elements of \mathcal{T}_H and that the number of such elements in Ω_i is uniformly bounded. If $\partial\Omega_i \cap \partial\Omega = \emptyset$, Ω_i is called a floating subdomain.

We also have a fine quasi uniform triangulation of each subdomain Ω_i with mesh size h_i . We denote $\max_i \{H_i/h_i\}$ by H/h . We assume that $\rho(x)$ is constant in each subdomain Ω_i and denote its value by ρ_i .

The finite element nodes on the boundaries of neighboring subdomains should match across the interface $\Gamma := \cup_{i \neq j} \partial\Omega_i \cap \partial\Omega_j$. We denote the space of finite element nodes on the interface Γ by Γ_h . We also define Γ_i , the interface on subdomain Ω_i , by $\Gamma_i := \Gamma \cap \partial\Omega_i$, and denote the space of finite element nodes on Γ_i by $\Gamma_{i,h}$. The interface can be partitioned into *faces*, *edges* and *vertices* in \mathbb{R}^3 and into *edges* and *vertices* in \mathbb{R}^2 ; see [47, chapter 4.2] for more detail.

We also define local bilinear forms and linear functionals by

$$a^{(i)}(u, v) := \int_{\Omega_i} \rho_i \nabla u \cdot \nabla v \, d\mathbf{x}, \quad f^{(i)}(v) = \int_{\Omega_i} f v \, d\mathbf{x}, \quad i = 1, \dots, N. \quad (2.11)$$

2.4 Notation

In the following, $W^{(i)}$ is the vector space of values at the nodes in $\overline{\Omega}_i$. Each $W^{(i)}$ can be decomposed into the vector space of subdomain interior nodal values and the vector space of subdomain interface nodal values, $W^{(i)} = W_I^{(i)} \oplus W_{\Gamma}^{(i)}$. $W_{\Gamma}^{(i)}$ can be further decomposed into the vector space of primal nodal values and the vector space of dual nodal values, $W_{\Gamma}^{(i)} = W_{\Pi}^{(i)} \oplus W_{\Delta}^{(i)}$. Terminologies of primal nodal values and dual nodal values came from the FETI-DP methods. In FETI-DP methods, we allow discontinuity for dual nodal values and ensure the continuity using Lagrange multiplier. We choose few degrees as primal values on each subdomain and the remaining interface nodal values are dual nodal values. For more detail, see [35].

Associated product spaces, which allow discontinuity across the interface, are

denoted by

$$\begin{aligned} W &:= \prod_{i=1}^N W^{(i)}, & W_I &:= \prod_{i=1}^N W_I^{(i)}, & W_\Gamma &:= \prod_{i=1}^N W_\Gamma^{(i)}, \\ W_\Pi &:= \prod_{i=1}^N W_\Pi^{(i)}, & \text{and} & & W_\Delta &:= \prod_{i=1}^N W_\Delta^{(i)}. \end{aligned}$$

Therefore, we have $W = W_I \oplus W_\Gamma$ and $W_\Gamma = W_\Pi \oplus W_\Delta$.

The finite element solutions are continuous across the interface and we denote the continuous subspace of W_Γ by \widehat{W}_Γ and the continuous subspace of W by \widehat{W} , respectively. For BDDC methods, we need a larger subspace $\widetilde{W}_\Gamma \subset W_\Gamma$, which can be written by

$$\widetilde{W}_\Gamma := W_\Delta \oplus \widehat{W}_\Pi = \left(\prod_{i=1}^N W_\Delta^{(i)} \right) \oplus \widehat{W}_\Pi,$$

where \widehat{W}_Π is the continuous, coarse-level, primal variable subspace. We will always assume that the basis has been changed so that each primal constraint corresponds to an explicit degree of freedom and W_Δ consists of functions with zero values at the primal degrees of freedom.

We define several restriction and extension operators. $R_{\Gamma\Delta}$ and $R_{\Gamma\Pi}$ are the restriction operators from the space \widetilde{W}_Γ onto W_Δ and \widehat{W}_Π , respectively. For each subdomain component, $R_\Delta^{(i)} : W_\Delta \rightarrow W_\Delta^{(i)}$, and $R_\Pi^{(i)} : \widehat{W}_\Pi \rightarrow W_\Pi^{(i)}$ map global interface vectors to their components on Γ_i , respectively. $R_\Gamma^{(i)} : \widehat{W}_\Gamma \rightarrow W_\Gamma^{(i)}$, $\widehat{R}_\Pi : \widehat{W}_\Gamma \rightarrow \widehat{W}_\Pi$ and $\widehat{R}_\Delta^{(i)} : \widehat{W}_\Gamma \rightarrow W_\Delta^{(i)}$ map \widehat{W}_Γ to proper components. $R_\Gamma : \widehat{W}_\Gamma \rightarrow W_\Gamma$ is the direct sum of $R_\Gamma^{(i)}$ and $\widetilde{R}_\Gamma : \widehat{W}_\Gamma \rightarrow \widetilde{W}_\Gamma$ is the direct sum of \widehat{R}_Π and $\widehat{R}_\Delta^{(i)}$.

Now we need to define positive scaling factors

$$\delta_i^\dagger(x) := \frac{\rho_i^\gamma}{\sum_{j \in \mathcal{N}_x} \rho_j^\gamma}, \quad x \in \Gamma_{i,h}$$

for $\gamma \in [1/2, \infty)$. Here \mathcal{N}_x is the set of indices of the subdomains which have x on their boundaries. The scaling factors give us a partition of unity:

$$\sum_{j \in \mathcal{N}_x} \delta_j^\dagger(x) = 1, \quad x \in \Gamma_h.$$

Let $D^{(i)}$ be the diagonal matrix with the elements $\delta_i^\dagger(x)$ corresponding to the node $x \in \Gamma_{i,h}$.

By multiplying each row of $R_\Gamma^{(i)}$, $R_\Delta^{(i)}$, and $\widehat{R}_\Delta^{(i)}$ with the corresponding $\delta_i^\dagger(x)$, we can define $R_{D,\Gamma}^{(i)}$, $R_{D,\Delta}^{(i)}$, and $\widehat{R}_{D,\Delta}^{(i)}$, respectively. The scaled restriction operators

$R_{D,\Gamma}$ and $R_{D,\Delta}$ are the direct sums of $R_{D,\Gamma}^{(i)}$ and $R_{D,\Delta}^{(i)}$, respectively. $\widetilde{R}_{D,\Gamma}$ is the direct sum of $\widehat{R}_{\Pi}^{(i)}$ and $\widehat{R}_{D,\Delta}^{(i)}$. From these definitions, we see that

$$R_{\Gamma}^T R_{D,\Gamma} = R_{D,\Gamma}^T R_{\Gamma} = I, \quad \widetilde{R}_{\Gamma}^T \widetilde{R}_{D,\Gamma} = \widetilde{R}_{D,\Gamma}^T \widetilde{R}_{\Gamma} = I. \quad (2.12)$$

2.5 Schur Complement Systems and Discrete Harmonic Extensions

We can rewrite $A^{(i)}$ with respect to interface and interior basis functions of $A^{(i)}$ and consider

$$\begin{bmatrix} A_{II}^{(i)} & A_{I\Gamma}^{(i)} \\ A_{\Gamma I}^{(i)} & A_{\Gamma\Gamma}^{(i)} \end{bmatrix} \begin{bmatrix} u_I^{(i)} \\ u_{\Gamma}^{(i)} \end{bmatrix} = \begin{bmatrix} 0 \\ f_{\Gamma}^{(i)} \end{bmatrix}.$$

Given $u_{\Gamma}^{(i)}$, we can calculate the interior values by solving

$$A_{II}^{(i)} u_I^{(i)} + A_{I\Gamma}^{(i)} u_{\Gamma}^{(i)} = 0. \quad (2.13)$$

This is a discrete harmonic function on Ω_i , see [47, chapter 4]. We use the notation $u^{(i)} := \mathcal{H}_i(u_{\Gamma}^{(i)})$ and call \mathcal{H}_i the discrete harmonic extension operator into Ω_i . We denote the piecewise discrete harmonic extension of u_{Γ} to the entire domain Ω by $\mathcal{H}(u_{\Gamma})$.

The related Schur complements are written as

$$S^{(i)} = A_{\Gamma\Gamma}^{(i)} - A_{\Gamma I}^{(i)} A_{II}^{(i)-1} A_{I\Gamma}^{(i)T}, \quad i = 1, \dots, N. \quad (2.14)$$

S is the direct sum of the $S^{(i)}$ on the product space W_{Γ} . Note that S is singular if there are any floating subdomains. Let $\widehat{S} := \sum_{i=1}^N R_{\Gamma}^{(i)T} S^{(i)} R_{\Gamma}^{(i)}$ and let

$$\widetilde{S} := \sum_{i=1}^N \begin{bmatrix} R_{\Gamma\Pi}^T R_{\Pi}^{(i)T} & R_{\Gamma\Delta}^T R_{\Delta}^{(i)T} \end{bmatrix} S^{(i)} \begin{bmatrix} R_{\Pi}^{(i)} R_{\Gamma\Pi} \\ R_{\Delta}^{(i)} R_{\Gamma\Delta} \end{bmatrix}. \quad (2.15)$$

They are Schur complements restricted to \widehat{W}_{Γ} and \widetilde{W}_{Γ} , respectively.

We have the following lemma on the discrete harmonic functions.

Lemma 6. *Let $u_{\Gamma}^{(i)}$ be the restriction of a finite element function u to $\partial\Omega_i \cap \Gamma$. Then, the discrete harmonic extension $u^{(i)} = \mathcal{H}_i(u_{\Gamma}^{(i)})$ of $u_{\Gamma}^{(i)}$ into Ω_i satisfies*

$$u^{(i)T} A^{(i)} u^{(i)} = \min_{v^{(i)}|_{\partial\Omega_i \cap \Gamma} = u_{\Gamma}^{(i)}} v^{(i)T} A^{(i)} v^{(i)}$$

and

$$u_{\Gamma}^{(i)T} S^{(i)} u_{\Gamma}^{(i)} = u^{(i)T} A^{(i)} u^{(i)}.$$

Analogously, if u_Γ is the restriction of a finite element function to Γ , the piecewise discrete harmonic extension $u = \mathcal{H}(u_\Gamma)$ of u_Γ into the interior of the subdomain satisfies

$$u^T Au = \min_{v|_\Gamma = u_\Gamma} v^T Av$$

and

$$u_\Gamma^T \widehat{S} u_\Gamma = u^T Au.$$

In practice, we do not need to calculate the Schur complement explicitly. The action of $S^{(i)}$ or $S^{(i)-1}$ can be calculated by solving proper Dirichlet or Neumann problems on Ω_i .

We can obtain the following reduced global problem on the interface by removing the interior part:

$$\widehat{S}_\Gamma u_\Gamma = g_\Gamma, \tag{2.16}$$

with

$$g_\Gamma = \sum_{i=1}^N R_\Gamma^{(i)T} \left(f_\Gamma^{(i)} - A_{\Gamma I}^{(i)} A_{II}^{(i)-1} f_I^{(i)} \right).$$

2.6 Overlapping Schwarz Methods

We present modern overlapping Schwarz methods which use Schur complements rather than classic overlapping Schwarz methods as in [23] and [24].

In this section, we assume that $\rho(x) \equiv 1$. We now extend each subdomain Ω_i to a larger region Ω'_i such that Ω'_i does not cut through any fine elements. This can be done by repeatedly adding a layer of elements. We assume that for $i = 1, \dots, N$, there exists $\delta_i > 0$, such that, if x belongs to Ω'_i , then

$$\text{dist}(x, \partial\Omega'_j \setminus \partial\Omega) \geq \delta_i$$

for a suitable $j = j(x)$, possibly equal to i , with $x \in \Omega'_j$. We denote the maximum of $\frac{H_i}{\delta_i}$ by

$$\frac{H}{\delta} := \max_i \left\{ \frac{H_i}{\delta_i} \right\}.$$

We also assume that the $\{\Omega'_i\}$ can be colored using at most N^c colors as explained in section 2.2. There is a partition of unity given by family of functions related to the overlapping subdomains. For a proof, we refer to [47, chapter 3.2] and [16, Lem. 2.4].

Lemma 7 (Partition of Unity). *Let $\{\Omega'_i\}$ be an overlapping partition with the overlap δ_i . Then, there exists a family of nonnegative functions in $W^{1,\infty}(\Omega)$, $\{\chi_i, 1 \leq$*

$i \leq N\}$, such that

$$\begin{aligned} \chi_i &= 0 \text{ on } \Omega \setminus \Omega_i \\ \sum_{i=1}^N \chi_i &= 1 \text{ on } \overline{\Omega} \\ \|\nabla \chi_i\|_{L^\infty} &\leq C\delta_i^{-1} \end{aligned}$$

where C is a constant independent of the δ_i and the H_i .

We also use a coarse space $W_0 \subset \widehat{W}$ of functions which are linear on the interface and discrete harmonic in each subdomain. The functions in W_0 have degrees of freedom at the subdomain vertices only. $R^{0T} : W_0 \rightarrow \widehat{W}$ is the matrix with columns representing the basis functions of W_0 .

Let $B(\Omega'_i)$ be the union of the nonoverlapping subdomains which intersect Ω'_i . We then have the following lemma related to the stable decomposition of Assumption 1.

Lemma 8. *For $u \in \widehat{W}$, there exists $u_0 \in W_0$ such that*

$$\|u - u_0\|_{L^2(\Omega_i)} \leq CH|u|_{H^1(B(\Omega'_i))}, \quad (2.17)$$

$$|u_0|_{H^1(\Omega_i)} \leq C|u|_{H^1(B(\Omega'_i))}. \quad (2.18)$$

The local spaces are the finite element spaces of functions that are piecewise linear on the fine meshes and vanish on the boundaries of the extended subdomain, Ω'_i :

$$W^{(i)} := \{u \in H_0^1(\Omega'_i) \mid u|_K \in P_1, K \in \mathcal{T}_i\} \subset \widehat{W}.$$

The local interpolators $R^{(i)T} : W^{(i)} \rightarrow \widehat{W}$ extend functions in $W^{(i)}$ by zero to the whole of Ω .

Given $\delta_i > 0$, let $\Omega_{i,\delta_i} \subset \Omega'_i$ be the set of points that are within a distance δ of $\partial\Omega'_i \setminus \partial\Omega$. We will need to use [47, lemma 3.10].

Lemma 9. *There exists a constant C such that, for $u \in H^1(\Omega'_i)$,*

$$\begin{aligned} \|u\|_{L^2(\Omega_{i,\delta_i})}^2 &\leq C\delta_i^2 \left(1 + \frac{H_i}{\delta_i}\right) \|u\|_{H^1(\Omega'_i)}^2 \\ &\leq C\delta_i^2 \left(1 + \frac{H_i}{\delta_i}\right) \|u\|_{H^1(B(\Omega'_i))}^2. \end{aligned}$$

We then define the overlapping additive preconditioned operator P_{ad} . We can prove a bound for the condition number of P_{ad} , refer [47, chapter 3.6].

Theorem 5. *The condition number of the additive Schwarz operator satisfies*

$$\kappa(P_{ad}) \leq C \left(1 + \frac{H}{\delta} \right)$$

where C depends on N^c , but is independent of h , H , and δ .

2.7 BDDC Methods

2.7.1 Algorithm

We consider the continuous space of interface nodal values, \widehat{W}_Γ , in BDDC methods to solve the reduced problem (2.16). Therefore, all functions are defined on interface only.

In BDDC methods, we need to choose the primal variables. We can choose \widehat{W}_Π to be spanned by vertex nodal finite element basis functions and edge cut-off functions of all the edges of Γ . An edge cut-off function is a piecewise linear function defined on the edge and has values 1 at all interface nodes except at the two ends of the edge where it vanishes. The local subspace $W_\Delta^{(i)}$ is the subspace of $W_\Gamma^{(i)}$ where the values at the subdomain vertices and the edge averages vanish.

We define a coarse Schur complement by

$$S_{\text{III}} := \sum_{i=1}^N R_{\text{II}}^{(i)T} \left\{ A_{\text{III}}^{(i)} - [A_{\text{II}}^{(i)} \ A_{\text{II}\Delta}^{(i)}] \begin{bmatrix} A_{\text{II}}^{(i)} & A_{\text{I}\Delta}^{(i)} \\ A_{\Delta\text{I}}^{(i)} & A_{\Delta\Delta}^{(i)} \end{bmatrix}^{-1} \begin{bmatrix} A_{\text{II}}^{(i)T} \\ A_{\text{II}\Delta}^{(i)T} \end{bmatrix} \right\} R_{\text{II}}^{(i)}, \quad (2.19)$$

and define an extension matrix $\Phi : \widehat{W}_\Pi \rightarrow \widetilde{W}_\Gamma$ by

$$\Phi = R_{\text{II}}^T - R_{\text{II}\Delta}^T \sum_{i=1}^N [0 \ R_{\Delta}^{(i)T}] \begin{bmatrix} A_{\text{II}}^{(i)} & A_{\text{I}\Delta}^{(i)} \\ A_{\Delta\text{I}}^{(i)} & A_{\Delta\Delta}^{(i)} \end{bmatrix}^{-1} \begin{bmatrix} A_{\text{II}}^{(i)T} \\ A_{\text{II}\Delta}^{(i)T} \end{bmatrix} R_{\text{II}}^{(i)}. \quad (2.20)$$

We will use $\Phi^T \widetilde{R}_{D,\Gamma}$ as the restriction operator for the coarse space.

We define S_Δ as the direct sum of subdomain Schur complements $S_\Delta^{(i)}$ which are defined by

$$S_\Delta^{(i)} := A_{\Delta\Delta}^{(i)} - A_{\Delta\text{I}}^{(i)} A_{\text{II}}^{(i)-1} A_{\text{I}\Delta}^{(i)}. \quad (2.21)$$

We use $S_\Delta^{(i)}$ as the local stiffness matrix and $\widehat{R}_{D,\Delta}^{(i)T}$ as the extension operator for each $W_\Delta^{(i)}$.

We then define the BDDC preconditioner as an additive preconditioner:

$$M_{\text{BDDC}}^{-1} := \widetilde{R}_{D,\Gamma}^T R_{\Gamma\Delta}^T S_\Delta^{-1} R_{\Gamma\Delta} \widetilde{R}_{D,\Gamma} + \widetilde{R}_{D,\Gamma}^T \Phi S_{\text{III}}^{-1} \Phi^T \widetilde{R}_{D,\Gamma}. \quad (2.22)$$

By some algebra, we can rewrite the BDDC preconditioner using \tilde{S} in (2.15) by

$$M_{\text{BDDC}}^{-1} = \tilde{R}_{D,\Gamma}^T \tilde{S}^{-1} \tilde{R}_{D,\Gamma} \quad (2.23)$$

and the Schur complement on \widehat{W} by

$$\widehat{S} = \tilde{R}_{\Gamma}^T \tilde{S} \tilde{R}_{\Gamma}. \quad (2.24)$$

2.7.2 Condition Number Bound

We follow the proof in [34], [49], and [50] to prove the condition number bound.

First, we show the lower bound. For a given $u_{\Gamma} \in \widehat{W}_{\Gamma}$, let $w_{\Gamma} := M_{\text{BDDC}} u_{\Gamma}$. By (2.12), we have that

$$\begin{aligned} u_{\Gamma}^T M_{\text{BDDC}} u_{\Gamma} &= u_{\Gamma}^T \tilde{R}_{\Gamma}^T \tilde{S} \tilde{S}^{-1} \tilde{R}_{D,\Gamma} w_{\Gamma} \\ &\leq \left(\tilde{R}_{\Gamma} u_{\Gamma}, \tilde{R}_{\Gamma} u_{\Gamma} \right)_{\tilde{S}}^{1/2} \left(\tilde{S}^{-1} \tilde{R}_{D,\Gamma} w_{\Gamma}, \tilde{S}^{-1} \tilde{R}_{D,\Gamma} w_{\Gamma} \right)_{\tilde{S}}^{1/2} \\ &= \left(u_{\Gamma}^T \tilde{R}_{\Gamma}^T \tilde{S} \tilde{R}_{\Gamma} u_{\Gamma} \right)^{1/2} \left(w_{\Gamma}^T \tilde{R}_{D,\Gamma}^T \tilde{S}^{-1} \tilde{S} \tilde{S}^{-1} \tilde{R}_{D,\Gamma} w_{\Gamma} \right)^{1/2} \\ &= \left(u_{\Gamma}^T \widehat{S} u_{\Gamma} \right)^{1/2} \left(u_{\Gamma}^T M_{\text{BDDC}} M_{\text{BDDC}}^{-1} M_{\text{BDDC}} u_{\Gamma} \right)^{1/2} \\ &= \left(u_{\Gamma}^T \widehat{S} u_{\Gamma} \right)^{1/2} \left(u_{\Gamma}^T M_{\text{BDDC}} u_{\Gamma} \right)^{1/2}. \end{aligned}$$

Therefore, we obtain $u_{\Gamma}^T M_{\text{BDDC}} u_{\Gamma} \leq u_{\Gamma}^T \widehat{S} u_{\Gamma}$.

Lemma 10. *Eigenvalues of the BDDC method are bounded below by 1.*

For the upper bound, we define an average operator $E_D : \widetilde{W}_{\Gamma} \rightarrow \widehat{W}_{\Gamma} \subset \widetilde{W}_{\Gamma}$ by

$$E_D := \tilde{R}_{\Gamma} \tilde{R}_{D,\Gamma}^T. \quad (2.25)$$

E_D is an identity operator on \widehat{W}_{Γ} .

We have the following lemma for E_D , see [47, Lemma 6.36] and [35, Lemma 1] for a proof:

Lemma 11.

$$|E_D u_{\Gamma}|_{\tilde{S}}^2 \leq C(1 + \log(H/h))^2 |u_{\Gamma}|_{\tilde{S}}^2, \quad u_{\Gamma} \in \widetilde{W}_{\Gamma}, \quad (2.26)$$

where C is independent of H , h , and ρ_i .

We define $w_\Gamma := M_{\text{BDDC}}u_\Gamma$ for a given $u_\Gamma \in \widehat{W}_\Gamma$ again. By Lemma 11, (2.23), (2.24), and (2.12), we have that

$$\begin{aligned}
u_\Gamma^T \widehat{S} u_\Gamma &= \left(u_\Gamma^T \widetilde{R}_\Gamma^T \right) \widetilde{S} \left(\widetilde{R}_\Gamma \widetilde{R}_{D,\Gamma}^T \widetilde{S}^{-1} \widetilde{R}_{D,\Gamma}^T w_\Gamma \right) \\
&= \left(\widetilde{R}_\Gamma u_\Gamma, \widetilde{R}_\Gamma u_\Gamma \right)_{\widetilde{S}}^{1/2} \left(E_D \widetilde{S}^{-1} \widetilde{R}_{D,\Gamma}^T w_\Gamma, E_D \widetilde{S}^{-1} \widetilde{R}_{D,\Gamma}^T w_\Gamma \right)_{\widetilde{S}}^{1/2} \\
&\leq \left(u_\Gamma^T \widetilde{R}_\Gamma^T \widetilde{S} \widetilde{R}_\Gamma u_\Gamma \right)^{1/2} C(1 + \log(H/h)) \left(\widetilde{S}^{-1} \widetilde{R}_{D,\Gamma}^T w_\Gamma, \widetilde{S}^{-1} \widetilde{R}_{D,\Gamma}^T w_\Gamma \right)_{\widetilde{S}}^{1/2} \\
&= C(1 + \log(H/h)) \left(u_\Gamma \widehat{S} u_\Gamma \right)^{1/2} \left(u_\Gamma^T M_{\text{BDDC}} u_\Gamma \right)^{1/2}.
\end{aligned}$$

We obtain $u_\Gamma \widehat{S} u_\Gamma \leq C(1 + \log(H/h))^2 u_\Gamma^T M_{\text{BDDC}} u_\Gamma$.

Therefore, we have the following bound for the BDDC operator.

Theorem 6. *The BDDC operator has the following bound of the condition number*

$$\kappa(M_{\text{BDDC}}^{-1} \widehat{S}) \leq C(1 + \log(H/h))^2$$

where C is independent of H , h , and ρ_i .

Lemma 10 is common to the BDDC operators for any problems. Therefore, we just need to estimate the upper bound of eigenvalues and to prove the property similar to Lemma 11 for the Reissner-Mindlin plate problem in chapter 5.

We can find a close relation between the BDDC methods and the FETI-DP methods, see [35] and [38] for more detail. For the FETI-DP methods, see [47] for definition and proofs. The preconditioned FETI-DP operator and the BDDC operator have the same eigenvalues if they use the same primal constraints.

Chapter 3

The Reissner-Mindlin Plate Theory

3.1 Introduction

Elasticity theory concerns the deformation of bodies under external forces and the calculation of the stress and strain of bodies from the deformation. In this theory, we consider bodies in \mathbb{R}^3 . We follow the presentations in [10, chapter 6].

Among materials with the linear elasticity property, we will mainly consider thin plates with a thickness t . By a reduction of dimension, we can describe the deformation of a thin plate by the displacement (w) and rotation (θ) variables in the Reissner-Mindlin Plate theory. If we impose the Kirchhoff condition, $\nabla w = \theta$, or $t = 0$, we obtain the Kirchhoff (biharmonic) problem. For the Kirchhoff plate, see [10, chapter 6.5], [9] and [12, chapter 5.9]. In the continuous case, the solution of the Reissner-Mindlin problem converges well to that of the Kirchhoff problem, see [3] and [4]. However, we can suffer from the locking if we do not use proper finite elements because the Kirchhoff condition is too severe on the discrete level. If we, e.g., use continuous piecewise linear functions to approximate both the displacement and rotation variables with a homogenous Dirichlet boundary condition, the rotation variables would vanish.

By introducing a reduction operator Π for θ and mixed finite element methods, we can avoid the locking problem. See [9, pp.195-232], [10, chapter 5.6], and [2, 5, 7, 1, 17, 18, 19, 20, 28, 29, 36, 46, 32, 6, 37, 44] for good finite elements on Reissner-Mindlin plate. In this chapter, we will introduce several finite elements for the Reissner-Mindlin Plate. We will also give some regularity results and convergence results from the Reissner-Mindlin Plate and the Kirchhoff Plate theory.

3.2 Linear Elasticity

We assume that we know the original body $\bar{\Omega}$ which is the closure of Ω , a bounded open set in \mathbb{R}^3 . We call $\bar{\Omega}$ the *reference configuration*. Under external force, we can view the deformation in terms of a mapping

$$\phi : \bar{\Omega} \longrightarrow B \subset \mathbb{R}^3,$$

where B is the deformed body of $\bar{\Omega}$. We refer to a point in the original body as x_R and to a point in the deformed body as x_B , i.e., $x_B = \phi(x_R)$.

Using the function I to denote the identity mapping, we can express ϕ as

$$\phi = I + u. \quad (3.1)$$

Here u is called the *displacement*. In the following, we assume that ϕ is sufficiently smooth. ϕ represents a *deformation*, if $\det(\nabla\phi) > 0$, because it maps a subdomain with positive volume into a subdomain with positive volume. If we use a linear approximation, we have

$$\begin{aligned} \|\phi(x_B + z_B) - \phi(x_B)\|_{l^2}^2 &\simeq \|\nabla\phi \cdot z_B\|_{l^2}^2 \\ &= z_B^T (\nabla\phi)^T \nabla\phi z_B. \end{aligned} \quad (3.2)$$

Therefore, the matrix

$$C := \nabla\phi^T \nabla\phi$$

describes the change of length and is called the *Cauchy-Green strain tensor*. The deviation of Cauchy-Green strain tensor from the identity matrix,

$$\varepsilon := \frac{1}{2}(C - I), \quad (3.3)$$

is called the *strain*. In the linear elasticity theory, we ignore higher order terms, i.e., keeping only the first order leads to the *symmetric gradient*:

$$\varepsilon_{ij} := \frac{1}{2} \left(\frac{\partial u_i}{\partial x_j} + \frac{\partial u_j}{\partial x_i} \right). \quad (3.4)$$

We assume that there are two types of external forces; surface forces and body forces. Mathematically we can express the body force by a function $f : B \rightarrow \mathbb{R}^3$ with a force $f dV$ acting on a volume element dV . Surface force can be written by a function $t(x_B, \mathbf{n}) : B \times S^2 \rightarrow \mathbb{R}^3$ where S^2 is the unit sphere in \mathbb{R}^3 denoting the space of the unit outward-pointing normal vector \mathbf{n} . If dA is the area element, then the surface force acting on dA is $t(x_B, \mathbf{n}) dA$. $t(x_B, \mathbf{n})$ is called the *Cauchy stress vector*.

We assume the following equilibrium state.

Assumption 4 (Axiom of Static Equilibrium). *There exists a vector field t such that in every subdomain V of B , the body forces f and the stresses t satisfy*

$$\int_V f(x_B) dx_B + \int_{\partial V} t(x_B, \mathbf{n}) ds = 0, \quad (3.5)$$

$$\int_V x_B \wedge f(x_B) dx_B + \int_{\partial V} x_B \wedge t(x_B, \mathbf{n}) ds = 0. \quad (3.6)$$

where \wedge is the vector product in \mathbb{R}^3 .

In the following, \mathbb{S}^3 denotes the space of symmetric 3×3 matrices, \mathbb{S}_+^3 the space of positive definite matrices in \mathbb{S}^3 , \mathbb{M}_+^3 the space of 3×3 matrices with positive determinants, \mathbb{Q}_+^3 the space of 3×3 orthogonal matrices with positive determinants, and $C^k(A, B)$ the space of C^k functions from the space A to the space B . Equilibrium axiom implies the existence of *Cauchy stress tensor*, T , as follows:

Theorem 7 (Cauchy's Theorem). *Let $t(\cdot, \mathbf{n}) \in C^1(B, \mathbb{R}^3)$, $t(x_B, \cdot) \in C^0(S^2, \mathbb{R}^3)$, and $f \in C(B, \mathbb{R}^3)$ in Assumption 4. Then there exists a symmetric tensor field $T \in C^1(B, \mathbb{S}^3)$ with the following properties:*

$$t(x_B, \mathbf{n}) = T(x_B)\mathbf{n}, \quad x_B \in B, \quad \mathbf{n} \in S^2, \quad (3.7)$$

$$\operatorname{div} T(x_B) + f(x_B) = 0, \quad x_B \in B, \quad (3.8)$$

$$T(x_B) = T^T(x_B), \quad x_B \in B. \quad (3.9)$$

We also assume that the material is frame indifferent.

Assumption 5 (Axiom of Material Frame-Indifference). *The Cauchy stress vector $t(x_B, \mathbf{n}) = T(x_B)\mathbf{n}$ is independent of the choice of coordinates, i.e., $Qt(x_B, \mathbf{n}) = t(Qx_B, Q\mathbf{n})$ for any $Q \in \mathbb{Q}_+^3$.*

We now define two properties of materials.

Definition 1. *A material is called elastic if there exists a mapping $\hat{T} : \mathbb{M}_+^3 \rightarrow \mathbb{S}^3$ which satisfies*

$$T(x_B) = \hat{T}(\nabla\phi(x_R)). \quad (3.10)$$

The mapping \hat{T} is called the response function.

Definition 2. *A material is called isotropic if*

$$\hat{T}(F) = \hat{T}(FQ), \quad \forall Q \in \mathbb{Q}_+^3. \quad (3.11)$$

So far we have discussed the argument on the deformed body B . With $\Sigma(x_R) := \det(\nabla\phi(x_R))(\nabla\phi(x_R))^{-1}T(\phi(x_R))(\nabla\phi(x_R))^{-T}$ and the neglected errors of the higher orders, we have

$$\operatorname{div}_R \Sigma + f_R = 0 \quad (3.12)$$

in a reference body. For Σ , we have the response function such as

$$\hat{\Sigma}(F) := \det(F)F^{-1}\hat{T}(F)F^{-T}.$$

We have the following theorem for an elastic material.

Theorem 8. *If a material is frame indifferent and isotropic, a response function $\hat{\Sigma} : \mathbb{M}_+^3 \rightarrow \mathbb{S}^3$ has the form $\hat{\Sigma}(F) = \sigma(FF^T)$ such that*

$$\begin{aligned} \sigma & : \mathbb{S}_+^3 \rightarrow \mathbb{S}^3 \\ \sigma(B) & = c_1 I + c_2 \operatorname{trace}(B)B + o(B) \quad \text{as } B \rightarrow 0. \end{aligned} \quad (3.13)$$

with proper constants c_1 and c_2 .

If we plug $C = \nabla\phi^T\nabla\phi = I + 2\varepsilon$ into $\sigma(C)$, we have

$$\sigma T(I + 2\varepsilon) = \tilde{c}_1 I + \tilde{c}_2 \operatorname{trace}(\varepsilon) + \tilde{c}_3 \varepsilon + o(\varepsilon) \quad \text{as } \varepsilon \rightarrow 0. \quad (3.14)$$

Normally, the situation $\varepsilon = 0$ corresponds to an unstressed condition and we assume that $\tilde{c}_1 = 0$. We can express the stress as follows if we ignore the terms of the higher orders:

$$\sigma = \lambda \operatorname{trace}(\varepsilon)I + 2\mu\varepsilon. \quad (3.15)$$

Here λ and μ are called the Lamé constants. We can express the Lamé constants in terms of the *Young's modulus of elasticity* E and the *Poisson ratio* ν :

$$\lambda = \frac{E\nu}{(1+\nu)(1-2\nu)}, \quad \mu = \frac{E}{2(1+\nu)}.$$

From this relation between ε and σ , we obtain the following boundary value problem:

$$\begin{aligned} -\operatorname{div} \sigma(x) & = f(x), & x \in \Omega, \\ \sigma(x) & = \lambda \operatorname{trace}(\varepsilon(x))I + 2\mu\varepsilon(x), & x \in \Omega, \\ u(x) & = 0, & x \in \Gamma_0 \subset \partial\Omega, \\ \sigma(x)\mathbf{n}(x) & = g(x), & x \in \Gamma_1 = \partial\Omega \setminus \Gamma_0. \end{aligned}$$

3.2.1 The Reissner-Mindlin Plate

In the following, we consider a thin plate with thickness t . Let the plate occupy the region $P_t = \Omega \times (-\frac{t}{2}, +\frac{t}{2})$, where Ω is a bounded domain of diameter 1 in \mathbb{R}^2 . We are interested in the case when the plate is thin, i.e., t is small. In this problem, we consider three displacement components u_i , $i = 1, 2, 3$. We use a reduction of dimension for the z -direction, and assume the following four conditions, cf. [10, chapter 6.5]:

- H1. The linearity hypothesis.
- H2. The displacement in the z -direction does not depend on the z -coordinate.
- H3. The points on the middle surface are deformed only in the z -direction.
- H4. The normal stress σ_{33} vanishes.

Under the above hypotheses, we can write the displacement components as,

$$\begin{aligned} u_i(x, y, z) &= -z\theta_i(x, y), \quad \text{for } i = 1, 2, \\ u_3(x, y, z) &= w(x, y). \end{aligned}$$

Using H4 with a reduction of dimension for the z -direction, we have a variational problem:

Minimize the Reissner-Mindlin energy

$$\begin{aligned} J(\theta, w) &= \frac{1}{2} \int_{\Omega} \mathcal{C}\varepsilon(\theta) : \varepsilon(\theta) \, dx dy + \frac{1}{2} \varrho t^{-2} \int_{\Omega} |\nabla w - \theta|^2 \, dx dy \\ &\quad - \int_{\Omega} g w \, dx dy + \int_{\Omega} \mathbf{f} \cdot \theta \, dx dy, \end{aligned}$$

where $\mathcal{C} = \mathbf{A}^{-1}$, $\mathbf{A}\tau = (1 + \nu)\tau/E - \nu \text{trace}(\tau)\mathbf{I}/E$, and \mathbf{I} is the 2 by 2 identity matrix. The Reissner-Mindlin equations are

$$\begin{aligned} -\text{div } \mathcal{C}\varepsilon(\theta) - \varrho t^{-2}(\nabla w - \theta) &= -\mathbf{f}, \\ -\text{div } (\nabla w - \theta) &= \varrho^{-1}t^2 g. \end{aligned} \tag{3.16}$$

For simplicity, we assume that θ and w vanish on $\partial\Omega$.

This problem can have a locking problem and we can handle that by using mixed finite element methods; see [9], [10]. By introducing the shear stress $\gamma = \varrho t^{-2}(\nabla w - \theta)$, we obtain the following variational problem, cf. [9], [8], [10, chapter 6.6]:

Find $\theta \in \mathbf{H}_0^1(\Omega)$, $w \in H_0^1(\Omega)$, and $\gamma \in \mathbf{L}^2(\Omega)$ such that

$$\begin{aligned} a(\theta, \phi) + (\gamma, \nabla v - \phi) &= (g, v) - (\mathbf{f}, \phi), \quad \phi \in \mathbf{H}_0^1(\Omega), v \in H_0^1(\Omega), \\ (\nabla w - \theta, \eta) - \varrho^{-1}t^2(\gamma, \eta) &= 0, \quad \eta \in \mathbf{L}^2(\Omega). \end{aligned} \tag{3.17}$$

Here $a(\theta, \phi) := \int_{\Omega} (\mathcal{C}\varepsilon(\theta), \varepsilon(\phi))$. For the bilinear form $a(\cdot, \cdot)$, there is Korn's inequality which ensures its positive definiteness on $\mathbf{H}_0^1(\Omega)$.

Lemma 12 (Korn's inequality). *Let $\Omega \subset \mathbb{R}^2$ be an open bounded set with a piecewise smooth boundary. In addition, suppose $\Gamma \in \partial\Omega$ has a positive one-dimensional measure. Then there exists a positive number $C(\Omega, \Gamma)$ which is independent of H_Ω such that*

$$\int_{\Omega} \varepsilon(u) : \varepsilon(u) \, dx dy \geq C(\Omega, \Gamma) \|u\|_{H^1(\Omega)}^2 \quad \text{for all } u \in H_\Gamma^1(\Omega). \quad (3.18)$$

Here $H_\Gamma^1(\Omega)$ is the closure of $\{u \in C^\infty(\Omega)^2 \mid u(x) = 0 \text{ for } x \in \Gamma\}$ with respect to the H^1 -norm.

Proof. See [10, chapter 6.3]. □

We know that $a(\theta, \theta)$ is not elliptic on the space $\mathbf{H}_0^1(\Omega) \times H_0^1(\Omega)$ because of the w component. Therefore, we cannot use the general theory of Section 1.4 directly. For the stability and other related issues, it is useful to introduce the Helmholtz decomposition. For a proof, see [10, Lemma 6.1].

Lemma 13. *Assume that $\Omega \subset \mathbb{R}^2$ is simply connected. Then every function $\gamma \in L^2(\Omega)$ is uniquely decomposable in the form*

$$\gamma = \nabla r + \text{curl } p$$

with $r \in H_0^1(\Omega)$ and $p \in H^1(\Omega)/\mathbb{R}$.

We can rewrite (3.17) as a perturbed Stokes equation:

Find $(r, \theta, p, w) \in H_0^1(\Omega) \times \mathbf{H}_0^1(\Omega) \times H^1(\Omega)/\mathbb{R} \times H_0^1(\Omega)$ such that

$$(\nabla r, \nabla v) = (g, v), \quad v \in H_0^1(\Omega), \quad (3.19)$$

$$a(\theta, \phi) - (\text{curl } p, \phi) = (\nabla r, \phi) - (\mathbf{f}, \phi), \quad \phi \in \mathbf{H}_0^1(\Omega), \quad (3.20)$$

$$-(\theta, \text{curl } q) - \varrho^{-1} t^2 (\text{curl } p, \text{curl } q) = 0, \quad q \in H^1(\Omega)/\mathbb{R}, \quad (3.21)$$

$$(\nabla w, \nabla s) = (\theta + \varrho^{-1} t^2 \nabla r, \nabla s), \quad s \in H_0^1(\Omega). \quad (3.22)$$

Now $a(\theta, \theta)$ is elliptic on $\mathbf{H}_0^1(\Omega)$ by Korn's inequality and if we check the inf-sup condition for each line of equations above, we can establish the existence and uniqueness of the solution. For more details, see Theorem 9 in subsection 3.2.2.

Note that for a known r with $t = 0$, (3.20) and (3.21) is the Stokes equation for $(\theta_2, -\theta_1, p)$. Therefore, there is a connection between the Reissner-Mindlin problem and the Stokes problem.

3.2.2 The Kirchhoff Plate

In addition to hypotheses H1-H4, we can assume the Kirchhoff condition:

H5. $\theta = \nabla w$.

Now θ is not independent being a function of w and we require that $w \in H_0^2(\Omega)$. The energy (3.16) becomes

$$J(\theta, w) = \frac{1}{2} \int_{\Omega} \mathcal{C}\varepsilon(\theta) : \varepsilon(\theta) \, dx dy + \int_{\Omega} \mathbf{f} \cdot \theta \, dx dy. \quad (3.23)$$

The variational problem (3.17) becomes:

Find $w \in H_0^2(\Omega)$ such that

$$a(\nabla w, \nabla v) = (g, v) - (\mathbf{f}, \nabla v), \quad v \in H_0^2(\Omega). \quad (3.24)$$

Let us denote the solution of this Kirchhoff plate problem by w^0 and define $\theta^0 := \nabla w^0$. As $t \rightarrow 0$, we know that $\theta \rightarrow \theta^0$ and $w \rightarrow w^0$. The two models have similar interior solutions but differ in a boundary layer of a width of order of t . You can find more results and examples on the differences of the two models in [3] and [4].

We have some regularity results and convergence results.

Theorem 9. *Let Ω be a convex polygon or a bounded domain with a smooth boundary in the plane. For any $t \in (0, 1]$, $\mathbf{f} \in \mathbf{H}^{-1}(\Omega)$, and $g \in H^{-1}(\Omega)$, there exists a unique solution $(r, \theta, p, w) \in H_0^1(\Omega) \times \mathbf{H}_0^1(\Omega) \times H^1(\Omega)/\mathbb{R} \times H_0^1(\Omega)$ satisfying (3.19)-(3.22). Moreover, if $\mathbf{f} \in \mathbf{L}^2(\Omega)$ and $g \in L^2(\Omega)$, then $\theta \in \mathbf{H}^2(\Omega)$, $w \in H^2(\Omega)$, and there exists a constant C independent of t , \mathbf{f} , and g such that*

$$\|\theta\|_{H^2(\Omega)} + \|w\|_{H^2(\Omega)} + t \|\gamma\|_{H^1(\Omega)} + \|\operatorname{div} \gamma\|_{L^2(\Omega)} \leq C(\|g\|_{L^2(\Omega)} + \|\mathbf{f}\|_{L^2(\Omega)}). \quad (3.25)$$

Finally, we have

$$\|\theta - \theta^0\|_{H^1(\Omega)} + \|w - w^0\|_{H^2(\Omega)} \leq Ct(\|g\|_{L^2(\Omega)} + \|\mathbf{f}\|_{L^2(\Omega)}). \quad (3.26)$$

Proof. See [9, pp.202-203]. □

3.3 Finite Elements for Reissner-Mindlin Plate

We can use conforming finite elements, i.e., $\Theta_h \subset \mathbf{H}_0^1(\Omega)$, $W_h \subset H_0^1(\Omega)$, and $\mathbf{S}_h \subset \mathbf{L}^2(\Omega)$. Let $\Pi : \mathbf{H}_0^1(\Omega) + \mathbf{S}_h \rightarrow \mathbf{S}_h$ be a reduction operator which will be specified later. Then, as in [9, 10], the discrete problem becomes:

Find $\theta_h \in \Theta_h$, $w_h \in W_h$, and $\gamma_h \in \mathbf{S}_h$ such that

$$\begin{aligned} a(\theta_h, \phi) + (\gamma_h, \nabla v - \Pi\phi) &= (g, v) - (\mathbf{f}, \phi), \quad \phi \in \Theta_h, v \in W_h \\ (\nabla w_h - \Pi\theta_h, \eta) - \varrho^{-1}t^2(\gamma_h, \eta) &= 0, \quad \eta \in \mathbf{S}_h. \end{aligned} \quad (3.27)$$

We now discuss some conforming finite elements.

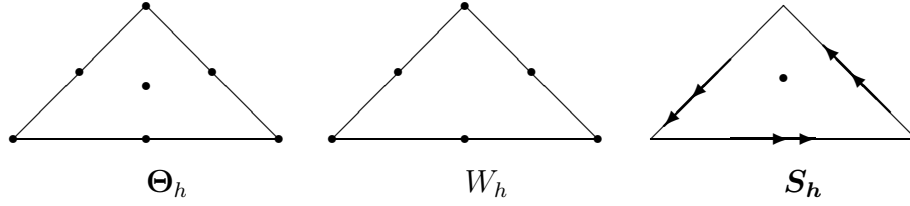


Figure 3.1: the MITC7 element.

3.3.1 The MITC7 Elements

For this element, we partition the domain into triangles. We choose, see [10, chapter 6.6], [9, pp.210-213], [21, pp.268-272],

$$\Theta_h = \mathbf{M}_{1,0}^1 + \mathbf{B}^3, \quad W_h = M_{1,0}^2, \quad \mathbf{S}_h = \mathbf{RT}_1^\perp$$

on the triangulation. Here $\mathbf{M}_{a,0}^k$ is the space of piecewise k th order polynomials in $\mathbf{H}_0^a(\Omega)$, $M_{a,0}^k$ the space of piecewise k th order polynomials in $H_0^a(\Omega)$, \mathbf{M}_a^k the space of piecewise k th order polynomials in \mathbf{H}^a , \mathbf{B}^k the space of piecewise k th order polynomial bubble functions, and \mathbf{RT}_1^\perp the space of Raviart-Thomas elements of order k , a subspace of $\mathbf{H}(\text{rot}, \Omega)$. More specifically, \mathbf{S}_h is defined by

$$\mathbf{S}_h := \{\gamma \in \mathbf{H}(\text{rot}, \Omega) \mid \gamma|_K \in (P_1(K))^2 + P_1(K)(y, -x)^T, \forall K\},$$

where $P_1(K)$ denotes the space of linear functions on the triangular element K . It can be proved that a function in $\mathbf{S}_h(K)$ is uniquely determined by assigning

- the moments up to first order of its tangential component on each edge of K (6 degrees of freedom) and
- its mean values over K (2 degrees of freedom).

For a given $u = (u_1, u_2)$, we define $\Pi : \mathbf{H}_0^1(\Omega) + \mathbf{S}_h \rightarrow \mathbf{S}_h$ by requiring that

$$\begin{aligned} \int_K \Pi u \, dx dy &= \int_K u \, dx dy, \\ \int_e (\Pi u \cdot \mathbf{t}) p_1(s) \, ds &= \int_e (u \cdot \mathbf{t}) p_1(s) \, ds \end{aligned}$$

for every triangle $K \in \mathcal{T}_h$ and every edge e of K . Here \mathbf{t} is the tangent vector to the edge e and $p_1(s)$ is any first order polynomial on each edge. Π is similar to the interpolation operator of the Raviart-Thomas element except that it is related to the rotation instead of the divergence.

For the MITC7 element, we have the following convergence theorem.

Theorem 10. For the MITC7 element and a sufficiently smooth solution (θ, γ, w) , we have for $1 \leq r \leq 2$

$$\|\theta - \theta_h\|_{L^2(\Omega)} + \|w - w_h\|_{L^2(\Omega)} \leq Ch^{r+1}(\|\theta\|_{H^{r+1}(\Omega)} + t\|\gamma\|_{H^r(\Omega)} + \|\gamma\|_{H^{r-1}(\Omega)}).$$

Proof. See [9, pp.212-213]. □

Considering the Helmholtz decomposition, functions of \mathbf{S}_h cannot be generally represented in the form

$$\gamma_h = \nabla r_h + \text{curl } p_h, \quad \forall \gamma_h \in \mathbf{S}_h,$$

with proper finite element spaces for r_h and p_h . However, the MITC7 element has a discrete Helmholtz decomposition with proper definitions.

First, the MITC7 element has the following 5 properties in terms of an auxiliary space

$$Q_h := \{q \in L_0^2(\Omega) \mid q|_K \in P_1(K), \forall K \in \mathcal{T}_h\}$$

where $L_0^2(\Omega)$ denotes the space of functions in $L^2(\Omega)$ with a vanishing mean.

P1: $\nabla W_h \subset \mathbf{S}_h$.

P2: $\text{rot } \mathbf{S}_h \subset Q_h$.

P3: $\text{rot } \Pi\phi = \Pi^0 \text{rot } \phi$ for $\phi \in \mathbf{H}_0^1(\Omega)$, with $\Pi^0 : L_0^2(\Omega) \rightarrow Q_h$ denoting the L^2 -projection.

P4: If $\eta \in \mathbf{S}_h$ satisfies $\text{rot } \eta = 0$, then $\eta = \nabla v$ for some $v \in W_h$.

P5: (Θ_h^\perp, Q_h) satisfies the inf-sup condition for the Stokes problem, i.e., there exists a constant C which is independent of h such that

$$\sup_{0 \neq \phi \in \Theta_h} \frac{(\text{rot } \phi, q)}{\|\phi\|_{H^1(\Omega)}} \geq C \|q\|_{L^2(\Omega)}, \quad \forall q \in Q_h. \quad (3.28)$$

We define the *discrete curl operator* curl_h as follows:

$$(\text{curl}_h q_h, \eta)_{L^2(\Omega)} = (q_h, \text{rot } \eta)_{L^2(\Omega)}, \quad \forall \eta \in \mathbf{S}_h. \quad (3.29)$$

Because $\mathbf{S}_h \subset \mathbf{H}_0(\text{rot}, \Omega)$, curl_h is well defined. Then, \mathbf{S}_h for the MITC7 element has a discrete Helmholtz decomposition described by the following theorem.

Theorem 11. Suppose properties P1, P2, and P5 hold. Then, there exists an L_2 -orthogonal decomposition such that

$$\mathbf{S}_h = \nabla W_h \oplus \text{curl}_h Q_h.$$

Proof. See [10, Theorem 6.6.5]. □

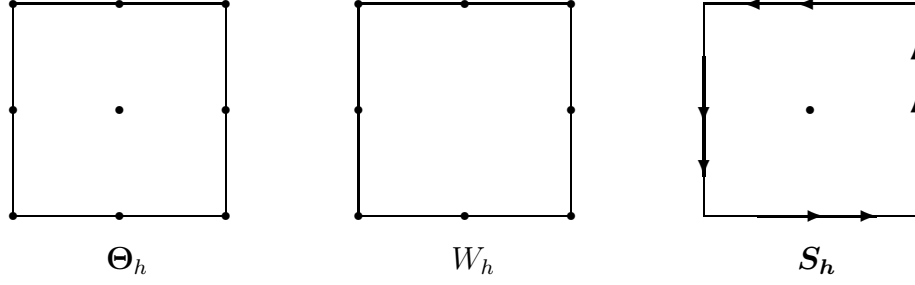


Figure 3.2: the MITC9 element.

This leads to an alternative discrete variational problem:

Find $(r_h, \theta_h, p_h, w_h) \in W_h \times \Theta_h \times Q_h \times W_h$ such that

$$\begin{aligned}
(\nabla r_h, \nabla v) &= (g, v), \quad v \in W_h, \\
a(\theta_h, \phi) - (\text{curl } p_h, \phi) &= (\nabla r_h, \phi) - (\mathbf{f}, \phi), \quad \phi \in \Theta_h, \\
-(\theta_h, \text{curl } q) - \varrho^{-1}t^2(\text{curl } p_h, \text{curl } q) &= 0, \quad q \in Q_h, \\
(\nabla w_h, \nabla s) &= (\theta_h + \varrho^{-1}t^2\nabla r_h, \nabla s), \quad s \in W_h.
\end{aligned} \tag{3.30}$$

In addition to these five properties, P1-P5, the MITC7 element has the following property.

P6: For each edge e of the element K , let \mathbf{t} be the tangent vector of e . Then the composite operator $(\Pi\theta|_e) \cdot \mathbf{t}$ depends only on $\theta|_e \cdot \mathbf{t}$.

3.3.2 The MITC9 Elements

In this element, we partition the domain into rectangles, see [9, pp.221-223] and [8]. On each element $K \in \mathcal{T}_h$, we choose,

$$\begin{aligned}
\Theta_h &= \{\theta \in \mathbf{H}_0^1(\Omega) \mid \theta|_K \in [\mathcal{Q}_2(K)]^2, \forall K \in \mathcal{T}_h\}, \\
W_h &= \{w \in H_0^1(\Omega) \mid w|_K \in [\mathcal{Q}_2(K) \cap P_3(K)], \forall K \in \mathcal{T}_h\}, \\
\mathbf{S}_h &= \{\gamma \in \mathbf{H}_0(\text{rot}, \Omega) \mid \\
&\quad \gamma|_K \in \text{span}[(1, x, y, xy, y^2) \times (1, x, y, x^2, xy)] \forall K \in \mathcal{T}_h\}
\end{aligned} \tag{3.31}$$

where $P_k(K)$ denotes the space of k th order polynomial functions on the rectangular element K and $\mathcal{Q}_2(K)$ the standard space of biquadratic polynomial functions.

For a given $u = (u_1, u_2)$, we define $\Pi : \mathbf{H}_0^1(\Omega) + \mathbf{S}_h \rightarrow \mathbf{S}_h$ by requiring that

$$\begin{aligned}
\int_K \Pi u \, dx dy &= \int_K u \, dx dy, \\
\int_e (\Pi u \cdot \mathbf{t}) p_1(s) \, ds &= \int_e (u \cdot \mathbf{t}) p_1(s) \, ds
\end{aligned}$$

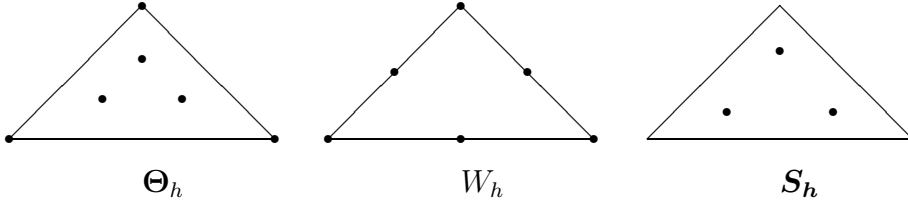


Figure 3.3: the Falk-Tu element with $k=2$.

for every rectangle $K \in \mathcal{T}_h$ and every edge e of K .

It is known that the MITC9 element satisfies the 6 properties P1-P6 of subsection 3.3.1 like the MITC7 element when we define the auxiliary space Q_h by

$$Q_h := \{q \in L_0^2(\Omega) : q|_K \in P_1(K), \forall K \in \mathcal{T}_h\}.$$

For a proof, see [17] and [18].

3.3.3 The Falk-Tu Elements

In the Falk-Tu element, see [9], [31], we choose

$$\Theta_h = \mathbf{M}_{1,0}^1 + \mathbf{B}^4, \quad W_h = M_{1,0}^2, \quad \mathbf{S}_h = \mathbf{M}_0^1$$

on the triangulation. Here $\mathbf{M}_{a,0}^k$ is the space of piecewise k th order polynomials in $\mathbf{H}_0^a(\Omega)$, $M_{a,0}^k$ the space of piecewise k th order polynomials in $H_0^a(\Omega)$, \mathbf{M}_a^k the space of piecewise k th order polynomials in \mathbf{H}^a , and \mathbf{B}^k the space of piecewise k th order polynomial bubble functions.

Note that we choose a discontinuous stress variable in the Falk-Tu element. The Π operator is defined as the L^2 projector from $\mathbf{H}_0^1(\Omega)$ to \mathbf{S}_h .

We have the following error estimate. For a proof, we refer to the lecture notes edited by Boffi and Gastaldi [9, pp.213-216].

Theorem 12. *For sufficiently smooth solutions of the continuous problem, we have*

$$\|\theta - \theta_h\|_{L^2(\Omega)} + \|w - w_h\|_{H^1(\Omega)} \leq Ch^2(\|\mathbf{f}\|_{L^2(\Omega)} + \|g\|_{L^2(\Omega)}) \quad (3.32)$$

where C is independent of h .

The k th order Falk-Tu elements are defined as follows; see [9], [31]:

$$\Theta_h = \mathbf{M}_{1,0}^{k-1} + \mathbf{B}^{k+2}, \quad W_h = M_{1,0}^k, \quad \mathbf{S}_h = \mathbf{M}_0^{k-1}. \quad (3.33)$$

Note that we again choose a discontinuous stress variable. The Π operator is again defined as the L^2 projector from $\mathbf{H}_0^1(\Omega)$ to \mathbf{S}_h .

We have an error estimate similar to Theorem 12. For a proof, see [9, p. 213].

Theorem 13. *For sufficiently smooth solutions of the continuous problem, we have for $1 \leq r \leq k - 1$*

$$\begin{aligned} & \|\theta - \theta_h\|_{L^2(\Omega)} + \|w - w_h\|_{H^1(\Omega)} \leq \\ & Ch^{r+1}(\|\theta\|_{H^{r+1}(\Omega)} + \|w\|_{H^{r+2}(\Omega)} + t\|\gamma\|_{H^r(\Omega)} + \|\gamma\|_{H^{r+1}(\Omega)}) \end{aligned} \quad (3.34)$$

where C is independent of h .

Chapter 4

Overlapping Methods Using the Falk-Tu Elements for the Reissner-Mindlin Plate

4.1 Introduction

In this chapter, we use the Falk-Tu elements to discretize the Reissner-Mindlin problem. For simplicity, we assume that the subdomains are shape-regular triangles. We first define coarse basis functions and local spaces for an overlapping method. We then show a $C(1 + \frac{H}{\delta})^3(1 + \log \frac{H}{h})^2$ bound for our overlapping method. As we saw in section 2.2, we can use the same coarse and local spaces to additive and multiplicative Schwarz methods. We also give numerical results on additive and multiplicative Schwarz methods.

4.2 Definition of the Operator \mathcal{C} and Bilinear Forms

We will consider the operator \mathbf{A} of subsection 3.2.1 in more detail and find a relation between $a(\theta, \theta)$ and the H^1 -norm of θ . Let,

$$\begin{aligned} \mathbf{A}\tau &:= \frac{1+\nu}{E}\tau - \frac{\nu \times \text{trace}(\tau)}{E}I \\ &= \frac{1}{E} \begin{pmatrix} 1 & -\nu & 0 \\ -\nu & 1 & 0 \\ 0 & 0 & 1+\nu \end{pmatrix} \begin{pmatrix} \tau_{11} \\ \tau_{22} \\ \tau_{12} \end{pmatrix}. \end{aligned} \tag{4.1}$$

Then \mathcal{C} , the inverse of \mathbf{A} , is defined by

$$\begin{aligned}
\mathcal{C}\varepsilon &:= \mathbf{A}^{-1}\varepsilon \\
&= \frac{E}{(1-\nu^2)} \begin{pmatrix} 1 & \nu & 0 \\ \nu & 1 & 0 \\ 0 & 0 & 1-\nu \end{pmatrix} \begin{pmatrix} \varepsilon_{11} \\ \varepsilon_{22} \\ \varepsilon_{12} \end{pmatrix} \\
&= \frac{E}{2(1+\nu)} \begin{pmatrix} \frac{2}{1-\nu} & \frac{2\nu}{1-\nu} & 0 \\ \frac{2\nu}{1-\nu} & \frac{2}{1-\nu} & 0 \\ 0 & 0 & 2 \end{pmatrix} \begin{pmatrix} \varepsilon_{11} \\ \varepsilon_{22} \\ \varepsilon_{12} \end{pmatrix} \\
&= \mu \begin{pmatrix} \frac{2}{1-\nu} & \frac{2\nu}{1-\nu} & 0 \\ \frac{2\nu}{1-\nu} & \frac{2}{1-\nu} & 0 \\ 0 & 0 & 2 \end{pmatrix} \begin{pmatrix} \varepsilon_{11} \\ \varepsilon_{22} \\ \varepsilon_{12} \end{pmatrix} \tag{4.2}
\end{aligned}$$

where

$$\mu := \frac{E}{2(1+\nu)}. \tag{4.3}$$

With

$$\varepsilon(\theta) := \frac{1}{2} \begin{pmatrix} 2\theta_x^1 & \theta_x^2 + \theta_y^1 \\ \theta_x^2 + \theta_y^1 & 2\theta_y^2 \end{pmatrix}, \tag{4.4}$$

define

$$a(\theta, \phi) := \int_{\Omega} (\mathcal{C}\varepsilon(\theta), \varepsilon(\phi)) \, dx dy \tag{4.5}$$

$$\begin{aligned}
&= \int_{\Omega} \left(\left(\begin{pmatrix} \frac{2\mu}{1-\nu}\theta_x^1 + \frac{2\mu\nu}{1-\nu}\theta_y^2 \\ \frac{2\mu\nu}{1-\nu}\theta_y^2 + \frac{2\mu\nu}{1-\nu}\theta_x^1 \\ \mu(\theta_x^2 + \theta_y^1) \end{pmatrix}, \begin{pmatrix} \phi_x^1 \\ \phi_y^2 \\ \frac{1}{2}(\phi_x^2 + \phi_y^1) \end{pmatrix} \right) \right) \, dx dy \\
&= \int_{\Omega} \left(\frac{2\mu}{1-\nu}\theta_x^1\phi_x^1 + \frac{2\mu\nu}{1-\nu}\theta_y^2\phi_x^1 + \frac{2\mu}{1-\nu}\theta_y^2\phi_y^2 + \right. \\
&\quad \left. \int_{\Omega} \left(\frac{2\mu\nu}{1-\nu}\theta_x^1\phi_y^2 + (\phi_x^2 + \phi_y^1)(\theta_x^2 + \theta_y^1)\mu \right) \, dx dy \right) \, dx dy. \tag{4.6}
\end{aligned}$$

Thus,

$$\begin{aligned}
\frac{a(\theta, \phi)}{\mu} &= \int_{\Omega} 2(\theta_x^1\phi_x^1 + \theta_y^2\phi_y^2 + \frac{1}{2}(\theta_x^2 + \theta_y^1)(\phi_x^2 + \phi_y^1)) \, dx dy + \\
&\quad \int_{\Omega} \frac{2\nu}{1-\nu}(\theta_x^1\phi_x^1 + \theta_y^2\phi_y^2 + \theta_y^2\phi_x^1 + \theta_x^1\phi_y^2) \, dx dy \\
&= 2 \int_{\Omega} \varepsilon(\theta) : \varepsilon(\phi) \, dx dy + \frac{2\nu}{1-\nu} \int_{\Omega} \operatorname{div} \theta \operatorname{div} \phi \, dx dy,
\end{aligned}$$

or

$$\begin{aligned}
a(\theta, \phi) &= 2 \int_{\Omega} \mu \varepsilon(\theta) : \varepsilon(\phi) \, dx dy + \frac{2\mu\nu}{1-\nu} \int_{\Omega} \operatorname{div} \theta \operatorname{div} \phi \, dx dy \\
&= \int_{\Omega} 2\mu \varepsilon(\theta) : \varepsilon(\phi) \, dx dy + \lambda \int_{\Omega} \operatorname{div} \theta \operatorname{div} \phi \, dx dy \\
&\quad \text{where } \lambda := \frac{2\mu\nu}{1-\nu}.
\end{aligned} \tag{4.7}$$

The bilinear form $a(\theta, \theta)$ is that of the standard linear elasticity operator. We can easily show that $a(\theta, \theta)$ is bounded by the square of the H^1 -seminorm of θ if the Lamé parameters μ and λ are bounded. More precisely, we get the bound

$$a(\theta, \theta) \leq \tilde{m} |\theta|_{H^1}^2 \tag{4.8}$$

with $\tilde{m} := \max(2\mu, \lambda)$.

We will use the scaled H^1 -norm for each subdomain:

$$\|u\|_{H^1(\Omega_i)}^2 = |u|_{H^1(\Omega_i)}^2 + \frac{1}{H_i^2} \|u\|_{L^2(\Omega_i)}^2. \tag{4.9}$$

4.3 Discrete Harmonic Extension

We use the Falk-Tu element to discretize (3.17). Because we choose a discontinuous stress variable, we can eliminate it on the element level as in [8], [23]. Then, the problem becomes:

Find $\theta_h \in \Theta_h$ and $w_h \in W_h$ such that

$$b((\theta_h, w_h), (\phi, v)) = (g, v) - (\mathbf{f}, \phi), \quad \phi \in \Theta_h, \quad v \in W_h \tag{4.10}$$

where b is defined by

$$b((\theta, w), (\phi, v)) := a(\theta, \phi) + \frac{\rho}{t^2} (\Pi\theta - \nabla w, \Pi\phi - \nabla v). \tag{4.11}$$

The discrete Reissner-Mindlin energy

$$b((\theta_h, w_h), (\theta_h, w_h)) = a(\theta_h, \theta_h) + \frac{\rho}{t^2} (\nabla w_h - \Pi\theta_h, \nabla w_h - \Pi\theta_h) \tag{4.12}$$

will be estimated later in the proof. We define $u := (\theta, w)$ and $\mathbf{U} := \Theta_h \times W_h$.

For natural boundary conditions, the dimension of the null space of this Reissner-Mindlin energy is 3. The first null element is given by $\theta = (0, 0)$ and $w = 1$, the second by $\theta = (1, 0)$ and $w = x$, and the third by $\theta = (0, 1)$ and $w = y$. These null space functions will play an important role for the subdomain problems defined later.

The energy of the interior part of u , which is orthogonal to discrete harmonic functions in b -seminorm, can be bounded by the sum of the energy of local components of u . Therefore, it is enough to consider discrete harmonic functions when establishing stable decompositions. From now on, we will assume that u is discrete harmonic in each subdomain.

Because the support of each bubble function is contained in a single element, the bubble functions are determined by the values of the piecewise linear parts of θ and w if u is discrete harmonic to minimize the Reissner-Mindlin energy. Therefore, we can consider the bubble function as a dependent functions in a discrete harmonic function.

Let us consider one element K only and assume that the piecewise linear part of θ and w are already determined. Let θ_L be the piecewise linear part of θ . Using the bubble basis functions θ_B^k , $k = 1, 2, \dots, 6$, we can write $\nabla w - \theta_L = \sum_{k=1}^6 \beta_k \Pi \theta_B^k$ with certain coefficients β_k .

Note that the square of the L^2 -norm of the divergence of θ_B is positive definite. Therefore, the two components of the a-seminorm are equivalent over the bubble function space and $a(\theta_B, \theta_B)$ is equivalent to $\tilde{m}|\theta_B|_{H^1}^2$.

Let us write the bubble function on the element K as $\theta_B = \sum_{k=1}^6 \alpha_k \beta_k \theta_B^k$. We can then choose optimal coefficients α_k , $k = 1, 2, \dots, 6$, for the bubble functions to minimize the Reissner-Mindlin energy of u . We know that the a-seminorm does not depend on the scaling and the square of the L^2 -norm of the bubble functions is on the order of h^2 .

Let β be the diagonal matrix with the diagonal entries $\beta_1, \beta_2, \dots, \beta_6$, and let $\alpha = (\alpha_1, \alpha_2, \dots, \alpha_6)^t$. Let F and G be the matrices representing the a-seminorm and the L^2 -norm of the bubble functions on a reference element, respectively. Let $\tilde{F} = \beta^t F \beta$, $\tilde{G} = \beta^t G \beta$, and let $\mathbf{1}$ be the 6-dimensional column vector with all entries 1. We know that $h^2 \mathbf{1}^t \beta^t \beta \mathbf{1}$ is equivalent to $\|\nabla w - \theta_L\|_{L^2(K)}^2$. Then the Reissner-Mindlin energy of $(\theta_L + \theta_B, w)$ is equivalent to

$$a(\theta_L, \theta_L) + \tilde{m} \alpha^t \tilde{F} \alpha + \frac{h^2}{t^2} (\mathbf{1} - \alpha)^t \tilde{G} (\mathbf{1} - \alpha).$$

This is minimized by

$$\begin{aligned} \alpha &= \frac{h^2}{t^2} \tilde{O}^{-1} \tilde{G} \mathbf{1} \quad \text{where} \\ O &:= \tilde{m} F + \frac{h^2}{t^2} G \quad \text{and} \\ \tilde{O} &:= \beta^t O \beta \\ &= \tilde{m} \tilde{F} + \frac{h^2}{t^2} \tilde{G} \end{aligned}$$

and

$$\mathbf{1} - \alpha = \tilde{m}\tilde{O}^{-1}\tilde{F}\mathbf{1}.$$

If we plug this α into the above energy formula, the Reissner-Mindlin energy is equivalent to

$$\begin{aligned} & a(\theta_L, \theta_L) + \tilde{m}\frac{h^2}{t^2}\frac{h^2}{t^2}\mathbf{1}^t\tilde{G}\tilde{O}^{-1}\tilde{F}\tilde{O}^{-1}\tilde{G}\mathbf{1} + \tilde{m}^2\frac{h^2}{t^2}\mathbf{1}^t\tilde{F}\tilde{O}^{-1}\tilde{G}\tilde{O}^{-1}\tilde{F}\mathbf{1} \\ &= a(\theta_L, \theta_L) + \tilde{m}\frac{h^2}{t^2}\mathbf{1}^t\beta^t\left(\frac{h^2}{t^2}GO^{-1}FO^{-1}G + \tilde{m}FO^{-1}GO^{-1}F\right)\beta\mathbf{1}. \end{aligned}$$

Because F , G , and O are positive definite, so are $GO^{-1}FO^{-1}G$ and $FO^{-1}GO^{-1}F$. We can bound the quadratic forms of these two positive definite matrices by each other in terms of \tilde{m} , h , and t . We then find that $GO^{-1}FO^{-1}G$ is equivalent to $c^{-2}\mathbf{I}$ where $c := \tilde{m} + \frac{h^2}{t^2}$. Similarly, $FO^{-1}GO^{-1}F$ is equivalent to $c^{-2}\mathbf{I}$.

The Reissner-Mindlin energy is equivalent to

$$\begin{aligned} & a(\theta_L, \theta_L) + \tilde{m}\frac{h^2}{t^2}\mathbf{1}^t\beta^t\left(\frac{h^2}{t^2}c^{-2}\mathbf{I} + \tilde{m}c^{-2}\mathbf{I}\right)\beta\mathbf{1} \\ &= a(\theta_L, \theta_L) + \tilde{m}\frac{h^2}{t^2}\mathbf{1}^t\beta^t(c^{-1}\mathbf{I})\beta\mathbf{1} \\ &= a(\theta_L, \theta_L) + c^{-1}\tilde{m}\frac{h^2}{t^2}\mathbf{1}^t\beta^t\beta\mathbf{1} \\ &= a(\theta_L, \theta_L) + \frac{\tilde{m}}{\tilde{m}t^2 + h^2}h^2\mathbf{1}^t\beta^t\beta\mathbf{1}. \end{aligned}$$

Using the equivalence of $h^2\mathbf{1}^t\beta^t\beta\mathbf{1}$ and $\|\nabla w - \theta_L\|_{L^2(K)}^2$, the Reissner-Mindlin energy is equivalent to

$$a(\theta_L, \theta_L) + \frac{\tilde{m}\|\nabla w - \theta_L\|_{L^2(K)}^2}{\tilde{m}t^2 + h^2}. \quad (4.13)$$

Overall, we can conclude that minimizing the Reissner-Mindlin energy over the (θ_L, θ_B, w) space is equivalent to minimizing the expression of the equation (4.13) over the (θ_L, w) space. This is called the stabilized Reissner-Mindlin energy of the (θ_L, w) space.

There are two terms: $a(\theta_L, \theta_L)$ and $\frac{\tilde{m}}{\tilde{m}t^2 + h^2}\|\nabla w - \theta_L\|_{L^2}^2$ in the stabilized Reissner-Mindlin energy. The a-seminorm increases linearly with \tilde{m} and the ratio between the two terms is $\frac{1}{\tilde{m}t^2 + h^2}$. If $t = 0$, this ratio is $\frac{1}{h^2}$ and larger than 1. If this ratio is small, then the problem is close to the linear elasticity problem; this ratio should be large for Reissner-Mindlin plate problem to be physically reasonable. If t is sufficiently small, then we can find \tilde{h} such that $\tilde{m}t^2 + h^2 = \tilde{h}^2$ and we can consider the case of $t > 0$ as being similar to the case of $t = 0$ with a mesh size \tilde{h} .

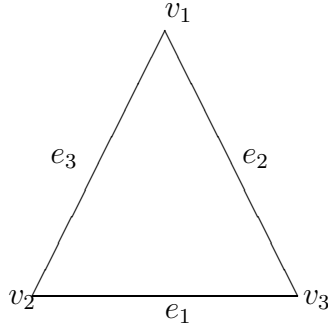


Figure 4.1: One subdomain and its vertices and edges.

Therefore, if t is bounded from above, we can consider t as being 0. In interesting problems for a Reissner-Mindlin plate, t is in this good range and we, therefore assume that t is 0 and $\Pi\theta = \nabla w$ from now on. Then, Reissner-Mindlin energy becomes

$$b(u, u) = a(\theta, \theta) \simeq a(\theta_L, \theta_L) + \frac{\tilde{m} \|\nabla w - \theta_L\|_{L^2(K)}^2}{h^2}$$

with the condition $\Pi\theta = \nabla w$.

4.4 The Coarse Problem

4.4.1 Coarse Basis Functions

We now provide details on our coarse basis functions. We define them on the interface and use their discrete harmonic extensions. We consider the subdomains Ω_i , one by one, to define the coarse basis functions. From now on, we consider only one of the floating subdomains Ω_i with $\partial\Omega_i \cap \partial\Omega = \emptyset$.

For each θ_i , $i = 1, 2$, we define a vertex basis function which vanishes at all interface nodes except at a subdomain vertex where its value is 1. We denote these vertex basis functions by θ_{i,v_k}^0 , $i = 1, 2$, $k = 1, 2, 3$. Because there are two components of θ , we have 6 vertex basis functions for each subdomain.

Lemma 14. *The Reissner-Mindlin energy of the vertex basis function θ_{i,v_k}^0 is bounded by $C\tilde{m}$ where C does not depend on H , h and δ , but depends on the shape regularity of the elements.*

Proof. We can find a bubble function θ_B such that the $\Pi\theta_B + \theta_L = 0$ where θ_L is a piecewise continuous linear functions with zero values at the interface and interior nodes except at the subdomain vertex being considered. This θ_B vanishes except in the elements which contain the subdomain vertex. The number of such elements are bounded by the shape regularity. The H^1 -seminorm of this function

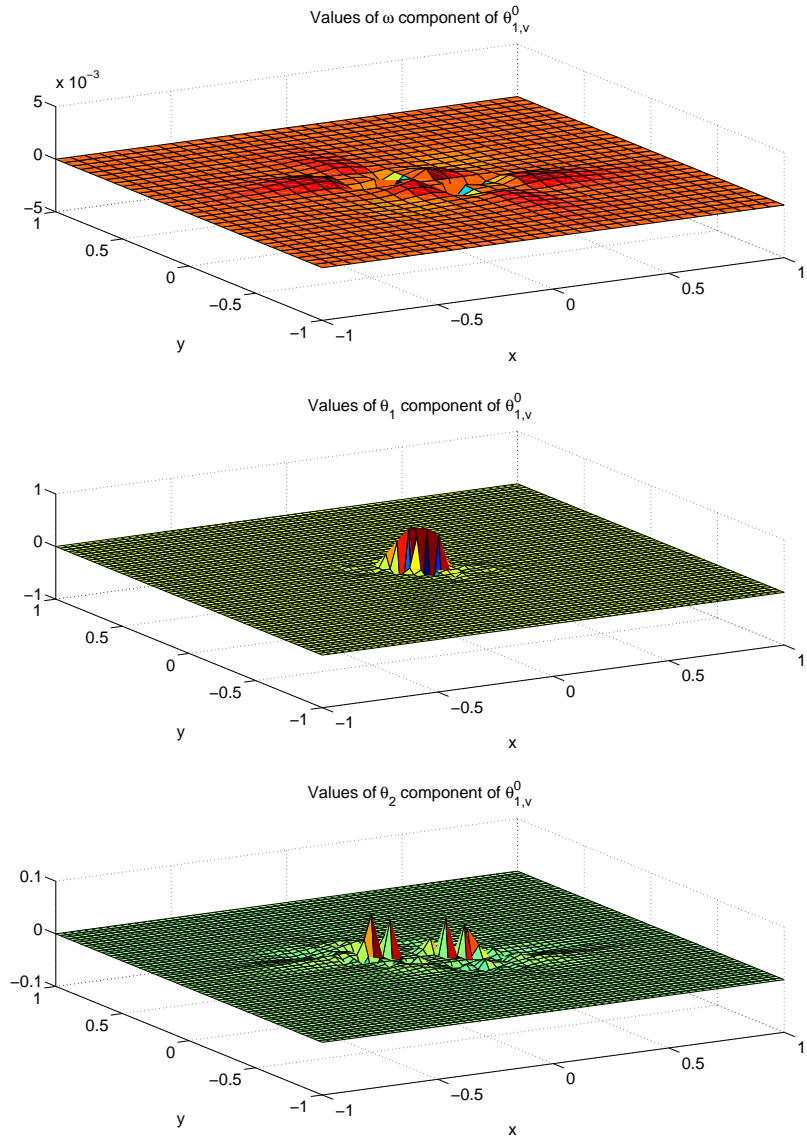


Figure 4.2: 3d plots of the θ vertex basis function $\theta_{1,v}^0$.

is bounded by a constant. Because $\nabla w = \Pi\theta$, the Reissner-Mindlin energy is equal to the square of the a-seminorm and we can bound the Reissner-Mindlin energy in terms of the square of the H^1 -seminorm. Because discrete harmonic functions have minimal energy, we can complete the proof. \square

For the other coarse basis functions, we need to prove several lemmas.

Lemma 15. *Let ξ_1, ξ_2, ξ_3 be the values of the barycentric functions of the subdomain at (x,y) . Let*

$$\Upsilon_i := \frac{\frac{1}{\xi_i^2}}{\frac{1}{\xi_1^2} + \frac{1}{\xi_2^2} + \frac{1}{\xi_3^2}}. \quad (4.14)$$

Then, the gradient of Υ_i is bounded by $\frac{C}{r}$ where r is the minimum distance to the two vertices of the edge e_i . The second order partial derivatives of Υ_i are bounded by $\frac{C}{r^2}$.

Proof. Without loss of generality, we prove the lemma for Υ_1 only. We use the Figure 4.1 of the triangle to define the indices of $e_1, e_2, e_3, v_1, v_2,$ and v_3 . Let $f := \xi_2^2 \xi_3^2$ and $g := \xi_1^2 \xi_2^2 + \xi_1^2 \xi_3^2$. Then,

$$\begin{aligned} \Upsilon_1 &= \frac{\frac{1}{\xi_1^2}}{\frac{1}{\xi_1^2} + \frac{1}{\xi_2^2} + \frac{1}{\xi_3^2}} \\ &= \frac{\xi_2^2 \xi_3^2}{\xi_2^2 \xi_3^2 + \xi_1^2 \xi_2^2 + \xi_1^2 \xi_3^2} \\ &= \frac{f}{f + g}. \end{aligned}$$

We can easily show that $f + g \geq C \min(\tilde{r}^2, r^2)$ where \tilde{r} is the minimum distance to the other vertex v_1 of the triangle which is not on the edge e_1 . Here, $\min(\tilde{r}, r)$ is the minimum distance to the three vertices of the triangle.

For f , we can also show that $f \leq Cr^2 \tilde{r}^4$.

We calculate the first order partial derivatives of f ,

$$\begin{aligned} f_x &= 2\xi_2 \xi_{2,x} \xi_3^2 + 2\xi_3 \xi_{3,x} \xi_2^2, \\ f_y &= 2\xi_2 \xi_{2,y} \xi_3^2 + 2\xi_3 \xi_{3,y} \xi_2^2, \end{aligned}$$

and find that $|f_x| \leq Cr\tilde{r}^3$ and $|f_y| \leq Cr\tilde{r}^3$.

The second order partial derivatives of f are

$$\begin{aligned}
f_{xx} &= 2((\xi_{2,x})^2\xi_3^2 + \xi_{2,xx}\xi_2\xi_3^2 + 2\xi_{3,x}\xi_{2,x}\xi_3\xi_2 \\
&\quad + (\xi_{3,x})^2\xi_2^2 + \xi_{3,xx}\xi_3\xi_2^2 + 2\xi_{2,x}\xi_{3,x}\xi_3\xi_2), \\
f_{xy} &= 2(\xi_{2,y}\xi_{2,x}\xi_3^2 + \xi_2\xi_{2,xy}\xi_3^2 + 2\xi_{2,x}\xi_{3,y}\xi_2\xi_3 \\
&\quad + \xi_{3,y}\xi_{3,x}\xi_2^2 + \xi_{3,xy}\xi_3\xi_2^2 + 2\xi_{3,x}\xi_{2,y}\xi_3\xi_2), \\
f_{yy} &= 2((\xi_{2,y})^2\xi_3^2 + \xi_{2,yy}\xi_2\xi_3^2 + 2\xi_{3,y}\xi_{2,y}\xi_3\xi_2 \\
&\quad + (\xi_{3,y})^2\xi_2^2 + \xi_{3,yy}\xi_3\xi_2^2 + 2\xi_{2,y}\xi_{3,y}\xi_3\xi_2),
\end{aligned}$$

and we find that $|f_{xx}|^2 \leq C\tilde{r}^2$, $|f_{xy}|^2 \leq C\tilde{r}^2$, and $|f_{yy}|^2 \leq C\tilde{r}^2$. Similarly, we can calculate the first and second order partial derivatives of g and obtain a bound of them by taking the maximum of the bounds of the two terms in g . We find that $|g| \leq Cr^2\tilde{r}^2$, $|g_x| \leq Cr\tilde{r}$, $|g_y| \leq Cr\tilde{r}$, $|g_{xx}|^2 \leq C$, $|g_{xy}|^2 \leq C$, and $|g_{yy}|^2 \leq C$.

We next calculate the partial derivative of Υ_1 with respect to x and find

$$\begin{aligned}
\frac{\partial\Upsilon_1}{\partial x} &= \frac{f_x(f+g) - f(f_x+g_x)}{(f+g)^2} \\
&= \frac{gf_x - fg_x}{(f+g)^2}.
\end{aligned}$$

If we use the bounds just derived, then

$$\begin{aligned}
\left|\frac{\partial\Upsilon_1}{\partial x}\right| &\leq \frac{Cr^2\tilde{r}^2r\tilde{r}^3 + Cr^2\tilde{r}^4r\tilde{r}}{C\min(r^2, \tilde{r}^2)^2} \\
&\leq Cr^3\tilde{r}^5\max(r^{-4}, \tilde{r}^{-4}) \\
&\leq C\max(r^{-1}\tilde{r}^5, r^3\tilde{r}) \\
&\leq C\max(r^{-1}, 1) \\
&\leq \frac{C}{r}.
\end{aligned}$$

Similarly, we get $|\frac{\partial\Upsilon_1}{\partial y}| \leq \frac{C}{r}$.

For the second order derivative of Υ_1 , we have

$$\begin{aligned}
\frac{\partial^2\Upsilon_1}{\partial x^2} &= \frac{(gf_{xx} + g_xf_x - f_xg_x - fg_{xx})(f+g)^2}{(f+g)^4} - \frac{2(f+g)(f_x+g_x)(gf_x - fg_x)}{(f+g)^4} \\
&= \frac{(gf_{xx} - fg_{xx})(f+g) - 2(f_x+g_x)(gf_x - fg_x)}{(f+g)^3}.
\end{aligned}$$

This can be bounded by

$$\begin{aligned}
\left| \frac{\partial^2 \Upsilon_1}{\partial x^2} \right| &\leq C \frac{(r^2 \tilde{r}^2 \tilde{r}^2 + r^2 \tilde{r}^4)(r^2 \tilde{r}^4 + r^2 \tilde{r}^2) + (r \tilde{r}^3 + r \tilde{r})(r^2 \tilde{r}^2 r \tilde{r}^3 + r^2 \tilde{r}^4 r \tilde{r})}{(f+g)^3} \\
&\leq C \frac{(r^2 \tilde{r}^4)(r^2 \tilde{r}^2) + (r \tilde{r})(r^3 \tilde{r}^5)}{(f+g)^3} \\
&\leq C \frac{r^4 \tilde{r}^6 + r^4 \tilde{r}^6}{\min(r^6, \tilde{r}^6)} \\
&\leq Cr^4 \tilde{r}^6 \max(r^{-6}, \tilde{r}^{-6}) \\
&\leq C \max(r^{-2} \tilde{r}^6, r^4) \\
&\leq C \max(r^{-2}, 1) \\
&\leq \frac{C}{r^2}.
\end{aligned}$$

Similarly, we get $|\frac{\partial^2 \Upsilon_1}{\partial y^2}| \leq \frac{C}{r^2}$.

Also,

$$\begin{aligned}
\frac{\partial^2 \Upsilon_1}{\partial x \partial y} &= \frac{(g_y f_x + g f_{xy} - f_y g_x - f g_{xy})(f+g)^2}{(f+g)^4} - \frac{2(f+g)(f_y + g_y)(g f_x - f g_x)}{(f+g)^4} \\
&= \frac{(g_y f_x + g f_{xy} - f_y g_x - f g_{xy})(f+g)}{(f+g)^4} - \frac{2(f_y + g_y)(g f_x - f g_x)}{(f+g)^3}.
\end{aligned}$$

This can be bounded by

$$\begin{aligned}
\left| \frac{\partial^2 \Upsilon_1}{\partial x \partial y} \right| &\leq C \frac{(r^2 \tilde{r}^4)(r^2 \tilde{r}^2) + (r \tilde{r})(r^3 \tilde{r}^5)}{(f+g)^3} \\
&\leq Cr^4 \tilde{r}^6 \max(r^{-6}, \tilde{r}^{-6}) \\
&\leq C \max(r^{-2} \tilde{r}^6, r^4) \\
&\leq \frac{C}{r^2}.
\end{aligned}$$

□

Lemma 16. *Under the same assumptions as in Lemma 15, the gradient of Υ_i , defined in (4.14), vanishes on the edges of a triangle.*

Proof. In the proof of Lemma 15, we have established that

$$\frac{\partial \Upsilon_1}{\partial x} = \frac{g f_x - f g_x}{(f+g)^2}$$

We have

$$\begin{aligned} gf_x &= (\xi_1^2 \xi_2^2 + \xi_1^2 \xi_3^2)(2\xi_2 \xi_{2,x} \xi_3^2 + 2\xi_3 \xi_{3,x} \xi_2^2) \\ &= 2\xi_1^2 \xi_2 \xi_3 (\xi_2^2 + \xi_3^2)(\xi_{2,x} \xi_3 + \xi_{3,x} \xi_2). \end{aligned}$$

Therefore, this term vanishes on the edges of a triangle. Similarly,

$$\begin{aligned} fg_x &= \xi_2^2 \xi_3^2 (2\xi_1 \xi_{1,x} \xi_2^2 + 2\xi_2 \xi_{2,x} \xi_1^2 + 2\xi_1 \xi_{1,x} \xi_3^2 + 2\xi_3 \xi_{3,x} \xi_1^2) \\ &= \xi_1 \xi_2^2 \xi_3^2 (2\xi_{1,x} \xi_2^2 + 2\xi_2 \xi_{2,x} \xi_1 + 2\xi_{1,x} \xi_3^2 + 2\xi_3 \xi_{3,x} \xi_1) \end{aligned}$$

which also vanishes on the edges. \square

Lemma 17. *Let Υ_i be the function defined by equation (4.14). Let M be a C^2 function on the closure of the triangle. For a given edge e_i , assume that M goes to 0 at least linearly at the two vertices of the edge e_i . Then, the gradient of $M\Upsilon_i$ is bounded by a constant and the second order partial derivatives of $M\Upsilon_i$ are bounded by $\frac{C}{r}$, where r is the minimum distance to the two vertices of the edge e_i . The value of $M\Upsilon_i$ is equal to that of M on the edge e_i and to 0 on the other edges. The gradient of $M\Upsilon_i$ is equal to that of M on the edge e_i and to 0 on the other edges.*

Proof. Let us consider the edge e_1 . Let $\tilde{M} = M\Upsilon_1$.

It is easy to see that the value of \tilde{M} is equal to that of M on the edge e_1 and to 0 on the other edges from the construction of Υ_1 .

By Lemma 16, on the edges of the triangle,

$$\begin{aligned} \frac{\partial \tilde{M}}{\partial x} &= \Upsilon_{1,x} M + \Upsilon_1 M_x \\ &= \Upsilon_1 M_x. \end{aligned}$$

Since Υ_1 vanishes on e_2 and e_3 and is equal to 1 on e_1 , we find that $\nabla(M\Upsilon_1) = \nabla M$ on the edge e_1 and that it vanishes on the other edges.

By Lemma 15, we can bound $|\frac{\partial \tilde{M}}{\partial x}|$ as

$$\begin{aligned} \left| \frac{\partial \tilde{M}}{\partial x} \right| &\leq |\Upsilon_{1,x} M| + |\Upsilon_1 M_x| \\ &\leq \frac{C}{r} r + C \\ &\leq C. \end{aligned}$$

Similarly, we have $|\frac{\partial \tilde{M}}{\partial y}| \leq C$.

If we use Lemma 16 again, we find that

$$\begin{aligned}
\left| \frac{\partial^2 \tilde{M}}{\partial x^2} \right| &\leq |\Upsilon_{1,xx} M| + 2|\Upsilon_{1,x} M_x| + |\Upsilon_1 M_{xx}| \\
&\leq \frac{C}{r^2} r + \frac{C}{r} + C \\
&\leq \frac{C}{r}.
\end{aligned}$$

Similarly, we have $|\frac{\partial^2 \tilde{M}}{\partial x \partial y}| \leq \frac{C}{r}$ and $|\frac{\partial^2 \tilde{M}}{\partial y^2}| \leq \frac{C}{r}$. \square

Lemma 18. *For a given vertex v_i , let e_j and e_k be the two edges adjacent to v_i . Let M_j and M_k be C^2 functions on the closure of the triangle going to 1 at least linearly at v_i . We also assume that M_j goes to 0 linearly at the other vertex of e_j and that M_k goes to 0 linearly at the other vertex of e_k . Let $\tilde{M} := \Upsilon_j M_j + \Upsilon_k M_k$. Then, $\nabla \tilde{M}$ is bounded by a constant and the second order partial derivatives of \tilde{M} are bounded by $\frac{C}{r}$, where r is the minimum distance to the vertices of the triangle. The value of \tilde{M} is equal to the value of M_j on the edge e_j , to the value of M_k on e_k , and vanishes on the third edge. The gradient of \tilde{M} is equal to the gradient of M_j on the edge e_j , to the gradient of M_k on the edge e_k , and vanishes on the other edge.*

Proof. Without loss of generality, we can assume that $j = 1$, $k = 2$, and $i = 3$. Let us define a linear function M_3 which vanishes on the edge e_3 and is equal to 1 at v_3 .

If we use the fact that $1 = \Upsilon_1 + \Upsilon_2 + \Upsilon_3$, we can express \tilde{M} as

$$\begin{aligned}
\tilde{M} &= \Upsilon_1 M_1 + \Upsilon_2 M_2 \\
&= \Upsilon_1 M_1 + \Upsilon_2 M_2 - M_3 + M_3 \\
&= \Upsilon_1 (M_1 - M_3) + \Upsilon_2 (M_2 - M_3) - \Upsilon_3 M_3 + M_3.
\end{aligned}$$

If we apply Lemma 17 to $\Upsilon_1 (M_1 - M_3)$, $\Upsilon_2 (M_2 - M_3)$, and $\Upsilon_3 M_3$, and add M_3 to the terms, we then can complete the proof. \square

We define a displacement vertex basis function $w_{v_k}^0$, $k = 1, 2, 3$, by giving w the value 1 at one of the subdomain vertices, 0 at the others, and making it linear on the edges of the subdomain. In addition to the definition of w on the interface, we give values for θ_i on the two edges of the subdomain vertex being considered such that $\theta = \frac{1}{\ell_j} \mathbf{t} \psi_{e_j}$ where ℓ_j is the length of the edge, \mathbf{t} the unit tangent vector of an edge adjacent to our chosen subdomain vertex, and ψ_{e_j} the edge cut-off function defined in section 2.7. Note that we make the value of θ equal to 0 at the subdomain vertices for continuity.

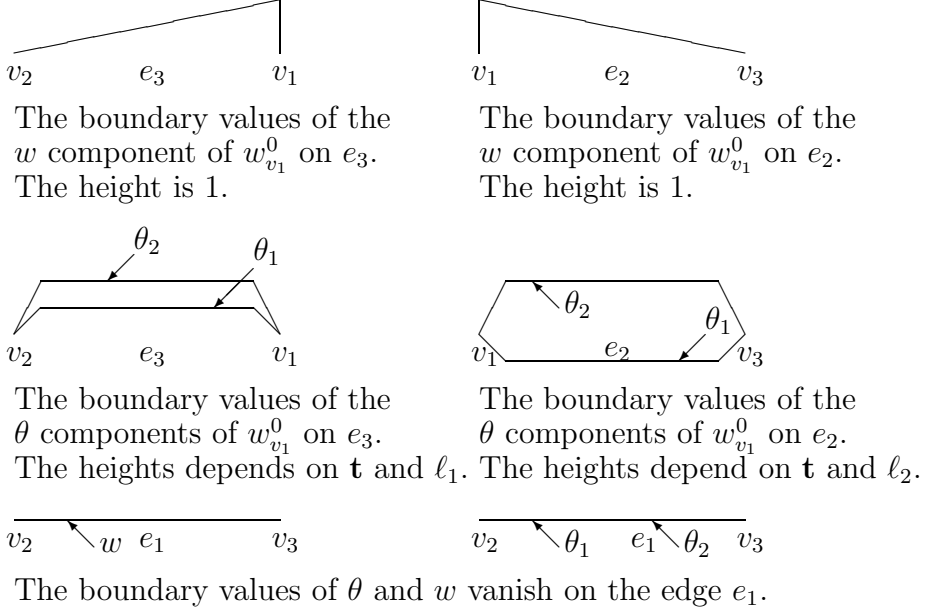


Figure 4.3: Values of $w_{v_1}^0$ on the interface.

Lemma 19. *The Reissner-Mindlin energy of the vertex basis function $w_{v_k}^0$ is bounded by $C \frac{\tilde{m}}{H^2} (1 + \log \frac{H}{h})$ where C does not depend on H , h , and δ , but depends on the shape regularity of the elements.*

Proof. Let us assume that the lengths of the three edges of a subdomain are ℓ_1, ℓ_2 , and ℓ_3 and that their relative lengths are bounded; this follows from the shape regularity of the subdomains. We first prove the lemma for $w_{v_1}^0$ using notation in Figure 4.1.

Let us assume that the vertex basis function has the value 1 at the vertex v_1 , and that the two edges e_2, e_3 of that vertex can be expressed by $a_2x + b_2y = c_2$ and $a_3x + b_3y = c_3$ respectively. (a_2, b_2) is the unit tangent vector of the edge e_2 from v_3 to v_1 , and (a_3, b_3) is the unit tangent vector of the edge e_3 from v_2 to v_1 and let (a'_i, b'_i) be the unit normal vector of the edge e_i .

Let again ξ_1, ξ_2, ξ_3 be the values of barycentric functions of the subdomain at (x, y) . Let

$$w_i = \frac{\frac{1}{\xi_i^2}}{\frac{1}{\xi_1^2} + \frac{1}{\xi_2^2} + \frac{1}{\xi_3^2}} \left(\frac{a_i}{\ell_i} x + \frac{b_i}{\ell_i} y + c_i \right)$$

for $i = 2, 3$, where c_i is chosen so that the equation $\frac{a_i}{\ell_i} x + \frac{b_i}{\ell_i} y + c_i = 1$ at our chosen vertex v_1 . Further, let $w = w_2 + w_3$. From Lemma 18, we know that w satisfies the boundary condition prescribed by the definitions of the basis function given above. We also know that the gradient of w is bounded by $\frac{C}{H}$ and that the

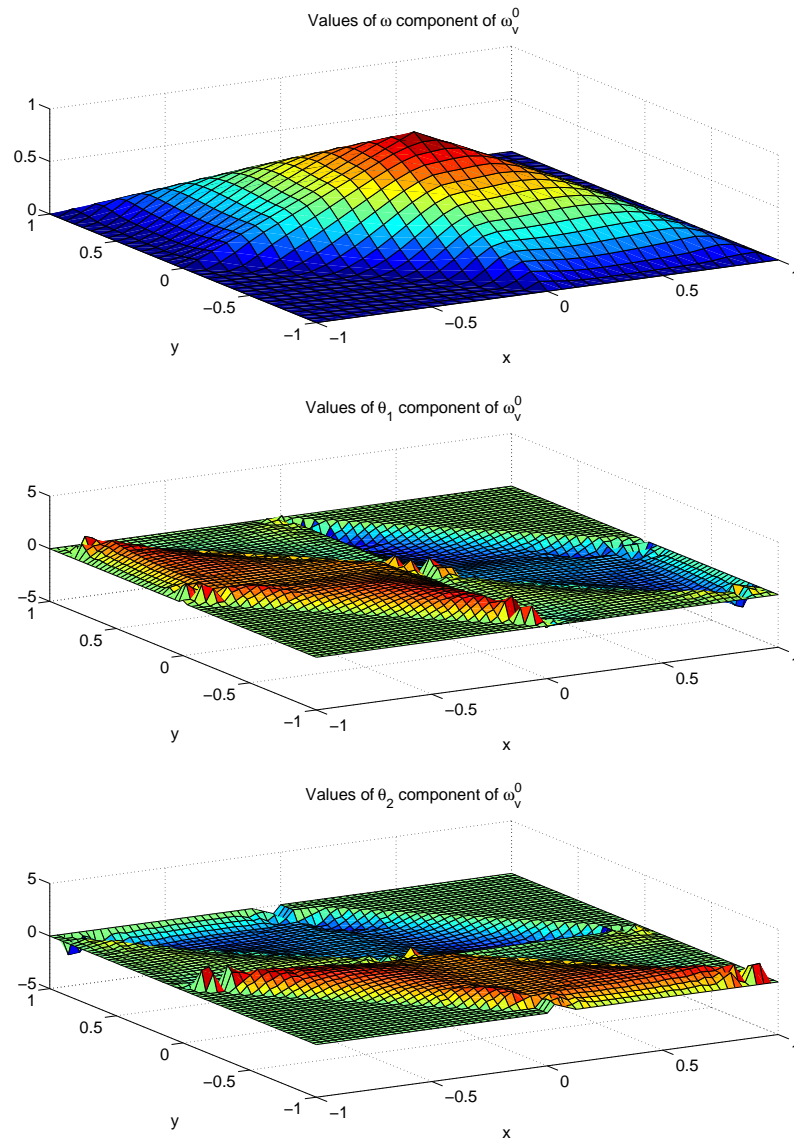


Figure 4.4: 3d plots of the w vertex basis function w_v^0 .

second derivatives of w are bounded by $\frac{C}{Hr}$ where r is the minimum distance to the vertices.

Then, define $w_h = \tilde{I}^h(w)$ and $\theta_L = I^h(\nabla w)$ on each element of the subdomain except in the elements next to each vertex where θ_L is defined by the linear components of θ . Here \tilde{I}^h is the standard second order interpolation operator to M_1^2 and I^h is the standard first order interpolation operator to \mathbf{M}_1^1 , see subsection 3.3.3 for the definitions of M_1^2 and \mathbf{M}_1^1 . We can easily find bubble functions by using the equation $\Pi\theta = \nabla w$ on each element. Because the scaling does not affect the H^1 -seminorm and there are a bounded number of elements next to any vertex because of the shape regularity, we can bound the a-seminorm of the basis function on the elements next to the vertices easily as in Lemma 14.

For each element K which does not touch a subdomain vertex, we have

$$|\theta_L|_{H^1(K)}^2 \leq \|\nabla^2 w\|_{L^2(K)}^2.$$

Therefore,

$$\begin{aligned} |\theta_L|_{H^1(\Omega_i)}^2 &\leq C \int_0^{2\pi} \int_{ch}^H \frac{1}{H^2 r^2} r dr d\theta + C \\ &\leq \frac{C}{H^2} (1 + \log \frac{H}{h}) + C. \end{aligned}$$

For the bubble function θ_B , we know that

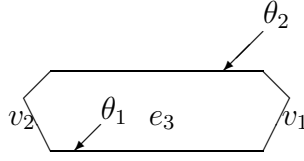
$$\Pi\theta_B = \nabla w_h - \theta_L = \nabla(\tilde{I}^h w) - I^h(\nabla w) = \nabla(\tilde{I}^h w - w) + (\nabla w - I^h(\nabla w)).$$

Therefore for each element K , which does not touch a subdomain vertex,

$$\begin{aligned} |\theta_B|_{H^1(K)}^2 &\leq \frac{C}{h^2} \|\theta_B\|_{L^2(K)}^2 \\ &\leq \frac{C}{h^2} (\|\nabla(\tilde{I}^h w - w)\|_{L^2(K)}^2 + \|\nabla w - I^h(\nabla w)\|_{L^2(K)}^2) \\ &\leq C (\|\nabla(\tilde{I}^h w - w)\|_{L^\infty(K)}^2 + \|\nabla w - I^h(\nabla w)\|_{L^\infty(K)}^2) \\ &\leq Ch^2 \|\nabla^2 w\|_{L^\infty(K)}^2 \\ &\leq C \frac{h^2}{H^2 r^2}. \end{aligned}$$

There are on the order of $\frac{H^2}{h^2}$ elements in each subdomain and the number of elements with a distance r from a vertex is about $\frac{r}{h}$. Therefore, to bound $|\theta_B|_{H^1(\Omega_i)}^2$, we need to estimate

$$C \sum_{i=1}^{\frac{H}{h}} \frac{1}{H^2} \frac{ih}{h} \frac{h^2}{i^2 h^2} = C \sum_{i=1}^{\frac{H}{h}} \frac{1}{H^2} \frac{h}{ih}$$



Boundary values of θ of $\theta_{e_3}^0$ on e_3 .
 All other boundary values of θ and w of $\theta_{e_3}^0$ are 0.

Figure 4.5: Values of $\theta_{e_3}^0$ on the interface.

where $r = ih$. This sum is bounded by $\frac{C}{H^2}(1 + \log\frac{H}{h})$.

In total, the square of the H^1 -seminorm of the function in the proof is bounded by $\frac{C}{H^2}(1 + \log\frac{H}{h})$. Because we choose θ and w such that $\Pi\theta = \nabla w$, we can bound the Reissner-Mindlin energy by $\frac{C\tilde{m}}{H^2}(1 + \log\frac{H}{h})$.

We can prove similar bounds for $w_{v_2}^0$ and $w_{v_3}^0$. \square

We define a rotational edge basis function $\theta_{e_k}^0$, $k = 1, 2, 3$, for each edge e_k by prescribing $\theta = \mathbf{n}\psi_{e_k}$ where \mathbf{n} is the unit normal vector of the edge e_k pointing into the right half plane, and ψ_{e_k} is the edge cut-off function. We set all the boundary values of w to zero.

Lemma 20. *The Reissner-Mindlin energy of the edge basis function $\theta_{e_k}^0$ is bounded by $C\tilde{m}(1 + \log\frac{H}{h})$ where C does not depend on H , h , and δ , but depends on the shape regularity of the elements of the subdomain.*

Proof. We have the same assumptions as in the proof of Lemma 19. Consider

$$w_k := \frac{\frac{1}{\xi_k^2}}{\frac{1}{\xi_1^2} + \frac{1}{\xi_2^2} + \frac{1}{\xi_3^2}}(a'_k x + b'_k y + c'_k)$$

where c'_k is chosen so that $w_k = 0$ on the edge e_k . As in Lemma 19, we can prove that the square of the H^1 -seminorm of this function is bounded by $C(1 + \log(\frac{H}{h}))$ using Lemma 17 instead of Lemma 18. \square

4.4.2 Coarse Interpolant in Stable Decomposition

In total, we have 9 vertex basis functions and 3 edge basis functions. Therefore, on average, we have 3 basis functions for each subdomain.

We now define a coarse interpolant u^0 by

$$u^0 = \sum_{k=1}^3 w(v_k)w_{v_k}^0 + \sum_{i=1}^2 \sum_{k=1}^3 \theta_i(v_k)\theta_{i,v_k}^0 + \sum_{k=1}^3 \frac{\int_{e_k} (I^h(\theta\psi_{e_k}) \cdot \mathbf{n}) ds}{\int_{e_k} \psi_{e_k} ds} \theta_{e_k}^0. \quad (4.15)$$

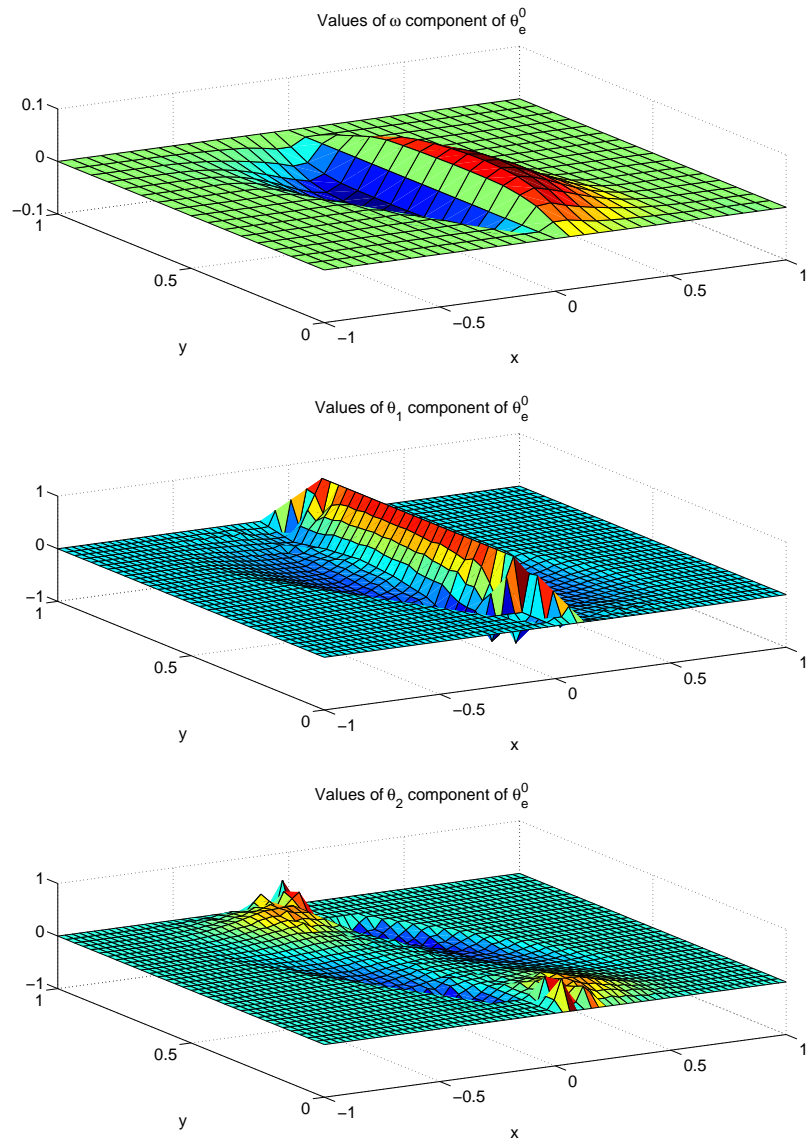


Figure 4.6: 3d plots of the θ edge basis function θ_e^0 .

We can easily check that this coarse interpolant reproduces all functions in the null space of the Reissner-Mindlin energy and thus satisfies the null space property, cf. [45].

From [47, remark 4.13], we know that

$$\|u\|_{L^\infty(\Omega_i)}^2 \leq C(1 + \log \frac{H}{h}) \|u\|_{H^1(\Omega_i)}^2, \quad u \in H^1(\Omega_i) \cap V. \quad (4.16)$$

And it is easy to prove that

$$\|u\|_{L^2(e)}^2 \leq 2H \|u\|_{H^1(\Omega_i)}^2$$

where e is an edge and that

$$\left| \frac{\int_e (I^h(u\psi_e) \cdot \mathbf{n}) ds}{\int_e \psi_e ds} \right| \leq C \sqrt{\int_e \frac{u^2}{H^2} ds} \sqrt{H} \leq C \frac{\|u\|_{L^2(e)}}{\sqrt{H}} \leq C\sqrt{2} \|u\|_{H^1(\Omega_i)}. \quad (4.17)$$

Using inequalities (4.16) and (4.17) and Lemmas 14, 19, and 20 of this section to bound the energy of the coarse interpolant (4.15), we obtain the following bound:

$$b(u^0, u^0)_{\Omega_i} \leq \frac{C\tilde{m}}{H^2} (1 + \log \frac{H}{h})^2 \|w\|_{H^1(\Omega_i)}^2 + C\tilde{m} (1 + \log \frac{H}{h})^2 \|\theta\|_{H^1(\Omega_i)}^2.$$

Using the equation $\nabla w = \Pi\theta$, we can show that

$$\frac{\|\nabla w\|_{L^2(\Omega_i)}^2}{H^2} \leq \frac{4\|\theta\|_{L^2(\Omega_i)}^2}{H^2}.$$

Because u^0 reproduces all the null space functions, we can use a Poincaré inequality by shifting by some null space functions and find that

$$\begin{aligned} b(u^0, u^0)_{\Omega_i} &\leq \frac{C\tilde{m}}{H^2} (1 + \log \frac{H}{h})^2 \|w\|_{H^1(\Omega_i)}^2 + C\tilde{m} (1 + \log \frac{H}{h})^2 \|\theta\|_{H^1(\Omega_i)}^2 \\ &\leq C\tilde{m} (1 + \log \frac{H}{h})^2 \|\theta\|_{H^1(\Omega_i)}^2. \end{aligned} \quad (4.18)$$

Lemma 21. *Under the condition of $\Pi\theta = \nabla w$, the a -seminorm and the H^1 -seminorm are equivalent for θ . This equivalence does not depend on H and h but depends on the shape regularity of elements and the Lamé constants. In particular, we have the relation $\|\theta\|_{H^1(\Omega_i)}^2 \leq \frac{C}{\mu} a(\theta, \theta)$.*

Proof. We can prove this lemma on each element of diameter h . Let us consider one element only and assume that one of its nodes is at $(0, 0)$. Then, we can use the following transformation to the reference element:

$$\begin{aligned}\tilde{w}(x, y) &= \frac{1}{h}(w(hx, hy) - w(0, 0)) + w(0, 0), \\ \tilde{\theta}(x, y) &= \theta(hx, hy).\end{aligned}$$

Then, $\nabla \tilde{w}(x, y) = \nabla w(hx, hy) = \Pi\theta(hx, hy) = \Pi\tilde{\theta}(x, y)$ on the reference element. We can easily see that the a -seminorm and the H^1 -seminorm are invariant under this dilation. Therefore, it is enough to prove the lemma on the reference element.

On each element, we have 12 basis functions for θ . Among them are three null basis functions for $a(\theta, \theta)$ and two null basis functions for the H^1 -norm. Two of these null basis functions are common. The remaining null basis function for $a(\theta, \theta)$ is $(-y, x)$ and this is not a valid basis function for this problem because of the condition $\nabla w = \Pi\theta$.

Because we consider a finite dimensional problem and the null space of the two seminorms are the same, the two seminorms are equivalent and we get the bound $|\theta|_{H^1(\Omega_i)}^2 \leq \frac{C}{\mu} a(\theta, \theta)$. \square

Using Lemma 21 and inequality (4.18), we can prove that

$$b(u^0, u^0)_{\Omega_i} \leq C \frac{\tilde{m}}{\mu} (1 + \log \frac{H}{h})^2 b(u, u)_{\Omega_i}. \quad (4.19)$$

We note that if the material becomes more incompressible, the decomposition becomes less stable.

If $\partial\Omega_i \cap \partial\Omega \neq \emptyset$ with a strictly positive measure, we can define similar basis functions except on $\partial\Omega$. In such a subdomain, we can prove a bound of the square of the a -seminorm by using a Friedrichs inequality.

If $\partial\Omega_i$ intersects $\partial\Omega$ only at one or a few points, we need to modify the proof. Let us assume that $\partial\Omega_i$ intersects $\partial\Omega$ at $(0, 0)$. Let us find $\bar{\theta}_1 x + \bar{\theta}_2 y + \hat{w}$ such that $\bar{\theta}_1 = \int_{\Omega_i} \theta_1 dx dy$, $\bar{\theta}_2 = \int_{\Omega_i} \theta_2 dx dy$, and $\hat{w} = \int_{\Omega_i} (w - \bar{\theta}_1 x - \bar{\theta}_2 y) dx dy$. Because θ_1 vanishes at a point, we have that

$$\begin{aligned}\|\theta_1\|_{L^\infty(\Omega_i)} &\leq \|\theta_1 - \bar{\theta}_1\|_{L^\infty(\Omega_i)} + |\bar{\theta}_1| \\ &\leq 2\|\theta_1 - \bar{\theta}_1\|_{L^\infty(\Omega_i)} \\ &\leq C \sqrt{1 + \log \frac{H}{h}} \|\theta_1 - \bar{\theta}_1\|_{H^1(\Omega_i)} \\ &\leq C \sqrt{1 + \log \frac{H}{h}} |\theta_1|_{H^1(\Omega_i)}\end{aligned} \quad (4.20)$$

which is a variation of inequality (4.16). Similarly, we have

$$\|\theta_2\|_{L^\infty(\Omega_i)}^2 \leq C(1 + \log \frac{H}{h})|\theta_2|_{H^1(\Omega_i)}^2 \quad (4.21)$$

We also have that

$$\int_e \frac{\theta \cdot n}{\ell} ds \leq C\|\theta\|_{L^\infty(\Omega_i)} \leq C\sqrt{1 + \log \frac{H}{h}}|\theta|_{H^1(\Omega_i)}. \quad (4.22)$$

which is a variation of inequality (4.17).

For w , we have

$$\begin{aligned} \|w\|_{L^\infty(\Omega_i)} &\leq \|w - \bar{\theta}_1 x - \bar{\theta}_2 y - \hat{w}\|_{L^\infty(\Omega_i)} + |\hat{w}| + \|\bar{\theta}_1 x + \bar{\theta}_2 y\|_{L^\infty(\Omega_i)} \\ &\leq 2\|w - \bar{\theta}_1 x - \bar{\theta}_2 y - \hat{w}\|_{L^\infty(\Omega_i)} + (|\bar{\theta}_1| + |\bar{\theta}_2|)H \\ &\leq C\sqrt{1 + \log \frac{H}{h}}\|w - \bar{\theta}_1 x - \bar{\theta}_2 y - \hat{w}\|_{H^1(\Omega_i)} + (|\bar{\theta}_1| + |\bar{\theta}_2|)H \\ &\leq C\sqrt{1 + \log \frac{H}{h}}|w - \bar{\theta}_1 x - \bar{\theta}_2 y - \hat{w}|_{H^1(\Omega_i)} + (|\bar{\theta}_1| + |\bar{\theta}_2|)H. \end{aligned} \quad (4.23)$$

Using the equation $\nabla(w - \bar{\theta}_1 x - \bar{\theta}_2 y - \hat{w}) = \Pi(\theta - (\bar{\theta}_1, \bar{\theta}_2))$, we can show that

$$\|\nabla(w - \bar{\theta}_1 x - \bar{\theta}_2 y - \hat{w})\|_{L^2(\Omega_i)}^2 \leq 4\|\theta - (\bar{\theta}_1, \bar{\theta}_2)\|_{L^2(\Omega_i)}^2.$$

The first term of (4.23) is bounded by

$$C\sqrt{1 + \log \frac{H}{h}}\|\theta - (\bar{\theta}_1, \bar{\theta}_2)\|_{L^2(\Omega_i)} \leq CH\sqrt{1 + \log \frac{H}{h}}|\theta|_{H^1(\Omega_i)}$$

by the Poincaré inequality. Also,

$$|\bar{\theta}_1| \leq H^2\|\theta_1\|_{L^\infty(\Omega_i)} \leq CH^2\sqrt{1 + \log \frac{H}{h}}|\theta_1|_{H^1(\Omega_i)}$$

We can obtain a similar bound for $|\bar{\theta}_2|$ and

$$\|w\|_{L^\infty(\Omega_i)} \leq CH\sqrt{1 + \log \frac{H}{h}}|\theta|_{H^1(\Omega_i)}. \quad (4.24)$$

Using Lemmas 14, 19, and 20 of this section and inequalities (4.20), (4.21), (4.24), and (4.22) instead of (4.16) and (4.17), we obtain the following bound:

$$b(u^0, u^0)_{\Omega_i} \leq C\tilde{m}(1 + \log \frac{H}{h})^2|\theta|_{H^1(\Omega_i)}^2. \quad (4.25)$$

Using Lemma 21 and inequality (4.25), we can prove that

$$b(u^0, u^0)_{\Omega_i} \leq C\frac{\tilde{m}}{\mu}(1 + \log \frac{H}{h})^2 b(u, u)_{\Omega_i}. \quad (4.26)$$

4.4.3 Additional Coarse Basis Functions

We can also define a w edge basis function on each edge. These basis functions are not necessary in our proof, however they make the constant in decomposition smaller. We will compare numerical results of the additive method with such w edge basis functions with results without them in section 4.10. In our experiments, the condition numbers of the preconditioned system with these additional basis functions are much smaller than those without.

On each edge of a subdomain, we prescribe the values of a quadratic which vanishes at the two subdomain vertices of the edge and has a maximum of 1 on the edge. In addition to the definition of w on the interface, we give values for θ in the subdomain such that $\theta = (\mathbf{t} \cdot \nabla w) \mathbf{t} \psi_{e_k}$ where \mathbf{t} is the unit tangent vector of the edge and ψ_{e_k} is the edge cut-off function. We denote these basis functions by $w_{e_k}^0$, $k = 1, 2, 3$.

Lemma 22. *The Reissner-Mindlin energy of the edge basis function $w_{e_k}^0$ is bounded by $\frac{C\tilde{m}}{H^2}(1 + \log\frac{H}{h})$ where C does not depend on H , h , and δ , but depends on the shape regularity of the elements of the subdomain.*

Proof. We have the same assumptions as in the proof of Lemma 19. w_i is defined by $\frac{\frac{1}{\xi_i^2}}{\frac{1}{\xi_1^2} + \frac{1}{\xi_2^2} + \frac{1}{\xi_3^2}} g(x, y)$ where $g(x, y)$ is the second order polynomial of (x, y) chosen so that $g(x, y)$ is 1 at the midpoint of the edge being considered and vanishes at all vertices and the midpoints of the other edges. $g(x, y)$ is the standard basis function in P_2 with a midpoint node. As in Lemma 19, we can prove that the square of the H^1 -seminorm of this function is bounded by $\frac{C}{H^2}(1 + \log\frac{H}{h})$ using Lemma 17 instead of Lemma 18. \square

Similarly, we can define θ edge basis functions related to the normal direction. But they did not give much improvement in our numerical experiments.

4.5 Local Problems

Let $w_d = w - w^0$, $\theta_{dL} = \theta_L - \theta_L^0$, and $\Pi\theta_{dB} = \nabla w_d - \theta_{dL}$. Then, $\Pi\theta_d = \theta_{dL} + \Pi\theta_{dB} = \nabla w_d$.

From Lemma 21 and inequality (4.19), we know that

$$|\theta_d|_{H^1(\Omega_i)}^2 \leq C \frac{\tilde{m}}{\mu^2} (1 + \log\frac{H}{h})^2 a(\theta, \theta)_{\Omega_i}. \quad (4.27)$$

If we use the Friedrichs inequality, we obtain

$$\|\theta_d\|_{L^2(\Omega_i)}^2 \leq C \frac{\tilde{m}}{\mu^2} (1 + \log\frac{H}{h})^2 H_i^2 a(\theta, \theta)_{\Omega_i}. \quad (4.28)$$

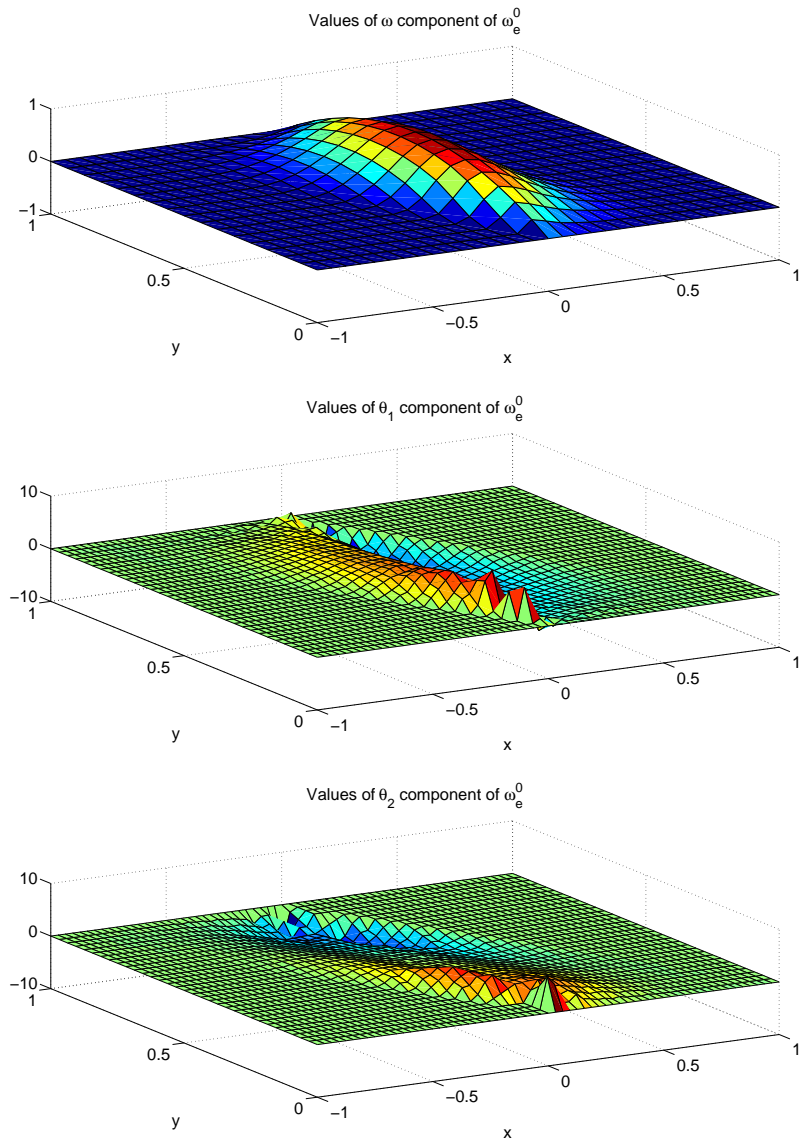


Figure 4.7: 3d plots of the w edge basis function w_e^0 .

From the equation $\Pi\theta = \nabla w$, we have the inequality $\|\nabla w\|_{L^2(\Omega_i)}^2 \leq \|\theta\|_{L^2(\Omega_i)}^2$. Therefore,

$$\|w_d\|_{H^1(\Omega_i)}^2 \leq C \frac{\tilde{m}}{\mu^2} (1 + \log \frac{H}{h})^2 H_i^2 a(\theta, \theta)_{\Omega_i}. \quad (4.29)$$

Similarly,

$$\|w_d\|_{L^2(\Omega_i)}^2 \leq C \frac{\tilde{m}}{\mu^2} (1 + \log \frac{H}{h})^2 H_i^4 a(\theta, \theta)_{\Omega_i}. \quad (4.30)$$

Let χ_i be nonnegative C^∞ functions in \mathbb{R}^2 such that

$$\begin{aligned} \chi_j &= 0 \text{ on } \Omega \setminus \Omega_j, \\ \sum_{j=1}^N \chi_j &= 1 \text{ on } \bar{\Omega}, \\ \|\nabla \chi_j\|_{L^\infty} &\leq C \delta_j^{-1}, \\ \|\nabla^2 \chi_j\|_{L^\infty} &\leq C \delta_j^{-2}. \end{aligned}$$

The construction of χ_j is standard, cf. [11].

We define the local components of the Schwarz decomposition as follows: $w_j := \tilde{I}^h(\chi_j w_d)$ and $\theta_{Lj} := I^h(\chi_j \theta_{dL} + w_d \nabla \chi_j)$. Here \tilde{I}^h is the standard interpolator onto the piecewise quadratic continuous functions on each element and I^h is the standard interpolator onto the piecewise linear continuous functions on each element as in Lemma 19. Because $\sum_j \chi_j = 1$ and $\sum_j \nabla \chi_j = 0$, the above formulas provide a decomposition. For the bubble functions, we use the condition $\nabla w = \Pi\theta$.

We need to use Lemma 9 of section 2.6 for the overlapping region. We know that derivatives of χ_j are nonzero only in a δ -neighborhood of the boundary of subdomains. We find using (4.27), (4.28), (4.29), and (4.30), that

$$\begin{aligned}
|\theta_{Lj}|_{H^1(\Omega_i)}^2 &= \|\nabla I^h(\chi_j \theta_{dL} + w_d \nabla \chi_j)\|_{L^2(\Omega_i)}^2 \\
&\leq \|\nabla(\chi_j \theta_{dL} + w_d \nabla \chi_j)\|_{L^2(\Omega_i)}^2 \\
&\leq C(\|\theta_{dL} \nabla \chi_j\|_{L^2(\Omega_i)}^2 + \|\chi_j \nabla \theta_{dL}\|_{L^2(\Omega_i)}^2 + \\
&\quad \|w_d \nabla^2 \chi_j\|_{L^2(\Omega_i)}^2 + \|\nabla \chi_j \nabla w_d\|_{L^2(\Omega_i)}^2) \\
&\leq C\left(\frac{1}{\delta_i^2} \|\theta_{dL}\|_{L^2(\Omega_i)}^2 + \|\nabla \theta_{dL}\|_{L^2(\Omega_i)}^2 + \right. \\
&\quad \left. \frac{1}{\delta_i^4} \|w_d\|_{L^2(\Omega_i, \delta_i)}^2 + \frac{1}{\delta_i^2} \|\nabla w_d\|_{L^2(\Omega_i)}^2\right) \\
&\leq C\left(\frac{1}{\delta_i^2} \|\theta_d\|_{L^2(\Omega_i)}^2 + \|\nabla \theta_d\|_{L^2(\Omega_i)}^2 + \right. \\
&\quad \left. \frac{1}{\delta_i^2} \left(1 + \frac{H_i}{\delta_i}\right) \|w_d\|_{H^1(B(\Omega'_i))}^2 + \frac{1}{\delta_i^2} \|w_d\|_{H^1(\Omega_i)}^2\right) \\
&\leq C \frac{\tilde{m}}{\mu^2} \left(\left(1 + \log \frac{H}{h}\right)^2 \frac{H_i^2}{\delta_i^2} a(\theta, \theta)_{\Omega_i} + \left(1 + \log \frac{H}{h}\right)^2 a(\theta, \theta)_{\Omega_i} + \right. \\
&\quad \left. \left(1 + \log \frac{H}{h}\right)^2 \left(1 + \frac{H}{\delta}\right)^3 a(\theta, \theta)_{B(\Omega'_i)} + \left(1 + \log \frac{H}{h}\right)^2 \left(\frac{H}{\delta}\right)^2 a(\theta, \theta)_{\Omega_i} \right) \\
&\leq C \frac{\tilde{m}}{\mu^2} \left(1 + \frac{H}{\delta}\right)^3 \left(1 + \log \frac{H}{h}\right)^2 b(u, u)_{B(\Omega'_i)}. \tag{4.31}
\end{aligned}$$

For the bubble functions on each element, we have

$$\begin{aligned}
|\theta_{Bj}|_{H^1(K)}^2 &\leq \frac{C}{h^2} \|\theta_{Bj}\|_{L^2(K)}^2 \\
&\leq \frac{C}{h^2} \|\nabla w_j - \theta_{Lj}\|_{L^2(K)}^2 \\
&= \frac{C}{h^2} \|\nabla(\tilde{I}^h(\chi_j w_d)) - I^h(\chi_j \theta_{dL} + w_d \nabla \chi_j)\|_{L^2(K)}^2 \\
&\leq \frac{C}{h^2} \|\nabla(\tilde{I}^h(\chi_j w_d)) - \nabla(\chi_j w_d) + \nabla(\chi_j w_d) \\
&\quad - I^h(\chi_j \theta_{dL} + w_d \nabla \chi_j)\|_{L^2(K)}^2 \\
&\leq \frac{C}{h^2} \|\nabla(\tilde{I}^h(\chi_j w_d)) - \nabla(\chi_j w_d)\|_{L^2(K)}^2 \\
&\quad + \frac{C}{h^2} \|\chi_j \nabla w_d - I^h(\chi_j \theta_{dL})\|_{L^2(K)}^2 \\
&\quad + \frac{C}{h^2} \|w_d \nabla \chi_j - I^h(w_d \nabla \chi_j)\|_{L^2(K)}^2. \tag{4.32}
\end{aligned}$$

The first term of (4.32) can be bounded by

$$\begin{aligned}
& C \|\nabla^2(\chi_j w_d)\|_{L^2(K)}^2 \\
& \leq C \|w_d \nabla^2 \chi_j + 2 \nabla \chi_j \nabla w_d + \chi_j \nabla^2(w_d)\|_{L^2(K)}^2 \\
& \leq C \|w_d \nabla^2 \chi_j\|_{L^2(K)}^2 + 2 \|\nabla \chi_j \nabla w_d\|_{L^2(K)}^2 + \|\chi_j \nabla \theta_d\|_{L^2(K)}^2.
\end{aligned}$$

If we add the above bound over the subdomain Ω_i , we then have

$$\begin{aligned}
\frac{C}{h^2} \|\nabla(\tilde{I}^h(\chi_j w_d)) - \nabla(\chi_j w_d)\|_{L^2(\Omega_i)}^2 & \\
& \leq C \left(\frac{1}{\delta_i^4} \|w_d\|_{L^2(\Omega_{i,\delta_i})}^2 + \frac{1}{\delta_i^2} \|\nabla w_d\|_{L^2(\Omega_{i,\delta_i})}^2 + \|\nabla \theta_d\|_{L^2(\Omega_i)}^2 \right) \\
& \leq C \frac{\tilde{m}}{\mu^2} \left(1 + \frac{H}{\delta}\right)^3 \left(1 + \log \frac{H}{h}\right)^2 b(u, u)_{B(\Omega'_i)}. \tag{4.33}
\end{aligned}$$

The second term of (4.32) is bounded similarly by

$$\begin{aligned}
\frac{C}{h^2} \|\chi_j \nabla w_d - I^h(\chi_j \theta_{dL})\|_{L^2(K)}^2 & \\
& \leq \frac{C}{h^2} \|\chi_j \nabla w_d - \chi_j \theta_{dL}\|_{L^2(K)}^2 + \frac{C}{h^2} \|\chi_j \theta_{dL} - I^h(\chi_j \theta_{dL})\|_{L^2(K)}^2 \\
& \leq \frac{C}{h^2} \|\chi_j \theta_{dB}\|_{L^2(K)}^2 + \frac{C}{h^2} \|\chi_j \theta_{dL} - I^h(\chi_j \theta_{dL})\|_{L^2(K)}^2 \\
& \leq C |\theta_{dB}|_{H^1(K)}^2 + C \|\nabla(\chi_j \theta_{dL})\|_{L^2(K)}^2.
\end{aligned}$$

Therefore, using the bound for the linear part of the θ in (4.33), we have

$$\begin{aligned}
\frac{C}{h^2} \|\chi_j \nabla w_d - I^h(\chi_j \theta_{dL})\|_{L^2(\Omega_i)}^2 & \\
& \leq C \frac{\tilde{m}}{\mu^2} \left(1 + \frac{H}{\delta}\right)^3 \left(1 + \log \frac{H}{h}\right)^2 b(u, u)_{B(\Omega'_i)}. \tag{4.34}
\end{aligned}$$

We can bound the sum of the third term of (4.32) over Ω_i by

$$\frac{C}{\mu^2} \left(1 + \frac{H}{\delta}\right)^3 \left(1 + \log \frac{H}{h}\right)^2 b(u, u)_{B(\Omega'_i)}.$$

4.6 The Additive and Multiplicative Operators

In total, we have the bound

$$\begin{aligned}
\sum_{j=0}^N b(u_j, u_j)_{\Omega_i} & \leq C \tilde{m} \sum_{j=0}^N |\theta_j|_{H^1(\Omega_i)}^2 \\
& \leq C \frac{\tilde{m}^2}{\mu^2} \left(1 + \frac{H}{\delta}\right)^3 \left(1 + \log \frac{H}{h}\right)^2 b(u, u)_{B(\Omega'_i)}.
\end{aligned}$$

Summing over the subdomains, the decomposition is stable with the bound

$$C_0^2 \leq C \left(\frac{\tilde{m}}{\mu}\right)^2 \left(1 + \frac{H}{\delta}\right)^3 \left(1 + \log \frac{H}{h}\right)^2.$$

Therefore, our overlapping method satisfies Assumption 1. Because we use exact solvers, Assumptions 2 and 3 are automatically satisfied. We can define the additive operator by (2.5) and the multiplicative operator by (2.6) and (2.7). We can use Theorem 4 to get a bound of the condition number of the additive operator.

Theorem 14. *In case exact solvers are employed on all subspaces, the condition number of the additive Schwarz operator, for sufficiently small t , is bounded by*

$$C \left(\frac{\tilde{m}}{\mu}\right)^2 \left(1 + \frac{H}{\delta}\right)^3 \left(1 + \log \frac{H}{h}\right)^2$$

where C depends on N^c , but is otherwise independent of t , h , H , and δ .

Similarly, we have a bounded condition number of the multiplicative operator. We show some numerical results in sections 4.10.

4.7 The Case of $t = \infty$

4.7.1 Coarse Problem

If $t = \infty$, the Reissner-Mindlin plate problem is just the linear elasticity problem. For more detail, see [23]. Bubble functions are zero in a discrete harmonic function. We define basis functions on the interface and then use discrete harmonic extensions of these boundary values. For each θ_i , we define a vertex basis function θ_{i,v_k}^0 , $i = 1, 2$, $k = 1, 2, 3$, which is linear on each edge and has the value 1 at a vertex.

Lemma 23. *The square of the a -seminorm of the vertex basis function θ_{i,v_k}^0 is bounded by $C\tilde{m}$ where C does not depend on H , h , and δ , but depends on the shape regularity of the elements of the subdomain.*

We define a coarse component u^0 of u by

$$u^0 = \sum_{i=1}^2 \sum_{k=1}^3 \theta_i(v_k) \theta_{i,v_k}^0.$$

This coarse interpolant reproduces both null space functions of θ of the a-seminorm. We have,

$$\begin{aligned} b(u^0, u^0)_{\Omega_i} &\leq C\tilde{m} \|\theta\|_{L^2(\Omega_i)}^2 \\ &\leq C\tilde{m} \left(1 + \log \frac{H}{h}\right) \|\theta\|_{H^1(\Omega_i)}^2 \\ &\leq C \frac{\tilde{m}}{\mu} \left(1 + \log \frac{H}{h}\right) b(u, u)_{\Omega_i} \end{aligned}$$

by using Korn's inequality, Lemma 12, after replacing $\|\theta\|_{H^1(\Omega_i)}^2$ by $\inf_{r \in RB} \|\theta - r\|_{H^1(\Omega_i)}^2$.

4.7.2 Local Problems

Let $w_d = w - w^0$ and $\theta_{dL} = \theta_L - \theta_L^0$. We define the local components as follows; $w_j := \tilde{I}^h(\chi_j w_d)$ and $\theta_{Lj} := I^h(\chi_j \theta_{dL})$. We find,

$$\begin{aligned} a(\theta_j, \theta_j)_{\Omega_i} &\leq C\tilde{m} |\theta_j|_{H^1(\Omega_i)}^2 \\ &\leq C\tilde{m} \|\nabla I^h(\chi_j \theta_d)\|_{L^2(\Omega_i)}^2 \\ &\leq C\tilde{m} (\|\theta_d \nabla \chi_j\|_{L^2(\Omega_i)}^2 + \|\chi_j \nabla \theta_d\|_{L^2(\Omega_i)}^2) \\ &\leq C\tilde{m} \left(\frac{1}{\delta^2} \|\theta_d\|_{L^2(\Omega_{i,\delta})}^2 + \|\nabla \theta_d\|_{L^2(\Omega_i)}^2\right) \\ &\leq C\tilde{m} \left(1 + \frac{H}{\delta}\right) \|\theta_d\|_{H^1(\Omega_i)}^2 \\ &\leq C\tilde{m} \left(1 + \frac{H}{\delta}\right) \left(1 + \log \frac{H}{h}\right) \|\theta\|_{H^1(\Omega_i)}^2 \end{aligned}$$

by Lemma 9. By replacing $\|\theta\|_{H^1(\Omega_i)}^2$ by $\inf_{r \in RB} \|\theta - r\|_{H^1(\Omega_i)}^2$, we obtain

$$\begin{aligned} a(\theta_j, \theta_j)_{\Omega_i} &\leq C \frac{\tilde{m}}{\mu} \left(1 + \frac{H}{\delta}\right) \left(1 + \log \frac{H}{h}\right) \|\theta\|_{H^1(\Omega_i)}^2 \\ &\leq C \frac{\tilde{m}}{\mu} \left(1 + \frac{H}{\delta}\right) \left(1 + \log \frac{H}{h}\right) a(\theta, \theta)_{\Omega_i}. \end{aligned}$$

The condition number is bounded by $C \frac{\tilde{m}}{\mu} \left(1 + \frac{H}{\delta}\right) \left(1 + \log \frac{H}{h}\right)$.

If we do not include the coarse basis functions of this section, then the condition number of the additive operator grows with the number of subdomains for large t , such as $t > 1$. When we added them in our numerical experiments, the additive method was quasi-optimal and scalable for any t , especially for large t . But it does not improve the condition number of the additive method for small t which are of more interest. The Reissner-Mindlin problem with large t does not have physical meaning and there is no strong reason for us to add unnecessary variable w to

the linear elasticity problem. If we were to include these coarse basis functions, we need to deal with a larger coarse space and it would increase the computation time.

4.8 Changes of Thickness t or the Lamé constants

It is of interest to consider cases where the thickness and the Lamé parameters change across the domain. For simplicity, we assume that the thickness and the Lamé constants are piecewise constant and that we can divide the domain into triangular subdomains such that t, μ , and λ are constants on each subdomain. We can see that the proof of previous sections does not depend on t, μ , and λ if t, λ and $\frac{\lambda}{\mu}$ are bounded from above. Therefore, we still get the same $C(\frac{m}{\mu})^2(1 + \log \frac{H}{h})^2(1 + \frac{H}{\delta})^3$ bound even when t, μ , and λ change over the domain.

4.9 Higher Order Falk-Tu Elements

We can use higher order Falk-Tu elements as in (3.33). Note that we again choose a discontinuous stress variable.

We can decompose Θ_h into two parts: the space of polynomials, Θ_{hL} , and the space of bubble functions, Θ_{hB} . On each element, we then have $a(\theta_L + \theta_B, \theta_L + \theta_B) \geq C(a(\theta_L, \theta_L) + a(\theta_B, \theta_B))$ for $\theta_L \in \Theta_{hL}$ and $\theta_B \in \Theta_{hB}$ because we consider a finite dimensional space. In discrete harmonic functions, we can consider θ_B as being dependent on θ_L and w . We know that $\nabla W_h \subset \Pi \Theta_{hB}$ and $\Theta_{hL} \subset \Pi \Theta_{hB}$, and that $w = \Pi \theta$ implies $\|w\|_{L^2}^2 \leq \|\theta\|_{L^2}^2$. Therefore, we can easily modify our proof for the higher order Falk-Tu elements and obtain the same bound.

4.10 Numerical Experiments

In the numerical experiments, L is the length of one side of a square domain, ν and E are the parameters of elasticity, H is the size of the coarse mesh, h that of the fine mesh, δ that of the overlap, and t the thickness of the plate. Results are given for the elasticity parameters $\nu = 0.8$ and $E = 0.1$. Experiments for each parameter set is done about 100 times with random right hand sides and the average iteration counts and condition numbers are given. We use the additive method (2.5) and symmetric multiplicative method (2.6) with the conjugate gradient algorithm to solve the linear system of equations. The stopping criteria for the conjugate gradient algorithm is $\frac{\|r_n\|_{L^2}}{\|r_0\|_{L^2}} \leq 10^{-7}$. We have calculated the condi-

Table 4.1: Results for $L = 1$, $\frac{H}{h} = 4$, $\frac{H}{\delta} = 4$, and decreasing $h = \frac{1}{n}$, and with an increasing number of subdomains $= \frac{n}{4} \times \frac{n}{4}$ without the w quadratic coarse basis functions.

n	Iter	cond	Iter	cond	Iter	cond	Iter	cond
t	10		0.1		0.001		0.00001	
12	36.3	70.5	31.1	29.8	80.2	379.6	81.5	383.2
24	63.5	309.9	38.0	42.3	153.2	662.8	162.4	704.6
36	92.2	772.7	49.9	79.3	191.3	851.7	207.9	949.9
48	122.0	1492.8	61.1	114.3	208.0	767.0	233.1	1015.7
60	150.2	2500.6	73.0	171.6	208.0	746.9	251.5	972.2
72	179.9	3823.5	87.0	236.3	215.0	714.4	265.9	1022.1
84	208.7	5483.0	101.7	308.0	209.9	607.7	281.0	976.6

Table 4.2: Results for $L = 1$, $\frac{H}{h} = 4$, $\frac{H}{\delta} = 4$, and decreasing $h = \frac{1}{n}$, and with an increasing number of subdomains $= \frac{n}{4} \times \frac{n}{4}$ with the w quadratic coarse basis functions.

n	Iter	cond	Iter	cond	Iter	cond	Iter	cond
t	10		0.1		0.001		0.00001	
12	35.2	70.5	25.1	17.5	58.0	77.5	59.3	78.1
24	64.0	310.1	37.0	35.9	66.0	69.1	68.7	72.4
36	93.0	772.9	49.0	73.7	67.6	68.1	73.7	75.2
48	121.9	1494.3	60.8	107.2	67.0	64.4	75.0	76.3
60	151.2	2503.0	74.0	161.7	65.0	66.6	75.2	77.4
72	180.1	3826.3	87.1	220.6	64.0	65.4	76.9	77.5
84	209.7	5484.9	100.7	291.6	62.0	62.6	77.0	76.6

tion number by constructing the matrix of coefficients (1.3) given by the conjugate gradient method given in section 1.3.

4.10.1 The Additive Operator

The condition number as a function of the number of subdomains are given in Tables 4.1 and 4.2. As expected, the condition number grows with the number of subdomains for large t , but it is bounded for small t .

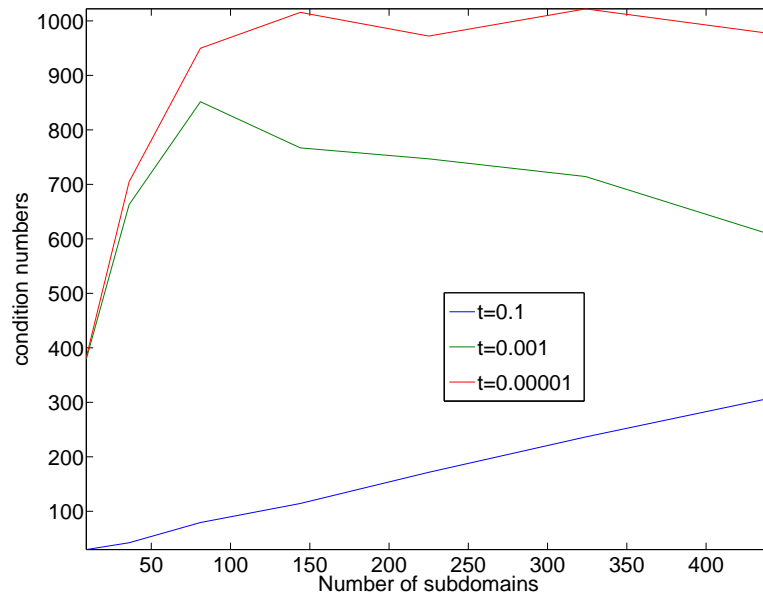


Figure 4.8: The condition number as a function of the number of subdomains without the w quadratic coarse basis functions.

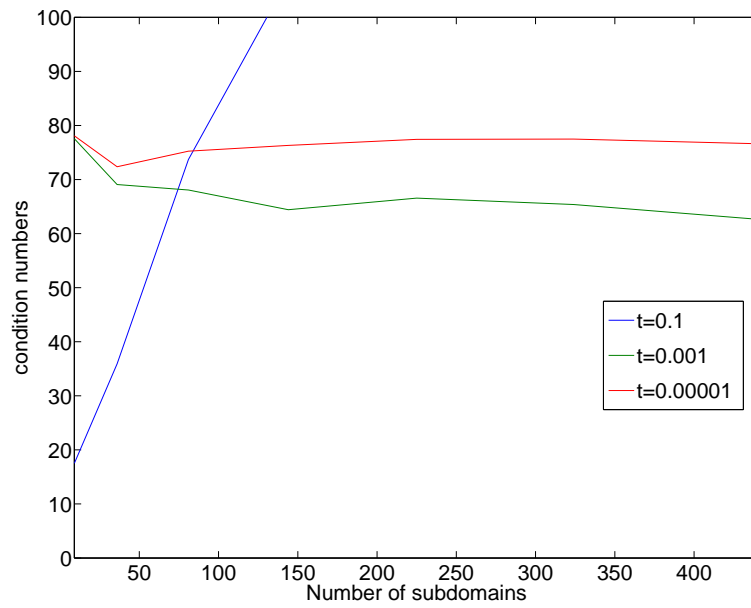


Figure 4.9: The condition number as a function of the number of subdomains with the w quadratic coarse basis functions.

Table 4.3: Results for $L = 1$, $\frac{H}{h} = 4$, $\frac{H}{\delta} = 4$, and decreasing $h = \frac{1}{n}$, and with an increasing number of subdomains $= \frac{n}{12} \times \frac{n}{12}$.

$\frac{H}{h}$	Iter	cond	Iter	cond
t	100		10	
12	41.6	17.50	40.0	18.13
24	45.0	20.69	43.7	18.61
36	46.0	21.09	44.0	18.21
48	46.0	20.07	44.9	17.96
60	46.0	18.90	44.5	18.92
72	46.0	18.08	44.7	19.69
84	46.0	18.38	45.0	20.24
96	46.0	18.76	45.0	20.57

If we add more coarse basis functions for the linear elasticity problem, we then can get condition number that does not increase as the number of subdomains increases for large t . The results with the extended coarse space for large t are in Table 4.3. These results do not depend on the number of subdomains.

Table 4.4: Results for $L = 1$, $h = \frac{1}{n}$, $\frac{H}{\delta} = 4$, the number of subdomains 3×3 , and increasing $\frac{H}{h} = \frac{n}{3}$ without the w quadratic coarse basis functions.

$\frac{H}{h}$	Iter	cond	Iter	cond	Iter	cond	Iter	cond	Iter	cond
t	1000		10		0.1		0.001		0.00001	
4	38.9	69.1	36.2	70.5	31.1	29.7	80.2	379.0	81.3	386.2
8	45.5	66.3	40.7	67.2	32.9	28.8	80.0	284.0	80.8	299.9
12	45.8	64.2	41.8	64.1	33.7	31.1	79.5	307.5	80.4	337.4
16	46.1	64.4	42.5	65.1	34.3	31.8	79.2	313.9	80.0	358.0
20	46.9	62.8	43.2	63.7	34.5	31.9	79.0	301.4	81.6	361.3
24	47.4	62.9	43.5	64.0	34.6	33.4	79.0	288.1	89.2	354.4
28	47.7	63.3	43.6	64.4	35.0	34.4	79.2	268.8	89.6	345.3

Table 4.5: Results for $L = 1$, $h = \frac{1}{n}$, $\frac{H}{\delta} = 4$, the number of subdomains 3×3 , and increasing $\frac{H}{h} = \frac{n}{3}$ with the w quadratic coarse basis functions.

$\frac{H}{h}$	Iter	cond	Iter	cond	Iter	cond	Iter	cond	Iter	cond
t	1000		10		0.1		0.001		0.00001	
4	39.0	69.4	35.2	70.4	25.1	17.5	58.0	78.1	59.1	79.0
8	46.2	65.6	41.6	66.1	28.0	17.2	59.5	79.0	61.9	82.5
12	47.0	65.5	42.6	63.9	29.4	19.0	60.0	80.4	64.2	88.0
16	47.6	64.7	43.6	64.0	30.2	20.2	59.3	83.9	64.9	90.2
20	48.0	64.1	44.0	63.8	31.0	20.7	59.3	81.9	66.5	92.9
24	48.1	64.2	44.4	63.7	31.0	21.1	59.6	78.1	67.3	94.2
28	48.1	64.4	44.3	63.6	31.0	21.6	60.1	74.9	67.8	94.5

Results with varying $\frac{H}{h}$ are given in Table 4.4, Table 4.5, Figure 4.10, and Figure 4.11.

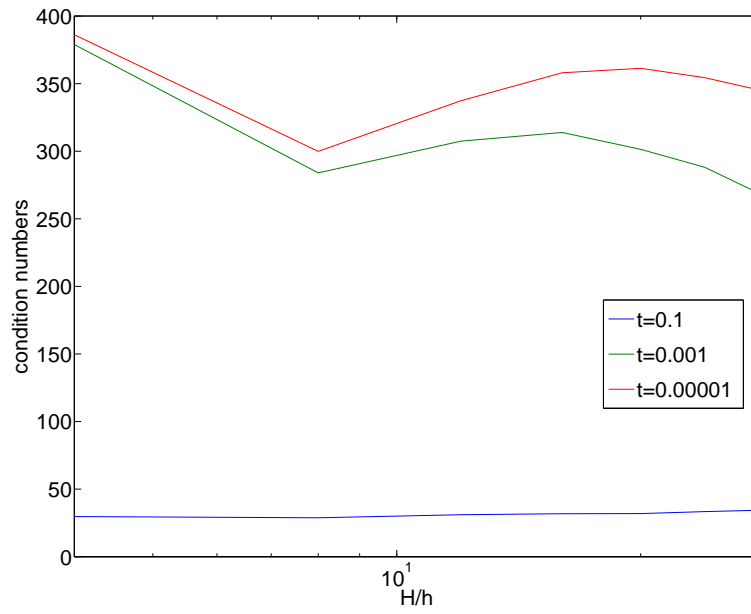


Figure 4.10: The condition number as a function of $\frac{H}{h}$ without the w quadratic coarse basis functions.

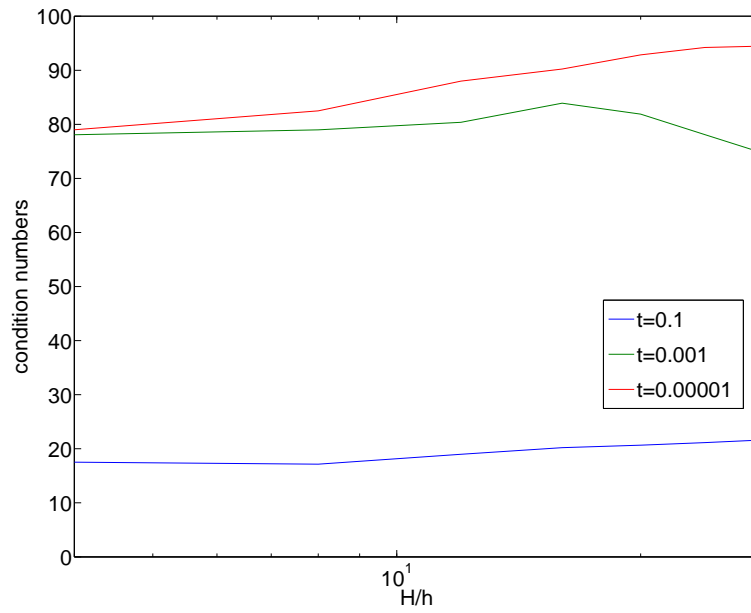


Figure 4.11: The condition number as a function of $\frac{H}{h}$ with the w quadratic coarse basis functions.

Table 4.6: Results for $h = \frac{1}{72}$, $\frac{H}{h} = 12$, and decreasing $\frac{H}{\delta} = 12, 6, 4, 3, 2.4, 2$ without the w quadratic coarse basis functions.

$\frac{H}{\delta}$	Iter	cond	Iter	cond	Iter	cond	Iter	cond
t	10		0.1		0.001		0.00001	
12	114.8	1439.2	62.1	96.3	484.9	7153.2	542.0	7387.8
6	93.5	564.2	51.0	56.4	210.4	1070.9	228.9	1324.4
4	73.9	290.6	45.0	47.1	145.3	581.9	162.1	804.3
3	61.4	162.3	40.1	41.1	116.9	438.9	132.6	620.3
2.4	50.9	96.6	36.4	36.7	72.8	216.9	110.1	463.6
2	42.2	59.0	32.7	29.8	83.1	293.0	94.6	398.9

Table 4.7: Results for $h = \frac{1}{72}$, $\frac{H}{h} = 12$, and decreasing $\frac{H}{\delta} = 12, 6, 4, 3, 2.4, 2$ with the w quadratic coarse basis functions.

$\frac{H}{\delta}$	Iter	cond	Iter	cond	Iter	cond	Iter	cond
t	10		0.1		0.001		0.00001	
12	116.2	1417.1	61.4	102.3	211.5	960.1	244.4	1033.7
6	94.5	525.2	48.0	47.7	94.7	139.0	102.8	151.8
4	74.9	287.0	41.0	38.4	68.9	77.2	79.0	96.4
3	62.4	165.1	36.0	32.9	60.0	53.9	67.0	67.5
2.4	51.4	96.7	33.0	25.1	53.3	44.0	60.5	57.4
2	42.6	59.2	29.0	22.2	48.2	39.8	55.1	50.9

Results with varying $\frac{H}{\delta}$ are given in Table 4.6, Table 4.7, Figure 4.12, and Figure 4.13. The condition number depends on $\frac{H}{\delta}$. It grows faster with $\frac{H}{\delta}$ when t is small.

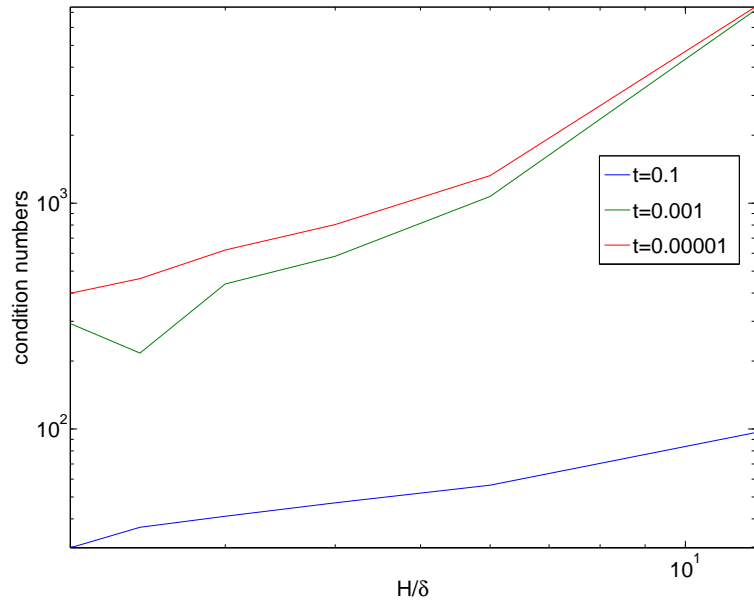


Figure 4.12: The condition number as a function of $\frac{H}{\delta}$ without the w quadratic coarse basis functions.

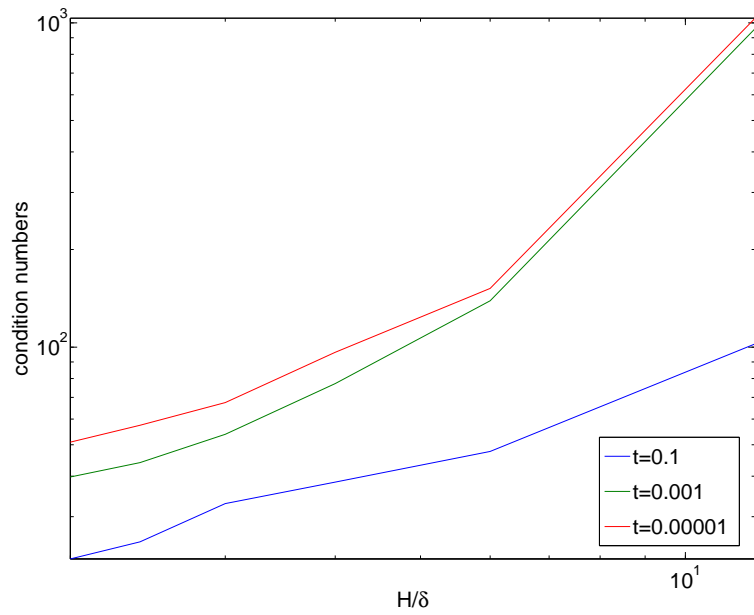


Figure 4.13: The condition number as a function of $\frac{H}{\delta}$ with the w quadratic coarse basis functions.

Table 4.8: Results for $L = 1$, $\frac{H}{h} = 4$, $\frac{H}{\delta} = 4$, decreasing $h = \frac{1}{n}$, and increasing the number of subdomains $= \frac{n}{4} \times \frac{n}{4}$ with the w quadratic coarse basis functions.

n	Iter	cond	Iter	cond	Iter	cond
t	0.1		0.001		0.00001	
12	6.0	1.59	15.9	6.10	16.0	6.26
24	9.0	2.50	19.0	5.66	19.0	5.96
36	13.0	4.32	19.0	5.45	20.0	6.22
48	16.0	6.18	18.9	5.33	21.0	6.37
60	20.0	8.87	18.0	5.05	21.0	6.50
72	23.8	11.55	18.0	4.76	21.7	6.55
84	27.2	14.90	17.0	4.49	22.0	6.54
96	31.0	20.15	16.9	4.27	22.0	6.56

4.10.2 The Multiplicative Operator

We have also tested the multiplicative operator numerically with the additional w quadratic basis functions in subsection 4.4.3. The multiplicative operator has much smaller condition number than the additive operator. Results of the multiplicative operator are given in Tables 4.8, 4.9, and 4.10 and Figures 4.14, 4.15, and 4.16.

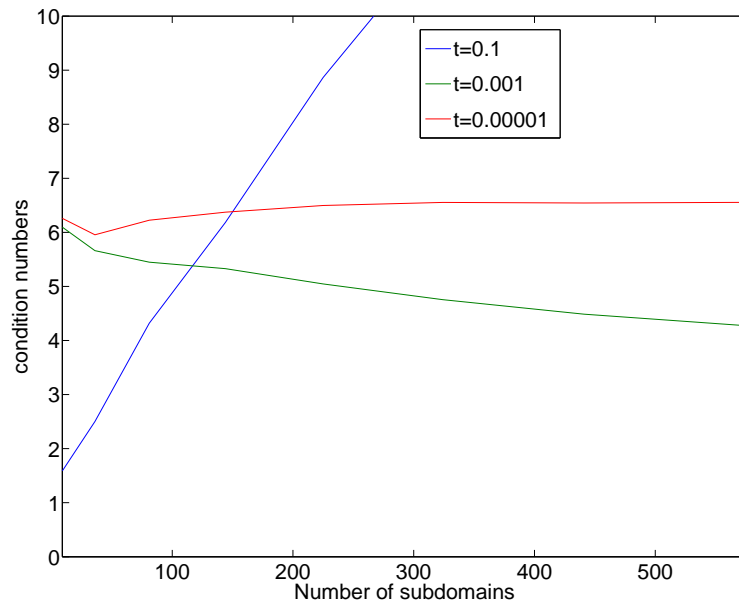


Figure 4.14: The condition number as a function of the number of subdomains with the w quadratic coarse basis functions.

Table 4.9: Results for $L = 1$, $h = \frac{1}{n}$, $\frac{H}{\delta} = 4$, the number of subdomains 3×3 , and increasing $\frac{H}{h} = \frac{n}{3}$ with the w quadratic coarse basis functions.

$\frac{H}{h}$	Iter	cond	Iter	cond	Iter	cond
t	0.1		0.001		0.00001	
4	6.0	1.59	15.9	6.17	15.9	6.20
8	7.0	1.79	16.0	6.61	16.6	6.99
12	7.0	1.91	15.8	6.40	16.6	7.13
16	7.0	1.99	15.5	5.90	16.6	6.87
20	8.0	2.05	15.6	5.72	16.6	6.82
24	8.0	2.10	15.2	5.74	16.8	7.13
28	8.0	2.14	15.0	5.83	16.9	7.65
32	8.0	2.18	15.0	5.95	16.9	8.15
36	8.0	2.21	15.0	6.04	17.0	8.55
40	8.0	2.24	15.0	6.09	17.0	8.86

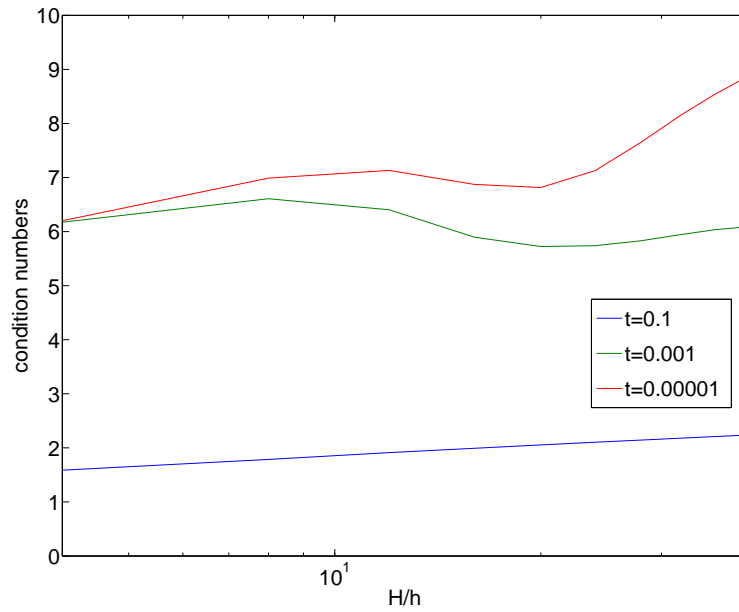


Figure 4.15: The condition number as a function of $\frac{H}{h}$ with the w quadratic coarse basis functions.

Table 4.10: Results for $h = \frac{1}{72}$, $\frac{H}{h} = 12$, and decreasing $\frac{H}{\delta} = 12, 6, 4, 3, 2.4, 2$ with the w quadratic coarse basis functions.

$\frac{H}{\delta}$	Iter	cond	Iter	cond	Iter	cond
t	0.1		0.001		0.00001	
12	17.0	6.11	57.3	57.76	62.8	66.98
6	13.0	4.02	24.2	10.33	28.0	13.30
4	10.0	3.18	19.0	6.42	22.0	8.37
3	9.0	2.62	15.3	5.19	18.2	6.61
2.4	8.0	2.32	13.7	4.34	16.0	5.37
2	7.0	2.07	12.0	3.73	13.6	4.58

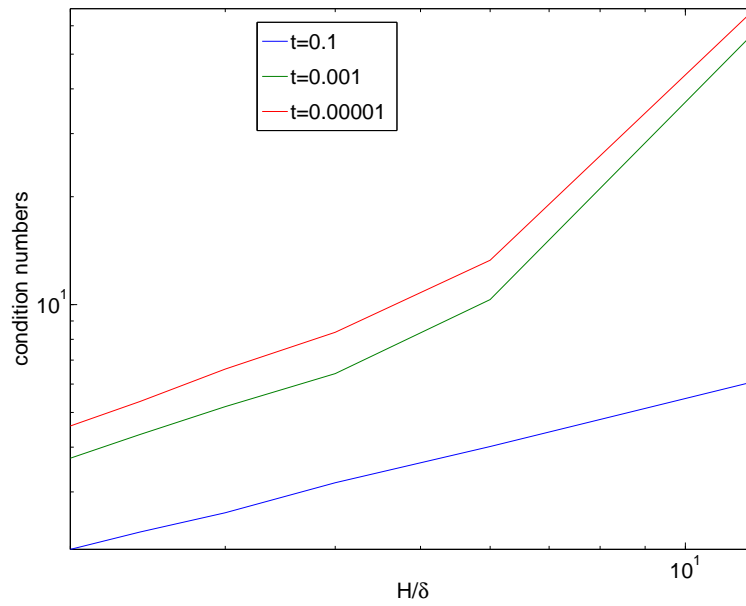


Figure 4.16: The condition number as a function of $\frac{H}{\delta}$ with the w quadratic coarse basis functions.

Chapter 5

BDDC methods for the Reissner-Mindlin Plate

5.1 Introduction

In this final chapter, we will discuss two BDDC methods for the Reissner-Mindlin Plate. They will differ in details and concern two different finite element models. Experimentally the performance of two different algorithms are quite similar. First, we will discuss work described in [8] while in the final section, and we will report on our own recent progress.

5.2 Notation

As in section 4.3, we can eliminate the stress variable for the discretized problem and obtain problem (4.10) where b is defined in (4.11):

Find $\theta_h \in \Theta_h$ and $w_h \in W_h$ such that

$$b((\theta_h, w_h), (\phi, v)) = (g, v) - (\mathbf{f}, \phi), \quad \phi \in \Theta_h, v \in W_h. \quad (5.1)$$

We will use notation similar to that of section 2.4 but replacing W by \mathbf{U} . In each subdomain, we have $\mathbf{U}^{(i)} := \Theta_h^{(i)} \times W_h^{(i)}$. We also define $\mathbf{U}^{(i)} := \mathbf{U}_\Gamma^{(i)} + \mathbf{U}_I^{(i)} := \mathbf{U}_\Pi^{(i)} + \mathbf{U}_\Delta^{(i)} + \mathbf{U}_I^{(i)}$. We also need to consider the product spaces \mathbf{U}_Γ , $\widehat{\mathbf{U}}_\Gamma$, and $\widetilde{\mathbf{U}}_\Gamma$.

$S^{(i)}$ is the Schur complement of the plate problem derived from the b operator in (4.11) on subdomain Ω_i . S is the direct sum of the $S^{(i)}$ on \mathbf{U}_Γ , \widehat{S} is the Schur complement restricted to $\widehat{\mathbf{U}}_\Gamma$, and \widetilde{S} the Schur complement restricted to $\widetilde{\mathbf{U}}_\Gamma$. Then, the discrete problem becomes:

Find $u_\Gamma \in \mathbf{U}_\Gamma$ such that $\widehat{S}u_\Gamma = \widehat{\mathbf{f}}_\Gamma$ for a proper $\widehat{\mathbf{f}}_\Gamma$.

For more notation of the spaces, restriction operators, and Schur complements, see section 2.4.

We define the positive scaling factors

$$\delta_i^\dagger(x) := N_x^{-1}, \quad x \in \Gamma_i \quad (5.2)$$

where N_x is the number of subdomains which have x on their boundaries. We will not include any vertex variables in the dual space and therefore $\delta_i^\dagger(x) \equiv \frac{1}{2}$ if x is a node of the dual space since all nodes for the dual space are on the edges. Therefore, we have

$$R_{\Gamma\Delta} \tilde{R}_{D,\Gamma}^T = \frac{1}{2} R_{\Gamma\Delta} \tilde{R}_\Gamma^T.$$

As in section 2.7, we can write a coarse stiffness matrix as

$$S_{\text{III}} = \sum_{i=1}^N R_{\text{II}}^{(i)T} S_{\text{III}}^{(i)} R_{\text{II}}^{(i)} \quad (5.3)$$

with

$$S_{\text{III}}^{(i)} = B_{\text{III}}^{(i)} - [B_{\text{II}}^{(i)} \quad B_{\text{II}\Delta}^{(i)}] \begin{bmatrix} B_{\text{II}}^{(i)} & B_{\text{I}\Delta}^{(i)} \\ B_{\Delta\text{I}}^{(i)} & B_{\Delta\Delta}^{(i)} \end{bmatrix}^{-1} \begin{bmatrix} B_{\text{II}}^{(i)T} \\ B_{\text{II}\Delta}^{(i)T} \end{bmatrix} \quad (5.4)$$

and the extension matrix $\Phi : \hat{\mathbf{U}}_{\text{II}} \rightarrow \tilde{\mathbf{U}}_\Gamma$ as defined by

$$\Phi = R_{\text{II}}^T - R_{\text{II}\Delta}^T \sum_{i=1}^N [0 \quad R_{\Delta}^{(i)T}] \begin{bmatrix} B_{\text{II}}^{(i)} & B_{\text{I}\Delta}^{(i)} \\ B_{\Delta\text{I}}^{(i)} & B_{\Delta\Delta}^{(i)} \end{bmatrix}^{-1} \begin{bmatrix} B_{\text{II}}^{(i)T} \\ B_{\text{II}\Delta}^{(i)T} \end{bmatrix} R_{\text{II}}^{(i)}. \quad (5.5)$$

We can use the exact local stiffness matrix, $S_\Delta^{(i)}$, which is defined by

$$S_\Delta^{(i)} := B_{\Delta\Delta}^{(i)} - B_{\Delta\text{I}}^{(i)} B_{\text{II}}^{(i)-1} B_{\text{I}\Delta}^{(i)}. \quad (5.6)$$

S_Δ is the direct sum of the $S_\Delta^{(i)}$.

We then define the BDDC preconditioner as in (2.22) in section 2.7:

$$M_{\text{BDDC}}^{-1} := \tilde{R}_{D,\Gamma}^T R_{\text{II}\Delta}^T S_\Delta^{-1} R_{\text{II}\Delta} \tilde{R}_{D,\Gamma} + \tilde{R}_{D,\Gamma}^T \Phi S_{\text{III}}^{-1} \Phi^T \tilde{R}_{D,\Gamma}. \quad (5.7)$$

5.3 BDDC Methods for MITC elements

In this section, we present the BDDC methods for the MITC elements as in [8]; some notations and representations have been modified. We assume that the subdomains are shape regular rectangles and use the MITC9 elements. We know that the MITC elements satisfy properties P1-P6 of subsection 3.3.1.

We choose $\hat{\mathbf{U}}_{\text{II}}$ as the space of the subdomain vertex nodal values. Each rectangular subdomain has 4 vertices and 12 primal variables and we have approximately

$\frac{12}{4} = 3$ coarse degrees of freedom per subdomain. The local space $\mathbf{U}_\Delta^{(i)}$ is defined as the subspace of $\mathbf{U}_\Gamma^{(i)}$ for which the values at the subdomain vertices vanish.

Let \mathcal{E}_i represent the set of the edges of Γ_i . For $u^{(i)} = (\theta^{(i)}, w^{(i)}) \in \mathbf{U}_\Gamma^{(i)}$ and the edge $e \in \mathcal{E}_i$, we first define the following edge seminorm on the rotation variables:

$$|\theta^{(i)}|_{\gamma(e)} := \inf_{\psi \in \mathbf{H}_0^1(\Omega), \psi|_e = \theta^{(i)}|_e} \|\varepsilon(\psi)\|_{L^2(\Omega_i)}. \quad (5.8)$$

We then define the interface seminorm of $u^{(i)}$,

$$|u^{(i)}|_{\tau(\Gamma_i)}^2 := \sum_{e \in \mathcal{E}_i} |u^{(i)}|_{\tau(e)}^2 \quad (5.9)$$

with

$$|u^{(i)}|_{\tau(e)}^2 := |\theta^{(i)}|_{\gamma(e)}^2 + ht^{-2} \|(\Pi\theta^{(i)} - \nabla w) \cdot \mathbf{t}\|_{L^2(e)}^2, \quad (5.10)$$

where \mathbf{t} is the unit tangent vector of the edge e . It follows from property P6 that $(\Pi\theta^{(i)} - \nabla w) \cdot \mathbf{t}$ is well defined on the edge e . Because we use shape regular subdomains, we can see that $|u^{(i)}|_{\tau(e)}$ and $|R^{(j)}R^{(i)T}u^{(i)}|_{\tau(e)}$ are equivalent for $e \in \Gamma_i \cap \Gamma_j$.

Using properties P1-P6, we can prove the following lemma for the interface seminorm $\tau(\Gamma_i)$. For a proof, see [8, section 5.2].

Lemma 24. *There exists a constant C , which is independent of H and h , such that,*

$$|u^{(i)}|_{\tau(\Gamma_i)}^2 \leq C |u^{(i)}|_{S^{(i)}}^2, \quad \forall u^{(i)} \in \mathbf{U}_\Gamma^{(i)}, \quad (5.11)$$

$$|u^{(i)}|_{\tau(\Gamma_i)}^2 \geq C(h/H) |u^{(i)}|_{S^{(i)}}^2, \quad \forall u^{(i)} \in R_\Gamma^{(i)} \widehat{R}_\Delta^{(i)T} \mathbf{U}_\Delta^{(i)}. \quad (5.12)$$

From this, we can easily prove an extension lemma.

Lemma 25 (extension lemma). *There exists a constant C , which is independent of H and h , such that,*

$$\left| R_\Gamma^{(i)} R_\Gamma^{(j)T} u^{(j)} \right|_{S^{(i)}}^2 \leq C(H/h) |u^{(j)}|_{S^{(j)}}^2, \quad \forall u^{(j)} \in R_\Gamma^{(j)} \widehat{R}_\Delta^{(j)T} \mathbf{U}_\Delta^{(j)}. \quad (5.13)$$

We can define an average operator E_D on $\widetilde{\mathbf{U}}_\Gamma$ as in section 2.7.

$$E_D := \widetilde{R}_\Gamma \widetilde{R}_{D,\Gamma}^T. \quad (5.14)$$

Let us denote the set of indices j such that $\overline{\Omega}_j \cap \overline{\Omega}_i \neq \emptyset$ by Ξ_i .

For a given $\tilde{u}_\Gamma = \Pi_i \tilde{u}^{(i)} \in \widetilde{\mathbf{U}}_\Gamma$ with $\tilde{u}^{(i)} \in \mathbf{U}_\Gamma^{(i)}$, define $u_{0,i}$ and u_0 as follows:

$$u_0 = \sum_{i=1}^N R_\Gamma^{(i)} \delta_i^\dagger u_{0,i} = \sum_{i=1}^N R_{D,\Gamma}^{(i)} u_{0,i} \quad (5.15)$$

and $u_{0,i}$ is a minimizer of $s^{(i)}(u^{(i)}, u^{(i)})$ among all functions $u^{(i)} \in \mathbf{U}_\Gamma^{(i)}$ such that $R_\Pi^{(i)} R_\Gamma^{(i)T} u^{(i)} = R_\Pi^{(i)} \tilde{R}_\Gamma^T \tilde{u}_\Gamma$. We also define $u_i = \tilde{u}^{(i)} - u_{0,i} \in R_\Gamma^{(i)} \hat{R}_\Delta^{(i)T} \mathbf{U}_\Delta^{(i)}$.

We then have

$$R_\Gamma^{(i)} E_D \tilde{u}_\Gamma = \sum_{j \in \Xi_i} R_\Gamma^{(i)} R_\Gamma^{(j)T} \delta_j^\dagger u_{j,0} + \frac{1}{2} \sum_{j \in \Xi_i} R_\Gamma^{(i)} R_\Gamma^{(j)T} u_j \quad (5.16)$$

and

$$\left| R_\Gamma^{(i)} E_D \tilde{u}_\Gamma \right|_{S^{(i)}}^2 \leq 2 \left| \sum_{j \in \Xi_i} R_\Gamma^{(i)} R_\Gamma^{(j)T} \delta_j^\dagger u_{j,0} \right|_{S^{(i)}}^2 + \frac{1}{2} \left| \sum_{j \in \Xi_i} R_\Gamma^{(i)} R_\Gamma^{(j)T} u_j \right|_{S^{(i)}}^2. \quad (5.17)$$

Using the extension lemma, the second term of (5.17) can be bounded by

$$\frac{CH}{h} \sum_{j \in \Xi_i} |u_j|_{S^{(j)}}^2 \leq \frac{CH}{h} \sum_{j \in \Xi_i} |\tilde{u}^{(j)}|_{S^{(j)}}^2. \quad (5.18)$$

The first term of (5.17) can be bounded by

$$\begin{aligned} & 2 \left| R_\Gamma^{(i)} \sum_{j \in \Xi_i} R_\Gamma^{(j)T} \delta_j^\dagger u_{j,0} \right|_{S^{(i)}}^2 \\ & \leq 4 |u_{i,0}|_{S^{(i)}}^2 + 4 \left| u_{i,0} - R_\Gamma^{(i)} \sum_{j \in \Xi_i} R_\Gamma^{(j)T} \delta_j^\dagger u_{j,0} \right|_{S^{(i)}}^2 \\ & \leq 4 |\tilde{u}^{(i)}|_{S^{(i)}}^2 + 4 \left| \sum_{j \in \Xi_i} R_\Gamma^{(i)} R_\Gamma^{(j)T} \delta_j^\dagger (R_\Gamma^{(j)} R_\Gamma^{(i)T} u_{i,0} - u_{j,0}) \right|_{S^{(i)}}^2 \\ & \leq 4 |\tilde{u}^{(i)}|_{S^{(i)}}^2 + \frac{CH}{h} \sum_{j \in \Xi_i} \left| R_\Gamma^{(i)} R_\Gamma^{(j)T} (R_\Gamma^{(j)} R_\Gamma^{(i)T} u_{i,0} - u_{j,0}) \right|_{\tau(\Gamma_{ij})}^2 \\ & \leq 4 |\tilde{u}^{(i)}|_{S^{(i)}}^2 + \frac{CH}{h} \sum_{j \in \Xi_i} \left(|u_{i,0}|_{\tau(\Gamma_{ij})}^2 + |u_{j,0}|_{\tau(\Gamma_{ij})}^2 \right) \\ & \leq 4 |\tilde{u}^{(i)}|_{S^{(i)}}^2 + \frac{CH}{h} \sum_{j \in \Xi_i} \left(|u_{i,0}|_{S^{(i)}}^2 + |u_{j,0}|_{S^{(j)}}^2 \right) \\ & \leq \frac{CH}{h} \sum_{j \in \Xi_i} |\tilde{u}^{(j)}|_{S^{(j)}}^2. \end{aligned} \quad (5.19)$$

By summing over the subdomains, we have

$$|E_D \tilde{u}_\Gamma|_{\tilde{S}}^2 \leq \frac{CH}{h} |\tilde{u}_\Gamma|_{\tilde{S}}^2, \quad \tilde{u}_\Gamma \in \tilde{\mathbf{U}}_\Gamma, \quad (5.20)$$

which is similar to Lemma 11. Following the arguments in section 2.7, we then have the following bound for the BDDC operator with the MITC elements.

Theorem 15. *The BDDC operator has the following bound of the condition number*

$$\kappa(M_{\text{BDDC}}^{-1}\widehat{S}) \leq \frac{CH}{h}$$

where C is independent of H and h .

In numerical experiments reported in [8], we can see that the bound of condition number is better than what the theory predicts; we can expect to have a bound which is the power of $(1 + \log \frac{H}{h})$.

5.4 BDDC Methods for Falk-Tu elements

In this section, we present our BDDC methods for the Falk-Tu elements. We assume that the subdomains are shape regular triangles.

We choose $\widehat{\mathbf{U}}_{\Pi}$ as the space of the subdomain vertex nodal values and the values $\int_{e_k} \theta \cdot \mathbf{n} ds$ for all edges. Each triangular subdomain has 3 vertices, 3 edges, and 12 primal variables and we have approximately $\frac{9}{6} + \frac{3}{2} = 3$ coarse degrees of freedom per subdomain. The local space $\mathbf{U}_{\Delta}^{(i)}$ is defined as the subspace of $\mathbf{U}_{\Gamma}^{(i)}$ where the values at the subdomain vertices and $\int_{e_k} \theta \cdot \mathbf{n} ds$ vanish.

We first tested an extension lemma on an edge e_{ij} numerically and calculated

$$\sup_{u^{(j)} \in R_{\Gamma}^{(j)} R_{\Gamma}^{(i)T} R_{\Gamma}^{(i)} \widehat{R}_{\Delta}^{(j)T} \mathbf{U}_{\Delta}^{(j)}} \frac{\left| R_{\Gamma}^{(i)} R_{\Gamma}^{(j)T} u^{(j)} \right|_{S^{(i)}}^2}{|u^{(j)}|_{S^{(j)}}^2}$$

for a number of values of H/h and t . If $u^{(j)} \in R_{\Gamma}^{(j)} R_{\Gamma}^{(i)T} R_{\Gamma}^{(i)} \widehat{R}_{\Delta}^{(j)T} \mathbf{U}_{\Delta}^{(j)}$, it vanishes at all nodes of $\partial\Omega_j \setminus e_{ij}$. The results in Table 5.1 and Figure 5.1 suggest that we have a constant bound.

Conjecture 1 (extension lemma). *There exists a constant C , which is independent of H and h , such that,*

$$\left| R_{\Gamma}^{(i)} R_{\Gamma}^{(j)T} u^{(j)} \right|_{S^{(i)}}^2 \leq C |u^{(j)}|_{S^{(j)}}^2, \quad \forall u^{(j)} \in R_{\Gamma}^{(j)} R_{\Gamma}^{(i)T} R_{\Gamma}^{(i)} \widehat{R}_{\Delta}^{(j)T} \mathbf{U}_{\Delta}^{(j)}. \quad (5.21)$$

Next, we tested an edge lemma on an edge e_{ij} numerically. For $u^{(i)} \in \mathbf{U}_{\Gamma}^{(i)}$, let $u_0^{(i)}$ be the coarse interpolant defined as (4.15) and $\psi_{e_{ij}}$ be the edge cut-off function of e_{ij} . We calculated

$$\sup_{u^{(i)} \in \mathbf{U}_{\Gamma}^{(i)}} \frac{\left| \psi_{e_{ij}}(u^{(i)} - u_0^{(i)}) \right|_{S^{(i)}}^2}{|u^{(i)}|_{S^{(i)}}^2} \quad (5.22)$$

Table 5.1: Maximum of the generalized eigenvalues for $H = 1$, $h = \frac{1}{k}$, and increasing $\frac{H}{h} = k$ between two interior subdomains for the extension lemma.

H/h	t=0.1	t=0.01	t=0.001	t=0.0001	t=0.000010
9	4.907158	10.953264	13.286568	13.336906	13.337417
18	5.417579	11.342027	13.208633	13.414581	13.416773
27	5.530311	11.634899	13.038411	13.426350	13.430772
36	5.571774	11.766864	12.788679	13.454008	13.462269
45	5.591386	11.839829	12.501084	13.447404	13.460537
54	5.602162	11.885327	12.262782	13.440867	13.459785
63	5.608703	11.915788	12.088357	13.434974	13.460689
72	5.612968	11.937174	12.078051	13.426620	13.460161

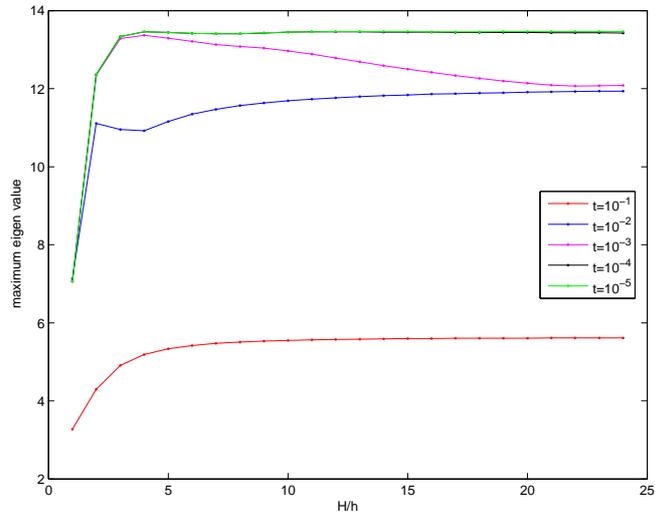


Figure 5.1: Maximum eigenvalue as a function of $\frac{H}{h}$ for the extension lemma.

Table 5.2: Maximum of the generalized eigenvalues for $H = 1$, $h = \frac{1}{k}$, and increasing $\frac{H}{h} = k$ for the edge lemma.

H/h	t=0.1	t=0.01	t=0.001	t=0.0001	t=0.000010
9	39.252590	293.059058	523.887444	530.591379	530.660677
18	43.503106	271.781051	697.637776	729.347650	729.696130
27	46.257163	262.949783	783.727702	856.560695	857.440410
36	48.442702	260.211920	826.903401	951.151252	952.829761
45	50.389569	259.449082	846.192946	1026.722797	1029.509209
54	52.288230	259.385027	851.902182	1089.687970	1093.882972
63	54.297223	259.587166	850.017478	1143.603560	1149.555093
72	58.094214	259.891252	844.084585	1190.658638	1198.521906

for a number of values of H/h and t . $\Pi_i u_0^{(i)}$ is continuous across the interface and $u^{(i)} - u_0^{(i)}$ vanishes at all primal variables. The results in Table 5.2 and Figure 5.2 suggest that we have a $C(1 + \log \frac{H}{h})^2$ bound.

Conjecture 2 (edge lemma). *There exists a constant C , which is independent of H and h , such that,*

$$\left| \psi_{e_{ij}}(u^{(i)} - u_0^{(i)}) \right|_{S^{(i)}}^2 \leq C(1 + \log \frac{H}{h})^2 |u^{(i)}|_{S^{(i)}}^2, \quad \forall u^{(i)} \in \mathbf{U}_\Gamma^{(i)}. \quad (5.23)$$

For a given $\tilde{u}_\Gamma = \Pi_i \tilde{u}^{(i)} \in \tilde{\mathbf{U}}_\Gamma$ with $\tilde{u}^{(i)} \in \mathbf{U}_\Gamma^{(i)}$, we have

$$\left| R_\Gamma^{(i)} E_D \tilde{u}_\Gamma \right|_{S^{(i)}}^2 \leq \left| \sum_{j \in \Xi_i} R_\Gamma^{(i)} R_\Gamma^{(j)T} \delta_j^\dagger \tilde{u}^{(j)} \right|_{S^{(i)}}^2 \quad (5.24)$$

$$\leq 2 \left| \tilde{u}^{(i)} \right|_{S^{(i)}}^2 + 2 \left| \tilde{u}^{(i)} - \sum_{j \in \Xi_i} R_\Gamma^{(i)} R_\Gamma^{(j)T} \delta_j^\dagger \tilde{u}^{(j)} \right|_{S^{(i)}}^2 \quad (5.25)$$

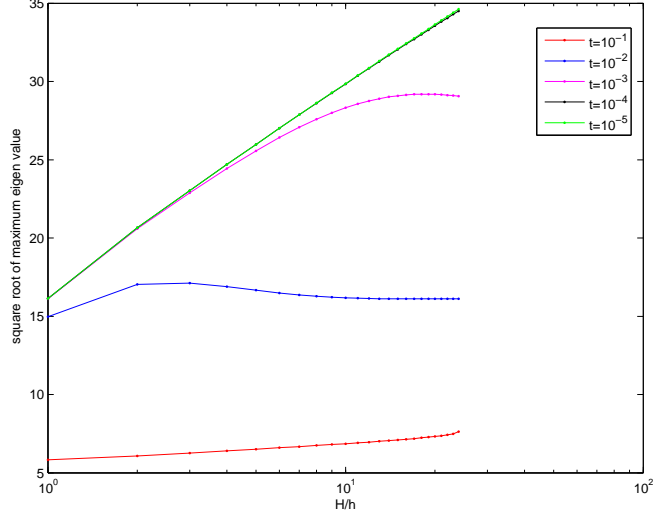


Figure 5.2: $\sqrt{\text{maximum eigenvalue}}$ as a function of $\frac{H}{h}$ for the edge lemma.

The second term is bounded by

$$\begin{aligned}
& \left| \tilde{u}^{(i)} - \sum_{j \in \Xi_i} R_\Gamma^{(i)} R_\Gamma^{(j)T} \delta_j^\dagger \tilde{u}^{(j)} \right|_{S^{(i)}}^2 \\
&= \left| R_\Gamma^{(i)} \sum_{j \in \Xi_i} R_\Gamma^{(j)T} \delta_j^\dagger (R_\Gamma^{(j)} R_\Gamma^{(i)T} \tilde{u}^{(i)} - \tilde{u}^{(j)}) \right|_{S^{(i)}}^2 \\
&\leq \frac{1}{4} \sum_{j \in \Xi_i} \left| R_\Gamma^{(i)} R_\Gamma^{(j)T} (R_\Gamma^{(j)} R_\Gamma^{(i)T} \tilde{u}^{(i)} - \tilde{u}^{(j)}) \right|_{S^{(i)}}^2 \\
&\leq \sum_{j \in \Xi_i} \left(\left| R_\Gamma^{(i)} R_\Gamma^{(j)T} R_\Gamma^{(j)} R_\Gamma^{(i)T} (\tilde{u}^{(i)} - u_0^{(i)}) \right|_{S^{(i)}}^2 + \left| R_\Gamma^{(i)} R_\Gamma^{(j)T} (\tilde{u}^{(j)} - u_0^{(j)}) \right|_{S^{(i)}}^2 \right) \\
&\leq C(1 + \log \frac{H}{h})^2 |u^{(i)}|_{S^{(i)}}^2 + C \sum_{j \in \Xi_i} \left| \psi_{e_{ij}} (\tilde{u}^{(j)} - u_0^{(j)}) \right|_{S^{(j)}}^2 \\
&\leq C(1 + \log \frac{H}{h})^2 \sum_{j \in \Xi_i} |u^{(j)}|_{S^{(j)}}^2. \tag{5.26}
\end{aligned}$$

By summing over the subdomains, we have

$$|E_D \tilde{u}_\Gamma|_{\tilde{S}}^2 \leq C(1 + \log \frac{H}{h})^2 |\tilde{u}_\Gamma|_{\tilde{S}}^2, \quad \tilde{u}_\Gamma \in \tilde{\mathbf{U}}_\Gamma, \tag{5.27}$$

which is similar to Lemma 11. Therefore, we can prove that the BDDC operator with the Falk-Tu elements have a $C(1 + \log \frac{H}{h})^2$ bound if our two conjectures hold.

Table 5.3: Results for $L = 1$, $\frac{H}{h} = 4$, and with an increasing number of subdomains.

NoS	λ_{max}	iter								
t	10^{-1}		10^{-2}		10^{-3}		10^{-4}		10^{-5}	
18	6.4	19.0	12.6	27.9	13.3	29.0	13.4	29.0	13.3	29.0
72	5.6	21.0	14.0	31.0	18.5	35.0	18.4	35.0	18.4	35.0
162	5.5	21.0	14.0	30.0	21.9	36.0	21.1	36.0	21.1	36.0
288	5.5	21.0	13.0	29.0	23.0	36.0	21.2	36.0	21.2	36.0
450	5.5	21.0	11.9	28.0	23.0	37.0	20.1	37.0	20.1	37.0
648	5.5	22.0	10.8	27.0	22.6	37.0	18.8	37.0	18.8	37.0
882	5.5	22.0	10.0	26.0	22.0	38.0	17.6	37.0	17.5	37.0
1152	5.5	22.0	9.4	25.0	21.3	38.0	16.5	38.0	16.4	38.0
1458	5.5	22.0	8.9	25.0	20.5	38.0	15.6	38.0	15.5	38.0
1800	5.5	22.0	8.6	25.0	19.7	38.0	14.9	38.0	14.8	38.0

5.4.1 Numerical Experiments

When discussing our numerical experiments, we use the same notation as in section 4.10. We also use the same elasticity parameters and stopping criteria as in that section. Because the minimum eigenvalue of our BDDC operator is bounded below by 1, we will report the maximum eigenvalue and the number of iterations only.

We have tested our BDDC methods with an increasing number of subdomains. The results are in given Table 5.3 and Figure 5.3. We see that the condition number does not grow with the number of subdomains.

We have also tested our BDDC methods with an increasing value of H/h . The results are given in Table 5.4 and Figures 5.4 and 5.5. They suggest a $C(1 + \log \frac{H}{h})^2$ bound.

Compared to results in [8], we see that the iteration counts are similar for two methods for the two different finite element. Examining the maximum eigenvalues, we find that the one of our methods is about twice as large as the one in [8].

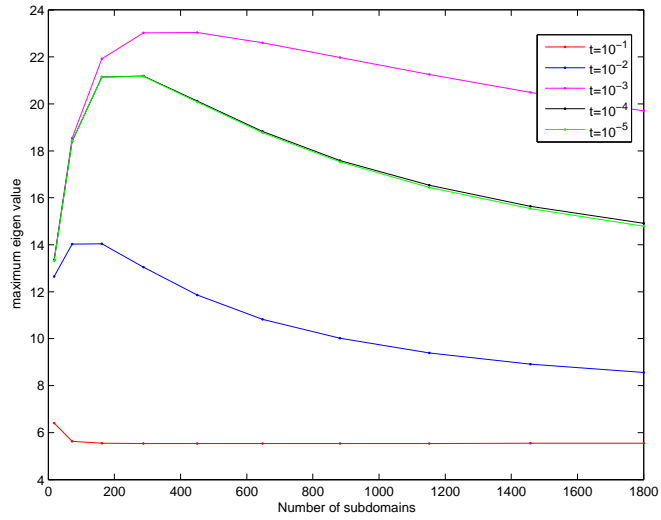


Figure 5.3: Maximum eigenvalue of the preconditioned system as a function of the number of subdomains

Table 5.4: Results for $L = 1$, number of subdomains 4×4 , and with an increasing H/h .

H/h	λ_{max}	iter								
t	10^{-1}		10^{-2}		10^{-3}		10^{-4}		10^{-5}	
3	5.2	18.3	10.9	27.0	11.2	28.9	11.2	29.0	11.2	28.9
4	6.0	20.0	13.1	30.7	14.9	32.0	14.9	32.0	14.9	32.0
5	6.6	21.0	14.4	32.0	16.8	35.0	16.9	35.0	16.9	35.0
6	7.1	22.0	15.2	33.0	18.0	37.0	18.0	37.0	18.0	37.0
7	7.5	23.0	15.9	34.0	18.9	38.0	18.9	38.0	18.9	38.0
8	7.9	24.0	16.5	35.0	19.6	40.0	19.6	40.0	19.6	40.0
9	8.3	25.0	17.1	35.9	20.4	41.0	20.3	41.0	20.3	41.0
12	9.2	26.0	18.6	37.0	22.7	43.7	22.3	43.9	22.3	43.9
15	10.0	27.0	19.8	38.0	25.6	46.0	24.4	46.0	24.3	46.0
18	10.6	28.0	20.9	39.0	28.1	48.0	26.3	48.0	26.2	48.0
21	11.2	28.9	21.7	40.0	30.3	50.0	28.5	49.9	28.5	49.9
24	11.6	29.3	22.6	40.4	33.6	51.9	29.9	51.2	29.8	51.4
27	12.1	30.0	23.2	41.0	35.2	53.0	31.5	53.0	31.1	53.0
30	12.7	30.9	23.7	41.5	37.1	54.0	32.9	54.0	32.9	54.0

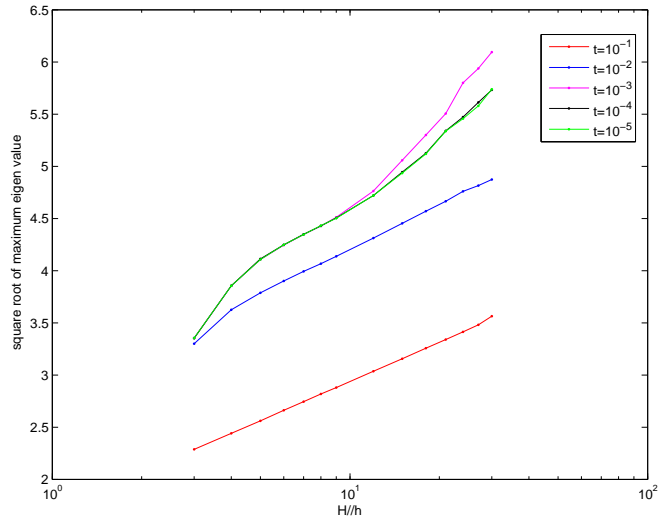


Figure 5.4: $\sqrt{\text{maximum eigenvalue}}$ of the preconditioned system as a function of H/h

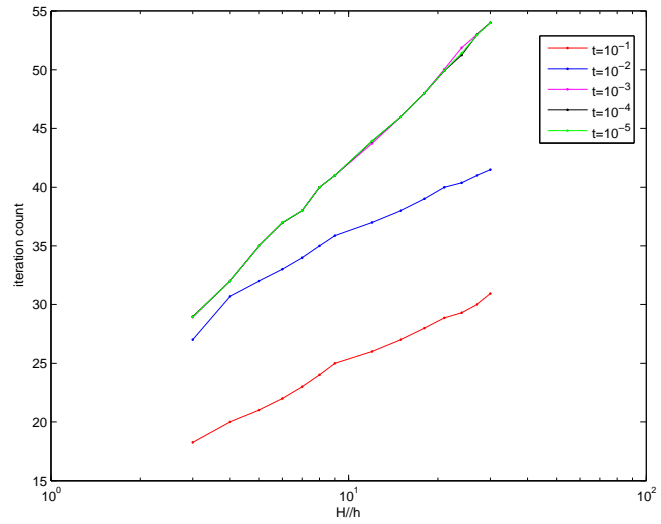


Figure 5.5: Iteration count of the preconditioned system as a function of H/h

Bibliography

- [1] Douglas N. Arnold, Franco Brezzi, Richard S. Falk, and L. Donatella Marini. Locking-free Reissner-Mindlin elements without reduced integration. *Comput. Methods Appl. Mech. Engrg.*, 196(37-40):3660–3671, 2007.
- [2] Douglas N. Arnold and Richard S. Falk. A uniformly accurate finite element method for the Reissner-Mindlin plate. *SIAM J. Numer. Anal.*, 26(6):1276–1290, 1989.
- [3] Douglas N. Arnold and Richard S. Falk. The boundary layer for the Reissner-Mindlin plate model. *SIAM J. Math. Anal.*, 21(2):281–312, 1990.
- [4] Douglas N. Arnold and Richard S. Falk. Asymptotic analysis of the boundary layer for the Reissner-Mindlin plate model. *SIAM J. Math. Anal.*, 27(2):486–514, 1996.
- [5] F. Auricchio and C. Lovadina. Analysis of kinematic linked interpolation methods for Reissner-Mindlin plate problems. *Comput. Methods Appl. Mech. Engrg.*, 190(18-19):2465–2482, 2001.
- [6] K.-J. Bathe and F. Brezzi. On the convergence of a four-node plate bending element based on Mindlin-Reissner plate theory and a mixed interpolation. In *The mathematics of finite elements and applications, V (Uxbridge, 1984)*, pages 491–503. Academic Press, London, 1985.
- [7] L. Beirão da Veiga. Finite element methods for a modified Reissner-Mindlin free plate model. *SIAM J. Numer. Anal.*, 42(4):1572–1591 (electronic), 2004.
- [8] L. Beirão da Veiga, C. Chinosi, C. Lovadina, and L. F. Pavarino. Robust BDDC preconditioners for Reissner-Mindlin plate bending problems and MITC elements. *SIAM J. Numer. Anal.*, 47(6):4214–4238, 2010.
- [9] Daniele Boffi, Franco Brezzi, Leszek F. Demkowicz, Ricardo G. Durán, Richard S. Falk, and Michel Fortin. *Mixed finite elements, compatibility conditions, and applications*, volume 1939 of *Lecture Notes in Mathematics*. Springer-Verlag, Berlin, 2008. Lectures given at the C.I.M.E. Summer School

held in Cetraro, June 26–July 1, 2006, Edited by Daniele Boffi and Lucia Gastaldi.

- [10] Dietrich Braess. *Finite elements*. Cambridge University Press, Cambridge, third edition, 2007. Theory, fast solvers, and applications in elasticity theory, Translated from the German by Larry L. Schumaker.
- [11] Susanne C. Brenner. A two-level additive Schwarz preconditioner for macro-element approximations of the plate bending problem. *Houston J. Math.*, 21(4):823–844, 1995.
- [12] Susanne C. Brenner and L. Ridgway Scott. *The mathematical theory of finite element methods*, volume 15 of *Texts in Applied Mathematics*. Springer, New York, third edition, 2008.
- [13] Susanne C. Brenner and Li-yeng Sung. Balancing domain decomposition for nonconforming plate elements. *Numer. Math.*, 83(1):25–52, 1999.
- [14] Susanne C. Brenner and Li-Yeng Sung. Multigrid algorithms for C^0 interior penalty methods. *SIAM J. Numer. Anal.*, 44(1):199–223 (electronic), 2006.
- [15] Susanne C. Brenner and Kening Wang. Two-level additive Schwarz preconditioners for C^0 interior penalty methods. *Numer. Math.*, 102(2):231–255, 2005.
- [16] M. Brezina and P. Vaněk. A black-box iterative solver based on a two-level Schwarz method. *Computing*, 63(3):233–263, 1999.
- [17] Franco Brezzi, Klaus-Jürgen Bathe, and Michel Fortin. Mixed-interpolated elements for Reissner-Mindlin plates. *Internat. J. Numer. Methods Engrg.*, 28(8):1787–1801, 1989.
- [18] Franco Brezzi, Michel Fortin, and Rolf Stenberg. Error analysis of mixed-interpolated elements for Reissner-Mindlin plates. *Math. Models Methods Appl. Sci.*, 1(2):125–151, 1991.
- [19] D. Chapelle and R. Stenberg. An optimal low-order locking-free finite element method for Reissner-Mindlin plates. *Math. Models Methods Appl. Sci.*, 8(3):407–430, 1998.
- [20] C. Chinosi, C. Lovadina, and L. D. Marini. Nonconforming locking-free finite elements for Reissner-Mindlin plates. *Comput. Methods Appl. Mech. Engrg.*, 195(25-28):3448–3460, 2006.

- [21] C. Constanda and M. E. Pérez, editors. *Integral methods in science and engineering. Vol. 2*. Birkhäuser Boston Inc., Boston, MA, 2010. Computational methods, Papers from the 10th International Conference (IMSE2008) held at the University of Cantabria, Santander, July 7–10, 2008.
- [22] Clark R. Dohrmann. A preconditioner for substructuring based on constrained energy minimization. *SIAM J. Sci. Comput.*, 25(1):246–258 (electronic), 2003.
- [23] Clark R. Dohrmann and Olof B. Widlund. An overlapping Schwarz algorithm for almost incompressible elasticity. *SIAM J. Numer. Anal.*, 47(4):2897–2923, 2009.
- [24] Clark R. Dohrmann and Olof B. Widlund. Hybrid domain decomposition algorithms for compressible and almost incompressible elasticity. *Internat. J. Numer. Methods Engrg.*, 82(2):157–183, 2010.
- [25] Maksymilian Dryja. An additive Schwarz algorithm for two- and three-dimensional finite element elliptic problems. In *Domain decomposition methods (Los Angeles, CA, 1988)*, pages 168–172. SIAM, Philadelphia, PA, 1989.
- [26] Maksymilian Dryja and Olof B. Widlund. Some domain decomposition algorithms for elliptic problems. In *Iterative methods for large linear systems (Austin, TX, 1988)*, pages 273–291. Academic Press, Boston, MA, 1990.
- [27] Maksymilian Dryja and Olof B. Widlund. Towards a unified theory of domain decomposition algorithms for elliptic problems. In *Third International Symposium on Domain Decomposition Methods for Partial Differential Equations (Houston, TX, 1989)*, pages 3–21. SIAM, Philadelphia, PA, 1990.
- [28] Ricardo Durán and Elsa Liberman. On mixed finite element methods for the Reissner-Mindlin plate model. *Math. Comp.*, 58(198):561–573, 1992.
- [29] Ricardo G. Durán, Erwin Hernández, Luis Hervella-Nieto, Elsa Liberman, and Rodolfo Rodríguez. Error estimates for low-order isoparametric quadrilateral finite elements for plates. *SIAM J. Numer. Anal.*, 41(5):1751–1772 (electronic), 2003.
- [30] M. Engeli, Th. Ginsburg, H. Rutishauser, and E. Stiefel. Refined iterative methods for computation of the solution and the eigenvalues of self-adjoint boundary value problems. *Mitt. Inst. Angew. Math. Zürich. No.*, 8:107, 1959.
- [31] Richard S. Falk and Tong Tu. Locking-free finite elements for the Reissner-Mindlin plate. *Math. Comp.*, 69(231):911–928, 2000.

- [32] Alexander Iosilevich, Klaus-Jürgen Bathe, and Franco Brezzi. Numerical inf-sup analysis of MITC plate bending elements. In *Plates and shells (Québec, QC, 1996)*, volume 21 of *CRM Proc. Lecture Notes*, pages 225–242. Amer. Math. Soc., Providence, RI, 1999.
- [33] Patrick Le Tallec, Jan Mandel, and Marina Vidrascu. A Neumann-Neumann domain decomposition algorithm for solving plate and shell problems. *SIAM J. Numer. Anal.*, 35(2):836–867 (electronic), 1998.
- [34] Jing Li and Olof Widlund. BDDC algorithms for incompressible Stokes equations. *SIAM J. Numer. Anal.*, 44(6):2432–2455, 2006.
- [35] Jing Li and Olof B. Widlund. FETI-DP, BDDC, and block Cholesky methods. *Internat. J. Numer. Methods Engrg.*, 66(2):250–271, 2006.
- [36] C. Lovadina. A new class of mixed finite element methods for Reissner-Mindlin plates. *SIAM J. Numer. Anal.*, 33(6):2457–2467, 1996.
- [37] Mikko Lyly. On the connection between some linear triangular Reissner-Mindlin plate bending elements. *Numer. Math.*, 85(1):77–107, 2000.
- [38] Jan Mandel and Clark R. Dohrmann. Convergence of a balancing domain decomposition by constraints and energy minimization. *Numer. Linear Algebra Appl.*, 10(7):639–659, 2003. Dedicated to the 70th birthday of Ivo Marek.
- [39] Jan Mandel, Radek Tezaur, and Charbel Farhat. A scalable substructuring method by Lagrange multipliers for plate bending problems. *SIAM J. Numer. Anal.*, 36(5):1370–1391 (electronic), 1999.
- [40] Aleksandr M. Matsokin and Sergey V. Nepomnyaschikh. A Schwarz alternating method in a subspace. *Soviet Math.*, 29(10):78–84, 1985.
- [41] Jindřich Nečas. *Les méthodes directes en théorie des équations elliptiques*. Masson et Cie, Éditeurs, Paris, 1967.
- [42] Sergey V. Nepomnyaschikh. *Domain Decomposition and Schwarz Methods in a Subspace for the Approximate Solution of Elliptic Boundary Value Problems*. PhD thesis, Computing Center of the Siberian Branch of the USSR Academy of Sciences, Novosibirsk, USSR, 1986.
- [43] Dianne P. O’Leary and Olof Widlund. Capacitance matrix methods for the Helmholtz equation on general three-dimensional regions. *Math. Comp.*, 33(147):849–879, 1979.

- [44] P. Peisker and D. Braess. Uniform convergence of mixed interpolated elements for Reissner-Mindlin plates. *RAIRO Modél. Math. Anal. Numér.*, 26(5):557–574, 1992.
- [45] Barry F. Smith, Petter E. Bjørstad, and William D. Gropp. *Domain decomposition*. Cambridge University Press, Cambridge, 1996. Parallel multilevel methods for elliptic partial differential equations.
- [46] Rolf Stenberg. A new finite element formulation for the plate bending problem. In *Asymptotic methods for elastic structures (Lisbon, 1993)*, pages 209–221. de Gruyter, Berlin, 1995.
- [47] Andrea Toselli and Olof Widlund. *Domain decomposition methods—algorithms and theory*, volume 34 of *Springer Series in Computational Mathematics*. Springer-Verlag, Berlin, 2005.
- [48] Lloyd N. Trefethen and David Bau, III. *Numerical linear algebra*. Society for Industrial and Applied Mathematics (SIAM), Philadelphia, PA, 1997.
- [49] Xuemin Tu. Three-level BDDC in three dimensions. *SIAM J. Sci. Comput.*, 29(4):1759–1780, 2007.
- [50] Xuemin Tu. Three-level BDDC in two dimensions. *Internat. J. Numer. Methods Engrg.*, 69(1):33–59, 2007.